GEOCHEMICAL STUDIES OF THE MOINE ROCKS IN WESTERN INVERNESS-SHIRE

Thesis presented for the Degree of Doctor of Philosophy in the University of London

Norman R. Charnley

Bedford College

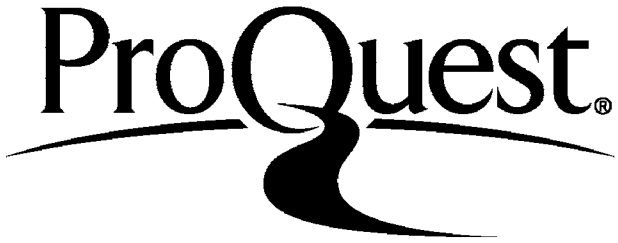

ABSTRACT

The aims of this work were to make a statistical study of variations in chemical composition within and between two major pelitic units in the Moine Series of Morar, western Inverness-shire, and to assess the metamorphic grade across the area by means of the calc-silicate bands found.

Two of the major pelitic units, the Lochailort Pelitic Group and the Garnetiferous Pelite, were sampled to a rigid sampling plan which allowed analysis of variance techniques to be applied to the results, in a study of chemical variation within each of the units. Stepwise linear discriminant function analysis of the data was also undertaken, to provide functions which could be used to separate the two units on the basis of their chemical compositions. These derived functions could also be used to classify unknown samples and assign them to their correct stratigraphic position.

Calc-silicate bands found as a minor rock type within the area may be used as precise indicators of metamorphic grade, since their chemistry determines their mineralogical response to metamorphism in a predictable fashion. Evidence from the less responsive pelites indicates that metamorphic grade rises generally eastwards across Morar, and a study of the calc-silicates, while confirming this, also provided evidence of a later, retrogressive event in the east of the area.

In order to obtain large numbers of chemical analyses, rapid X-ray fluorescence analytical techniques were employed. For major element analysis a fusion method of sample preparation was adopted, and a new method of calibration was devised which allows a large range of rock compositions to be analysed using a single set of linear calibration regression equations.

ACKNOWLEDGMENTS

The work described in this thesis was carried out during the tenure of a Natural Environment Research Council grant, which I gratefully acknowledge.

I am indebted to my supervisor, Dr D. Powell, for introducing me to the Moines and their problems, and for his help and encouragement both in the field and in London.

I should like to thank the staff and research students of the Geology Department who helped in this work, in particular

Dr I.L. Gibson, for his advice and criticisms during the course of this work, particularly in the development of the X-ray techniques used;

Mr J.B. Jackson, for providing a constant source of stimulating discussion, comments and criticism, and for his unstinting help in the preparation of fusion standards for the X-ray calibrations;

Mr H.S. Lloyd, who performed the wet chemical analyses used in this work, and Miss Mary Burtoft, who typed this thesis.

I should also like to thank Dr P. Pal of the Physics Department, Bedford College, for introducing me to the delights of matrix algebra, and showing the way to the solution of the mass absorption problem described in Appendix I.

I am also very grateful for all those who made my periods of field work in Morar so enjoyable, particularly Tommy and Betty Gillan, who provided food, warmth and innumerable cups of coffee at the end of each day's work.

Finally, I should like to thank Sian for her constant patience, support and encouragement at all stages of this work, and for her help in explaining it to other people.

CONTENTS

LIST OF TABLES

LIST OF FIGURES

Chapter 1 INTRODUCTION

Location of area

The rocks considered in this study are from the Morar area of western Inverness-shire, which lies on the west coast of Scotland, some 40km west of Fort William along the A830 (the "Road to the Isles"). Apart from the low-lying, fairly flat coastal strip between Arisaig and Mallaig, the area is generally mountainous with steep-sided glaciated valleys providing a vertical relief of up to 800m. (Figure 1.1).

Geological Setting

Apart from small outcrops of Lewisian rocks within the Morar antiform, the area comprises metamorphic sediments of the Moine Series. In Scotland rocks of the Moine Series outcrop over a wide area, from the Grampian Highlands (where they are thought to be represented by the Central Highland Granulites) northwards across the Great Glen Fault to the Moine Thrust zone, which marks the north west boundary of the Caledonian orogenic belt in Scotland (Figure 1.2). The whole Moine Series thus lies within this orogenic belt, forming part of the "metamorphic Caledonides".

Although subject to study for almost ninety years the position of the Moine Series in the stratigraphic column is not known with certainty, nor has a stratigraphic succession been established which can be applied over the whole Moine outcrop. Correlation of at least part of the Moine with the Torridonian is generally accepted, though not proven (Kennedy, 1951; Sutton and Watson, 1964), and isotope studies indicate that older rocks of the Moine west of the Great Glen were deposited at least 780my and possibly as much as 1000my ago (Long and Lambert, 1963).

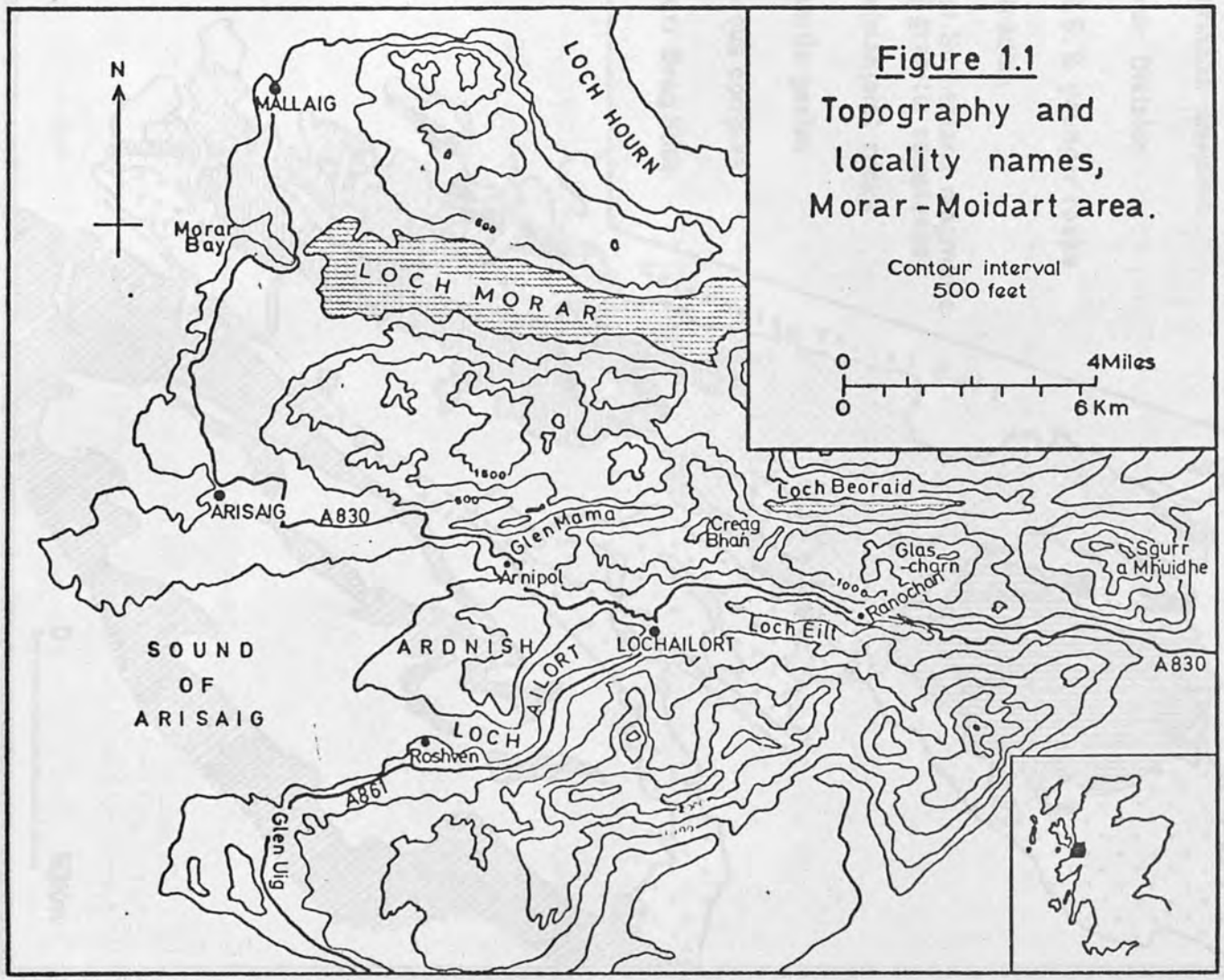
N
MALLAIG
LOCH HOURN
Morar Bay
LOCH MORAR
600
0
1800
800
ARISAIG
A830
Glen Mama
Arnipol
Creag Bhan
Loch Beoraid
Glas-charn
Sgurr a Mhuidhe
1000
Ranochan
Loch Eilt
SOUND OF ARISAIG
ARDNISH
LOCHAILORT
A830
LOCH AILORT
Roshven
A861
Glen Uig
Figure 1.1
Topography and locality names, Morar-Moidart area.
Contour interval 500 feet
0
4Miles
0
6Km

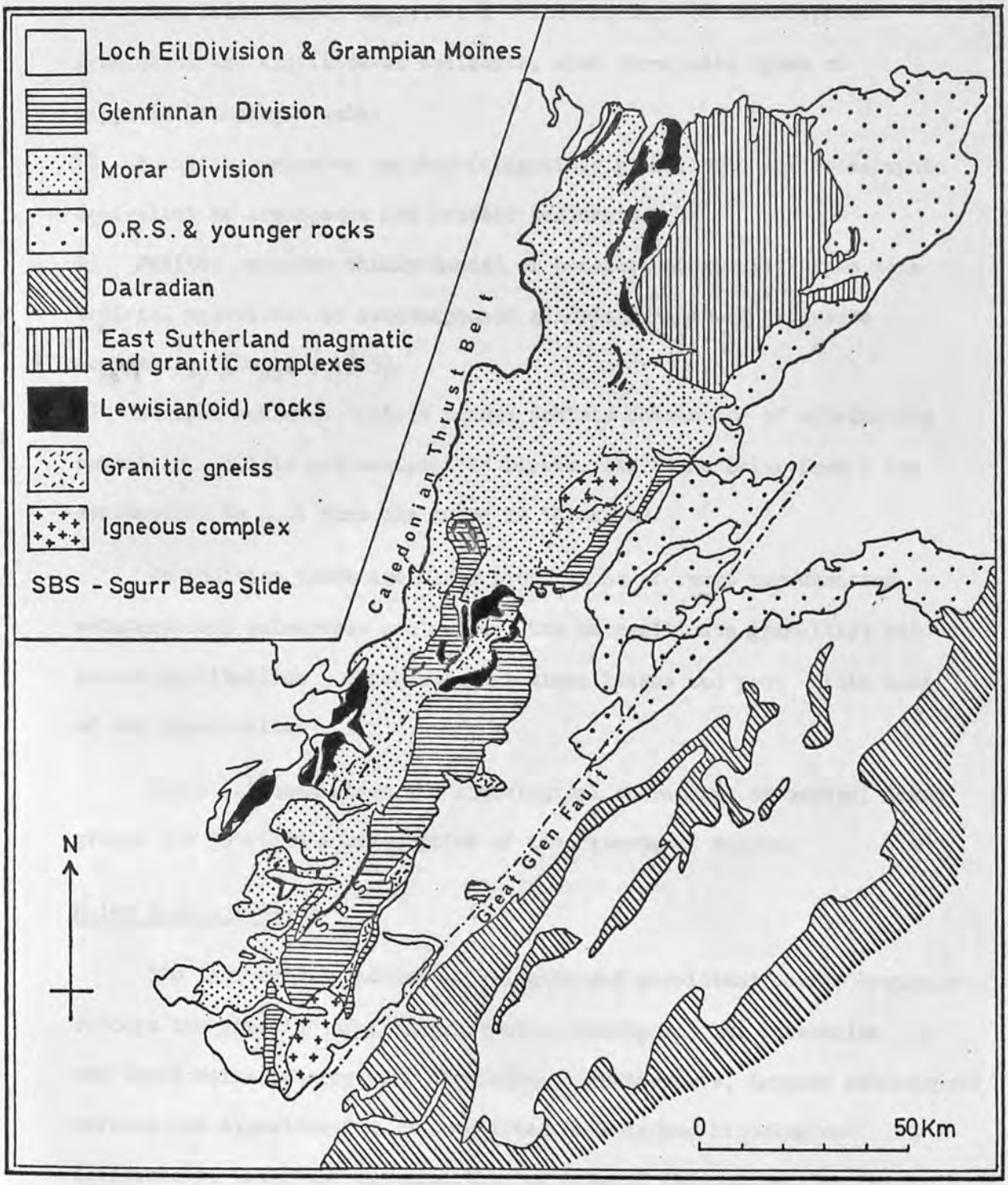

Figure 1.2 Distribution of the Moine rocks of Scotland

Moine Series Lithology

The Moine Series comprises a thick sequence of metamorphosed arenaceous and argillaceous sediments, with three main types of mappable lithologic unit:

1) Psammite: massive quartzo-feldspathic granulites, the metamorphic equivalent of arenaceous and arkosic sediments.

2) Pelite: massive thinly banded or homogeneous garnetiferous mica schists, equivalent to metamorphosed silty sediments of greywacke composition (Butler, 1965).

3) Striped schists: thinly banded schists consisting of alternating psammitic, pelitic and semipelitic layers, the bands being from a few centimetres to more than one metre in thickness.

In addition there are minor proportions of rocks representing metamorphosed calcareous sediments; the calc-silicate granulites and garnet amphibolites , which occur as minor lenses and pods within some of the larger units.

Table 1.1 summarises the lithological characters of several named groups and provides a description of the "standard" Moines.

Moine Stratigraphy

The lack of distinctive lithologies and persistent marker horizons renders the erection of a comprehensive stratigraphical succession for the whole Moine outcrop very difficult. Furthermore, intense metamorphic effects and migmatisation in some areas have masked lithological differences, while the superposition of several fold phases further obscures the order of deposition.

TABLE 1.1 Summary of lithological characters of rock formations of western Inverness-shire (after Johnstone et al., 1969)

7. LOCH EIL PSAMMITE	Variably quartzose psammitic granulite (locally a micaceous 'salt and pepper' type) with very subordinate bands of pelitic and semipelitic schist. Calc-silicate ribs and lenticles present throughout and locally abundant.
6. GLENFINNAN STRIPED SCHIST	Banded siliceous granulite (locally quartzite) and pelitic gneisses. Pods or lenses of metasedimentary amphibolites and calc-silicate granulites occur.
5. LOCHAILORT PELITE	Pelitic gneiss, with subordinate psammitic or semipelitic stripes. Metasedimentary amphibolite and calc-silicate lenses are usually present.
4. UPPER MORAR PSAMMITE	Dominantly psammitic granulite, often pebbly, with common semipelitic bands; calc-silicate ribs present throughout.
3. MORAR (Striped and Pelitic) SCHIST	A dominantly pelitic assemblage locally divided into: a. Rhythmically striped and banded pelite, semipelitic schists and micaceous psammitic rocks with abundant calc-silicate ribs. b. Pelitic schists with some subordinate semipelite stripes. c. Laminated grey, semipelitic and micaceous granulites, locally with thin siliceous and calc-silicate ribs.
2. LOWER MORAR PSAMMITE	Micaceous and siliceous psammitic granulites locally pebbly; subordinate semipelitic rocks developed locally and more thickly towards the top; calc-silicate ribs rare except towards the top; heavy-mineral bands present, but most common near the base.
1. BASAL PELITE	Dominantly pelitic and semipelitic schists, thinly banded with psammite. Apparently typified by abundant contorted quartz veins. May be tectonically mixed 'slide' schist.
LEWISIAN	Eastern type. Hornblende and biotite gneisses and eclogites, associated with metasediments such as marbles, pelitic gneisses, graphitic schists. Western type. Typically migmatitic hornblende and biotite gneisses. Locally retrograded to biotite-rich schists.

Johnstone et al. (1969) divided the Moines of the Northern Highlands into three major groups - the Morar, Glenfinnan and Loch Eil Divisions - which form three belts of strata (Fig. 1.2), the Morar Division being the most westerly. These divisions are not strictly stratigraphic groups, as the boundaries between them may be major slide surfaces, and although characteristic sets of rocks are present, strata from neighbouring divisions may be infolded.

The Morar Division comprises a recognisable stratigraphic succession (1-4, Table 1.1) which was first established in western Morar (Richey and Kennedy, 1939), and was later modified and extended by Ramsay and Spring (1962) and Powell (1964) (Table 1.2).

The Morar Division gives way to the Glenfinnan Division in the east. The full stratigraphic sequence and identity of beds in the Glenfinnan Division are still incompletely known, although in southern Inverness-shire and Argyll Brown et al. (1970) and Dalziel (1966) have suggested a stratigraphy (Units 5 & 6, Table 1.1; see also Table 1.2). The details of the Loch Eil Division, which lies to the east of the Glenfinnan Division, are also uncertain, but the typical lithology is given in Unit 7, Table 1.1.

The junction between the Glenfinnan and Morar Divisions is tectonic in part, marked by the Sgurr Beag slide (Tanner, 1970; Tanner et al.,1970), but is held to be stratigraphic in places (Powell, 1964,1974; Dalziel, 1966; Brown et al.,1970). If essentially a stratigraphic contact, then current bedding evidence would indicate that the older rocks lie to the west, so that Table 1.1 is essentially a stratigraphic sequence. However, if movement on the Sgurr Beag slide has caused appreciable tectonic shortening, the Morar schists may be the equivelent of the

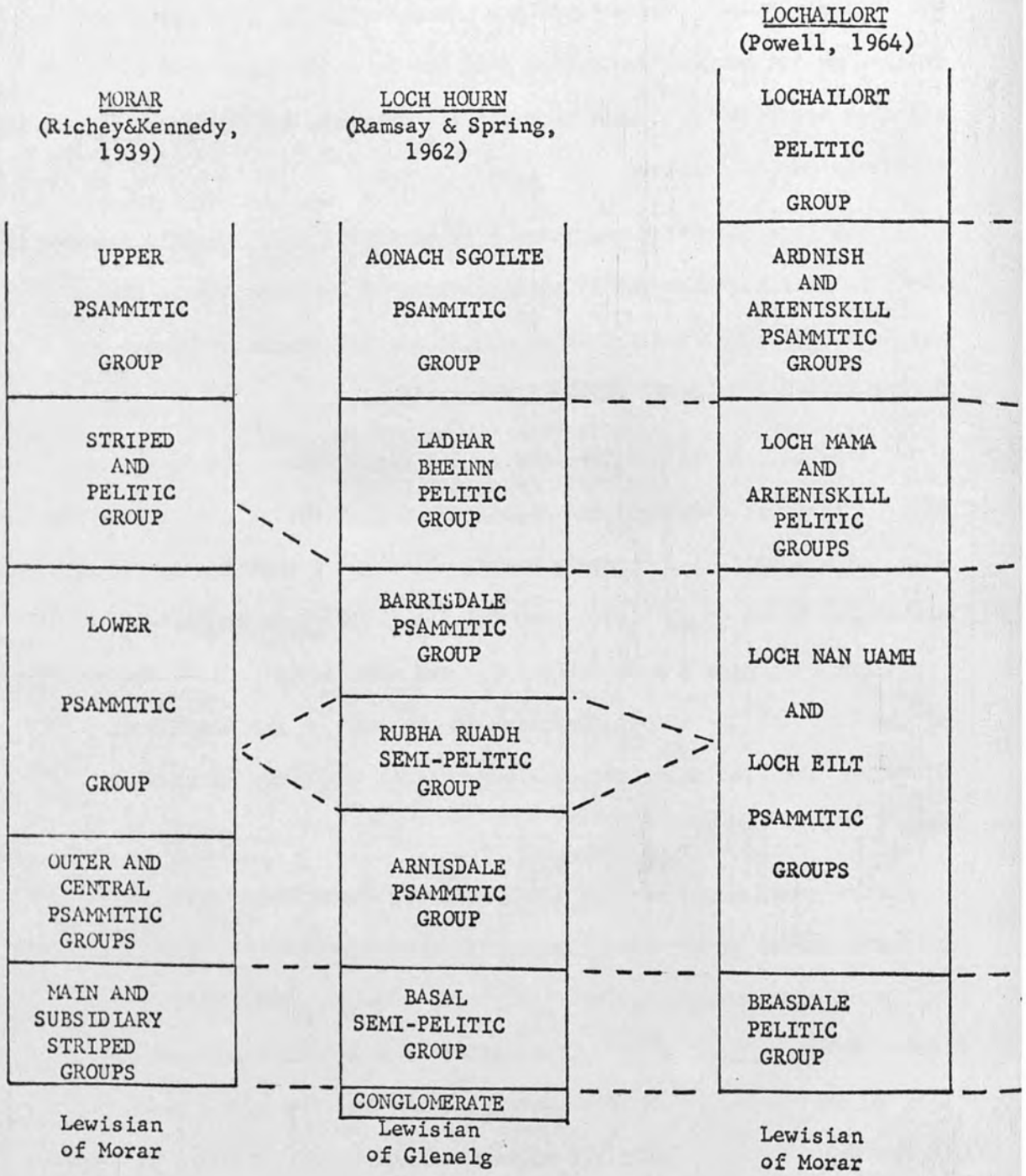

TABLE 1.2 Stratigraphical successions in the Moine Series.

(after Johnstone et al., 1969)

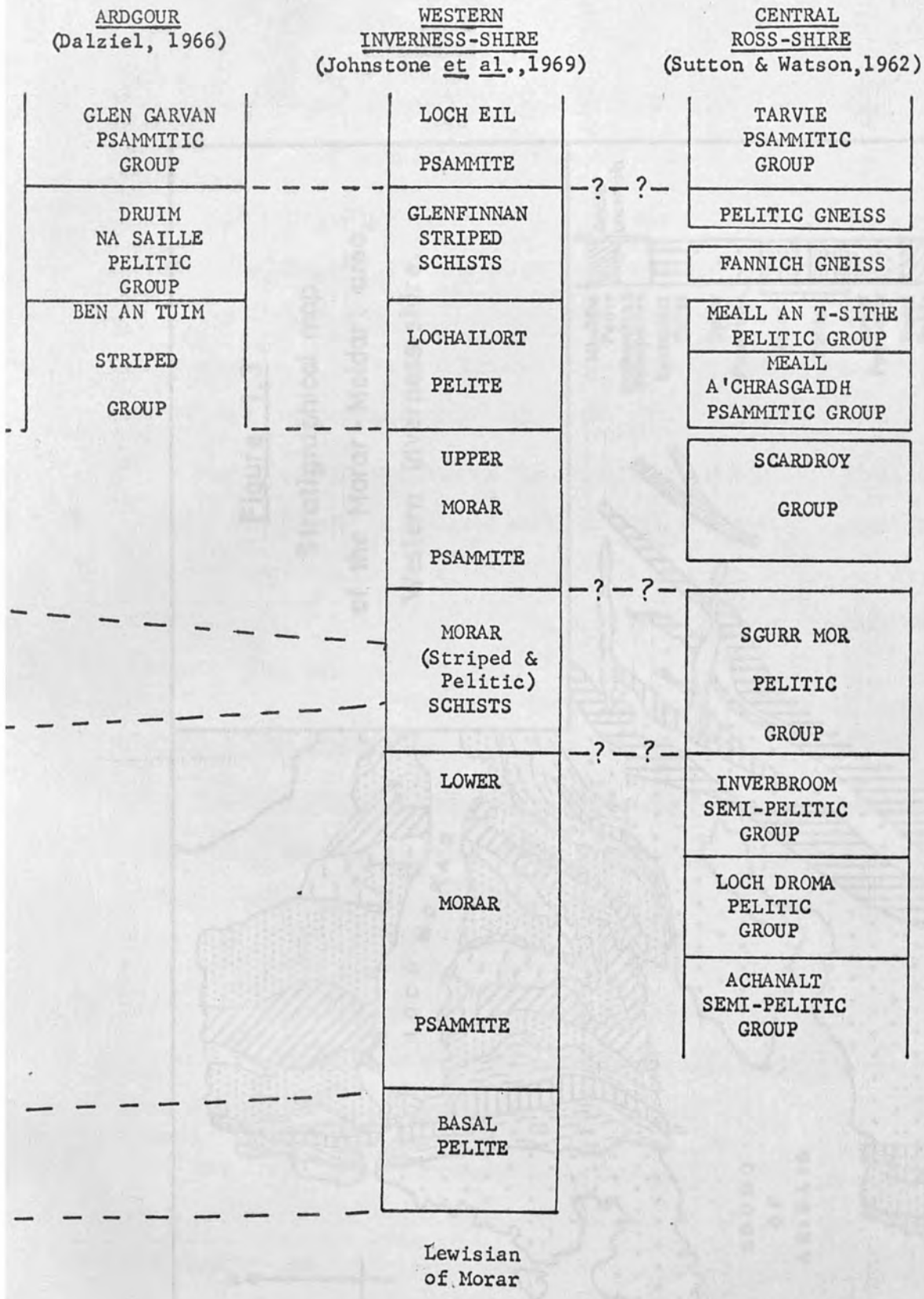

TABLE 1.2 (continued)

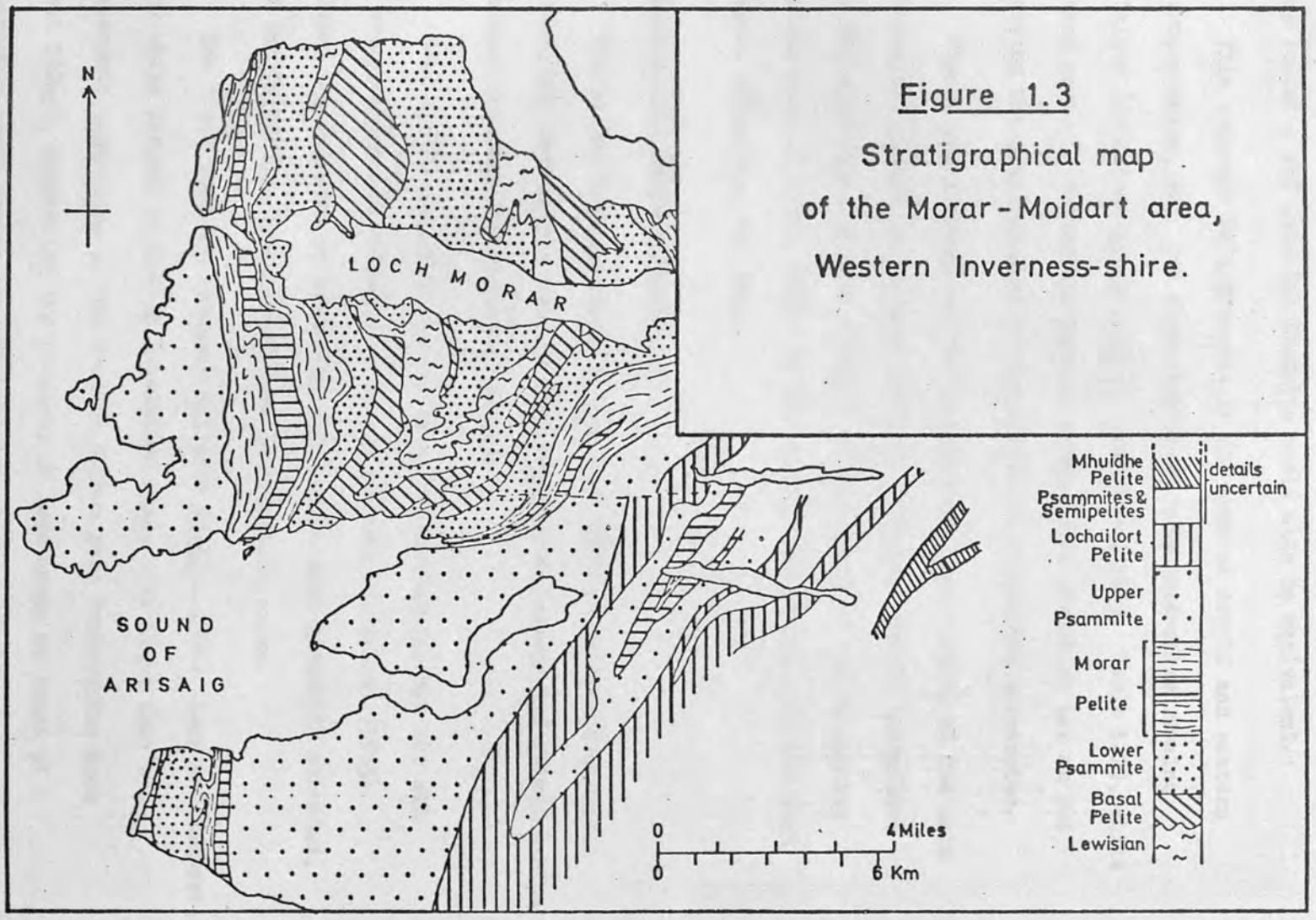

Figure 1.3

Stratigraphical map of the Morar - Moidart area, Western Inverness-shire.

Glenfinnan Striped Schists and the Lochailort Pelite, while the Upper Morar Psammite and Loch Eil Psammite could also be equivalent.

This sequence is applicable in the area of Argyll and western Inverness-shire, but its extension north into Ross-shire remains tentative (Johnstone et al., 1969; Johnstone, 1975; Table 1.2), while further north in Sutherland intense metamorphic reworking has as yet prevented the establishment of any useful stratigraphic succession.

Figure 1.3 illustrates the geographical distribution of the main lithological groups in the area studied. To the west of Lochailort dips are generally moderate (30-50°) with a dominant strike running slightly east of north, while to the east of Lochailort dips are much steeper, often near vertical.

Structural and metamorphic history

The Moines have undergone a long and complex tectono-metamorphic history, and controversy remains over the timing, extent and relationships of metamorphic and deformational events.

Read (1934) argued in favour of a Pre-Torridonian age for all the metamorphism and deformation of the Moines, but Bailey (1955) reviewed the evidence to reach the conclusion, more generally accepted, that the Caledonian orogeny had been the dominant event.

The first isotopic research (Giletti et al., 1961; Long and Lambert, 1963) while largely producing Caledonian ages, also found that syn-metamorphic pegmatites in the western Moines gave Precambrian ages (about 730my), suggesting the presence in some areas at least of a Precambrian event (named the "Morarian" by Lambert, 1969). Further isotopic and structural research has confirmed the existence of Precambrian tectono-metamorphic events (Powell, 1974; van Breemen et al., 1974; Winchester, 1974a) but debate continues on which events constitute

the Caledonian, and which the Precambrian. The Precambrian metamorphism is apparently post-D1, and D3 can be dated at about 445my (van Breemen et al., 1974), but while Powell (1974) maintains that D2 accompanied the Precambrian metamorphism, van Breemen et al. (1974) have dated D2 as post Arenig in age (less than 490my). The areal extent of the two major metamorphic episodes also remains to be defined, although it would appear that to a great extent the Caledonian metamorphism has destroyed the traces of the Morarian metamorphism (Winchester, 1974a).

Objectives of the study

1) "Chemical stratigraphy"

In an attempt to approach problems of correlations of rock groups within the Moine from a new direction, a study was undertaken of the differences in chemical composition between two of the major pelitic units in the Moine succession of Morar, the Lochailort Pelite and the Garnetiferous Pelite of the Morar Striped and Pelitic Group (Fig.1.2). These two pelites are considered to be integral parts of the Morar Succession but of different age by Powell (1964, 1974), whilst Tanner et al. (1970) regard the Lochailort Pelite as part of the Glenfinnan Division, which is largely allochthonous over much of its outcrop. These authors recognise one locality where rocks equivalent, at least in part, to the Lochailort Pelite stratigraphically overlie the Morar Succession (Tanner et al., p.303). Chemical labelling of these two pelite groups could therefore provide a means whereby the stratigraphical status of the pelites within the Glenfinnan Division might be indicated, as well as providing supporting evidence for the stratigraphical separation of the two groups.

The statistical technique of linear discriminant function analysis has been used in this study because it provides a sound basis for assessing a "chemical stratigraphy". The mathematical background to the method is given in Appendix II, and the results in Chapter 4. It was necessary during the study to consider variation in chemical composition within each of the large pelitic units sampled, and in order to examine variation arising from different sources sampling to a rigid plan was undertaken and analysis of variance techniques employed to examine the data. This was felt to be an essential addition to the study because variation between units cannot be properly considered without some knowledge of the form and amount of variation within those units. The results of this analysis are given in Chapter 3.

2) Calc-silicates as indicators of metamorphic grade

The main lithologies of the Moine Series are not very responsive to changes in grade of metamorphism, their chemical compositions precluding the development of distinctive index minerals. Because of this an examination was undertaken of the chemistry and mineralogy of the calc-silicate bands which occur throughout the area, emphasis being placed on their value as indicators of metamorphic grade (Kennedy, 1949). The conclusions drawn from this examination are detailed in Chapter 5.

3) Techniques of analysis

In order to obtain the large number of chemical analyses needed, a rapid X-ray fluorescence technique was developed for the analysis of major element constituents in rocks. This was made of general use, rather than specific to this study, so that people with little or no

experience in laboratory techniques could undertake analyses. A simple fusion method of sample preparation was thus adopted, and a new method of calibration devised which allows analysis of a wide range of rock types using only one straight calibration line for each element. Sample preparation is described in Chapter 2, and the calibration method is described in detail in Appendix I.

Chapter 2. COLLECTION AND ANALYSIS OF SAMPLES

Introduction

The main aim when developing the method of analysis for major element constituents by XRF was simplicity in use, so that people with little or no experience of laboratory techniques could undertake analyses. To this end, a simple fusion technique of sample preparation was adopted, and a method devised which allowed analysis of a wide range of rock types using only one straight calibration line for each element.

Collection and preparation of samples

In collecting samples in the field, the freshest possible specimens were taken, and in most cases a hammer and chisels were sufficient to obtain reasonably sized fresh hand specimens. However, in sampling the Lochailort Pelitic Group for the statistical studies, smooth glaciated outcrop surfaces prevented the desired random sampling. As a result a portable drill was used, being an adapted two-stroke chain saw engine, with a water jacket arrangement round the chuck shaft which allowed water to be pumped down through the shaft to the tip of the diamond bit. The drill itself weighed 18 kg and water carrier, hosepipe, petrol can and tool kit added about another 16 kg. Hand held, the drilling rate was slow, taking an hour or more to obtain a core 3-4 cms in diameter and 15-20 cm long.

To prepare the samples for crushing, a small high speed diamond lapping wheel was used to remove any weathered material present. Extraction of the calc-silicate bands was made easier by first sawing the samples into slabs 1-2 cms thick, and removing most of the unwanted matrix with a hammer and chisel.

The samples were crushed using first a large Sturtevant jaw crusher for the larger samples, reducing them to fragments less than 1 cm. A roller crusher then reduced these fragments, or smaller samples, to sand size. Where possible the samples were split while at the 0.25-0.5 cm size, to reduce the load to be finely ground in the Tema swing mill at the last stage. For the calc-silicates, an agate barrelled swing mill was used, but for the pelitic rocks this entailed an unduly long crushing period to reduce the micaceous minerals, and a tungsten carbide barrelled mill was substituted.

Sample preparation for XRF analysis

The fusion method adopted for major element analysis by XRF was similar to that of Padfield and Gray (1971), using a flux based on sodium tetraborate. Fusion techniques have the advantage of eliminating the mineralogical, chemical and particle size effects inherent in the use of pressed powder pellets, and the low proportion of rock in the fusion (12%) reduces interelement absorption effects. Unfortunately, the sodium tetraborate flux prevents analysis of sodium from the fused discs, and sodium determinations are made from pressed powder pellets. These are unsatisfactory, as already noted, and flux based on lithium tetraborate is to be tried in the future, so that all major elements can be determined from one fusion disc. (When starting this work lithium tetraborate was in short supply and regarded as prohibitively expensive.)

Flux and weighing

A single fusion disc is made up from the following weights:

0.400g rock powder
2.800g anhydrous sodium tetraborate } Flux
0.055g sodium carbonate }

The sodium carbonate is added to reduce the viscosity of the melt; originally, sodium nitrate was also added to assist oxidation, but

heavy staining of the Pt-Au crucibles makes it unsuitable, and instead fusion time was extended to ensure complete oxidation.

The flux is prepared in 2kg batches, this being enough for 700 individual discs. The borax and sodium carbonate are first dried at about 105°C, then weighed, mixed and ground in an agate-barrelled Tema swing mill.

Both flux and rock powder to be analysed are dried at 105°C before weighing, to drive off interstitial moisture. Four fusion discs are prepared for each sample, being weighed out as two portions into sealable plastic tubes, each holding enough mixture for two discs. Each portion acts as a check on the other against gross weighing errors, and weighing time is also reduced. Since the balance used reads to 0.0001g, and weighing to $\pm$0.0002g is straightforward, errors arising from weighing should be negligible.

After weighing, four or five small glass balls (3.5-4.5mm diameter) are added to the rock-flux mixture, and the plastic tubes sealed and shaken in a Glen Creston mill for 5-10 minutes, to ensure thorough mixing of the rock powder and flux. Any errors arising from this mixture sticking to the glass balls or the plastic tubes, or even from the flux or rock sticking preferentially, appear to be no greater than those produced by weighing rock and flux directly into crucibles, so that samples can be weighed out while the crucibles are in the furnace.

Melting

The glass balls are removed, and the rock-flux mixture transferred to crucibles of 95%Pt-5%Au alloy. (The melt does not wet the surface of these, making cleaning of the crucibles much easier, as the solidified glass just springs off, or falls off if the crucible surface is gently flexed.) The mix is then fused in an electric furnace at 1050-1100°C

for about 30 minutes, although rocks with high silica, spinel or chromite contents may need longer to ensure complete fusion. The crucible is then removed from the furnace and placed on a silica triangle over three meka burners, and the melt is swirled around to remove bubbles and ensure homogeneity before casting into discs.

Casting

The method of casting the melt to form discs originally used was that described by Padfield and Gray (1971), i.e. the melt was poured onto a hot (250°C) polished steel plate, and pressed with a small flat aluminium plunger into a disc within a ring of copper wire. This required a fair degree of skill, and a certain amount of luck, with a high proportion of the discs cracking, inconsistencies in their surface qualities, and a tendency for the copper rings to spread open too far to fit the sample holders of the X-ray spectrometer.

Improvements were made by using a larger plunger, and rings die-stamped from thin brass sheet, which improved surface reproducibility, and reduced the incidence of cracking considerably. Now a method very similar to that of Harvey et al. (1972) has been adopted, in which a plunger assembly is mounted on the hotplate, and is used to press the melt into aluminium formers, producing discs needing no supporting ring, and with very good surface reproducibility.

The sets of prepared discs are stored in small sealable polythene bags, and kept in a dessicator until analysed because they are hygroscopic; absorbed water destroys the surface finish of the discs and markedly reduces count rates obtained from them.

Trace element pellets

These pressed powder pellets are used for trace element analysis, and also determination of Na. 6g of rock powder are weighed and mixed with 1g PF resin (a form of powdered bakelite), and pressed at 12 tonnes to form pellets. Baking at 120°C for 10-15 minutes hardens the resin to form durable pellets.

Analytical conditions and procedure

(a) Major element analysis

A Philips PW1212 semi-automatic X-ray spectrometer is used for all the analyses. This can be set up to run through a number of angles, for each characteristic emission line, with several pre-programmed options for each angle:

(i) X-ray tube. A tube with Ag target is used for all the major elements, run at 36Kv, 44mA (1584 watts). The use of the silver target is essentially a compromise, the convenience of not using two or more tube targets (e.g. Cr and W) being offset by the poorer excitation of some of the elements. Excitation of Si and Al is good, and although excitation for elements P to Fe is poorer, a sufficiently high count rate is produced by all common rock types. Poor excitation of Ca is even an advantage in one way, reducing interference of CaKβ escape peak on PKα to negligible proportions.

(ii) Diffracting crystals. Three crystals are mounted on a carrier, and can be changed automatically. RAP ((001), 2d 26.12 Å) is used for elements Na to P, and LiF(200) (2d 2.848 Å) for all the others. LiF(220) (2d 4.027 Å) is used for Fe, as a convenient way of reducing the count rate.

(iii) Detector. A gas flow proportional counter is used for all major element determinations. With a 90%argon-10% methane gas. The window is 2μm aluminised polycarbonate, giving good transmission of the long wave-lengths of Na and Mg Kα. (1μm mylar windows, although giving better transmission, have very much shorter lives under vacuum.)

(iv) Pulse height selector. A narrow energy "window" is used for Na,Mg,P,Al and Si to eliminate high energy scattered silver radiation. (Philips settings 1.5 lower level, 2.5 window.)

(v) Collimator. (In specimen-analyser crystal path) A coarse collimator (size 480 μm) is used for elements Na to P, and a fine collimator (Slit size 160μm) for the other major elements.

(vi) Vacuum. The optical path is enclosed in an evacuated system, for better transmission of the longer wavelengths.

(vii) Channels. Up to 15 preset angles can be run through automatically in one program. Only ten are needed for major elements, since backgrounds are low enough to be regarded as negligible.

For analysis, three of the four prepared discs are selected by counting the Si radiation on each disc and taking the closest three (this is a rough check on the disc surface reproducibility, and is not usually needed with the new disc making procedure). A synthetic enamel standard is used to check the short term drift in the detector. For each element the principal K line is measured, first on the standard, then on the three discs, the whole program being run through twice. Output of channel number and counts is onto printed paper tape and punched cards . (Punched paper tape output is also available, but less convenient for processing.)

The punched cards are processed using a specially written computer program, via the remote terminal to the University of London computer system. For each element, the program performs several checks and calculations:

(i) Counts on the standard are checked for "drift" against a given average standard count for that element, and an estimate of the drift for each cycle printed (this is a check that the machine is correctly set up and behaving properly - abnormally different count rates on the standard indicate that something is wrong).

(ii) Counts from the three discs are then corrected for drift, and the drift corrected counts for each cycle are compared. This is done by dividing the difference between the two sets of counts by the square root of their average (an approximation to the standard deviation of the counts). If the result exceeds 5 ("standard deviations") there is a strong possibility that the analysis will fall outside the limits of the counting statistics.

(iii) The three sets of averaged, drift-corrected counts are used to find an initial value of the elements concerned, using calibration terms read in from cards.

(iv) The three sets of counts are compared to check that none of them falls outside the expected statistical limits. If any does, only the two closest are taken, and appropriate indications and error messages are printed out.

(v) The initial element percentages are averaged, taking all three values or any two selected under section (iv), and the initial analysis printed out. This analysis is then corrected for mass absorption effects and the final analysis printed.

Details of the analytical conditions for each element are summarised in Table 2.1 and an explanation of corrections and calibration techniques can be found in Appendix I.

Element	Count Time (secs.)	Collimator	Pulse Height Selector setting ++	Analyser Crystal	°2θ	Counts/%
p	100	Coarse	1.5-2.5	R.A.P.	27.33	10000
Si	100	Coarse	1.5-2.5	R.A.P.	31 71	2000
Al	100	Coarse	1 5-2.5	R.A.P.	37.70	1500
Mg	100	Coarse	1.5-2.5	R.A.P.	44.50	1300
Na	100	Coarse	1.5-2.5	R.A.P	54.29	1900
Fe	10	Fine	External	LiF(220)	85.87	3000
Mn	10	Fine	External	LiF(200)	63 02	10000
Ti	10	Fine	External	LiF(200)	86.23	3200
Ca	10	Fine	External	LiF(200)	113.21	6000
K	10	Fine	External	LiF(200)	136.79	1600

Total running time 70 minutes for 9 elements + 15 minutes for Na.

All analysis with X-ray optical path under vacuum and sample spinning. Ag target 36Kv 44mA

++Pulse height selector settings refer to Philips PW1212 inbuilt system.

TABLE 2.1 Conditions for major element analysis by X-ray Fluorescence

b) Trace element analysis

Trace elements are analysed in two programs, one using a silver target X-ray tube to determine Nb,Zr,Y,Rb,Sr and Zn, the other using a tungsten target tube to determine Nd,Ce,Ba and La. Full details of the two programs are summarised in Tables 2.2 and 2.3.

Calibrations had been erected by standard spiking techniques, and mass absorption corrections were applied to the results. For the lanthanide elements mass absorption constants were derived from the major element analysis, but for the other elements a mass absorption coefficient was estimated by measuring backscattered silver radiation from the sample for use in a calibrated polynomial.

Position	Count Time (secs.)	$^{o}2\theta$
Nb & Zr Background	20	20.52
Nb Kα	40	21.37
Nb Background	20	21 85
Y Background	20	23.05
Y Kα	40	23.75
Sr & Y Background	20	24.44
Sr Kα	40	25.09
Rb & Sr Background	20	25.89
Rb Kα	40	26.58
Rb Background	20	27.35
Zr Background	20	19.51
Zr Kβ	40	20.04
Ag backscatter	20	16.02
Zn Background	40	41.23
Zn Kα	40	41.74

All analysis with Ag target . 70Kv 20mA
X-ray optical path under vacuum, sample spinning, fine collimator
Pulse Height selector set at3.25 lower level 3.50 window
LiF(200) analysing crystal . Scintillation counter.

Y corrected -.19/ppm Rb. Mass absorption correction made by measuring Ag backscatter

Total running time 1 hour

TABLE 2.2 Conditions for trace element analysis by X-ray fluorescence

Position	Count Time (secs.)	$^{o}2\theta$
Nd background	100	94.40
Nd $L\beta_1$	100	99.05
Ce $L\beta_1$	100	111.62
Ce background	100	117.30
Ti $K\beta_1$	20	123.95
Ba $L\beta_1$	100	128.80
La + Ba background	100	134.83
La $L\alpha_1$	100	138.70

All analysis with W target 60Kv 28mA

X-ray optical path under vacuum, sample spinning, coarse collimator

Pulse height selector 3.25 lower level, 3.50 window.

LiF(220) analyser crystal. Flow counter.

Corrections for peak overlaps are made in the following ratios:

Ba - .003ppm/ ppm Ti

Ba - .816ppm / ppm Ce

Ce - .093ppm / ppm Nd

Nd + .014ppm/ ppm Ba

TABLE 2.3 Conditions for analysis of the lanthanide trace elements by X-ray fluorescence.

Chapter 3. ANALYSIS OF VARIANCE EXPERIMENT

Introduction

In considering variation within a layer of rock, whether in chemical composition, density, permeability, or any other measurable variable, it is apparent that variation can arise from a number of sources. This variation may be on a large scale, such as in lateral changes in lithology, on the smaller scale of differences between two parts of the same hand specimen, or the variability may arise from sources such as analytical error.

Analysis of variance is a statistical technique which allows variation to be quantified and assigned to these differing sources, with some estimate of the contribution of each to the over-all variation. The sampling design employed determines the appropriate form of the analysis and the sources of variation which can be examined. The technique is of fundamental importance in many aspects of numerical and statistical geology.

Shaw (1954, 1956) made a study of trace and major element geochemistry in pelitic rocks, but was mainly concerned with detecting variations produced by metamorphism. Butler (1965) was also concerned with chemical changes during metamorphism of Moine rocks in Ardnamurchan, but in addition made a general chemical study of the major Moine lithologies. He concluded that the massive garnetiferous mica schists (such as those considered in this study) represent original sediments of greywacke or silt composition, with high CaO and Na_2O contents and low K_2O contents indicating immaturity. The psammites, with high Al_2O_3, Na_2O and K_2O contents represent arkoses or feldspathic quartzites.

Of particular relevance to this study is the work of Steveson (1971) who employed analysis of variance to try and detect differences produced by metamorphism within the Glen Mama and Arieniskill Pelitic Groups of the Morar area, the two groups being stratigraphic equivalents at different metamorphic grades. In considering sampling design for the discriminant function experiment to be described later, it was realised that a design which would also allow an analysis of variance study would be most suitable, inasmuch as it allows within-group variations to be studied, as well as variation between groups. In fact, the comparison of two different populations can only be seriously attempted when some estimate has been made of the variability of each of the populations considered, in this case two major pelitic units of the Moine succession in Morar, the Lochailort Pelitic Group and the Garnetiferous Pelite of the Morar Striped and Pelitic Group.

Inspection of Steveson's results lead to the adoption of a similar sampling plan, it being the most productive of results from a comparatively small number of samples and analyses. The sampling plan was also one of the most suitable for the discriminant function study, in providing a large random sample of the two groups under consideration.

Units studied

1) The Garnetiferous Pelite of the Morar Striped and Pelitic Group (Unit 2b of Richey and Kennedy, 1939) consists of a series of garnetiferous pelitic schists with subordinate semipelites and rare psammitic bands and lenses. The group was sampled to the south of Arisaig, where the schists dip 30-40° WNW so that northwest-southeast traverses provide a section across the succession. The metamorphic grade at this point in this area is uppermost greenschist facies or lowest almandine-amphibolite facies, and the pelites typically consist of quartz+plagioclase+muscovite +brown biotite+garnet$^{+}_{-}$chlorite, with accessory amounts of zircon, apatite, sphene and opaque iron oxides.

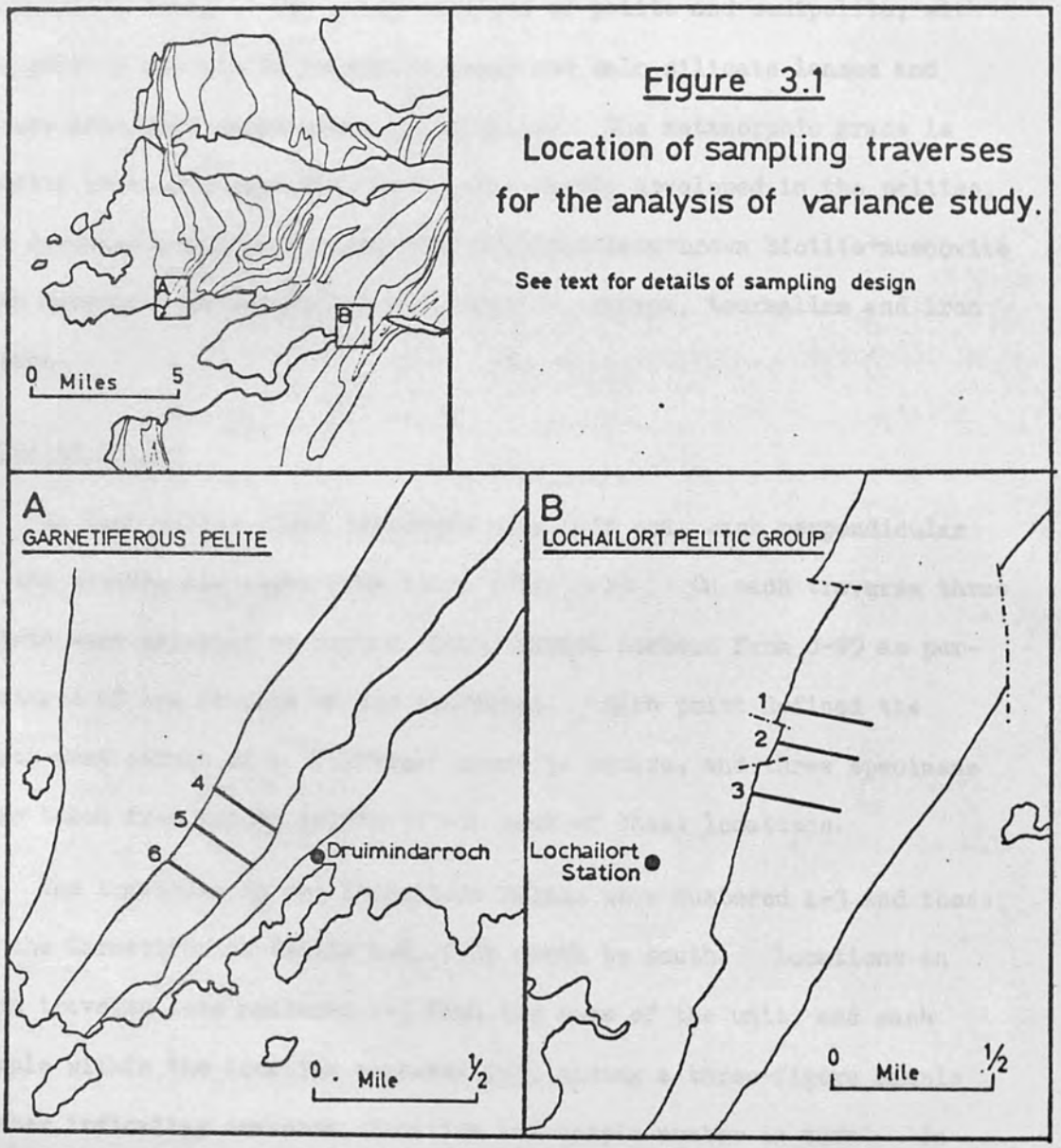
A
B
0 Miles 5
Figure 3.1
Location of sampling traverses for the analysis of variance study.
See text for details of sampling design
A
GARNETIFEROUS PELITE
4
5
6
Druimindarroch
0 Mile ½
B
LOCHAILORT PELITIC GROUP
1
2
3
Lochailort Station
0 Mile ½

2) The Lochailort Pelitic Group (Powell, 1964) outcrops just east of Lochailort village, and lies in the core of the Glenshian synform, a large isoclinal fold plunging gently NNE, and with an almost vertical axial plane. The western limb of the synform was sampled for the statistical study. The group consists of pelite and semipelite, with subordinate amounts of psammitic rocks and calc silicate lenses and garnet amphibolites as minor lithologies. The metamorphic grade is kyanite zone, although kyanite is very rarely developed in the pelites, the dominant assemblage being quartz+plagioclase+brown biotite+muscovite with accessory amounts of zircon, apatite, sphene, tourmaline and iron oxides.

Sampling design

In each pelite three traverses were laid out, each perpendicular to the strike, and about 200m apart (Fig. 3.1). On each traverse three points were selected at random, using random numbers from 0-99 as percentages of the lengths of the traverses. Each point defined the north-west corner of a "location" about 5m square, and three specimens were taken from random points within each of these locations.

The traverses in the Lochailort Pelite were numbered 1-3 and those in the Garnetiferous Pelite 4-6, from north to south. Locations on each traverse were numbered 1-3 from the base of the unit, and each sample within the location numbered 1-3, giving a three-figure sample number indicating traverse, location and sample number in turn. In addition the suffix K was added to indicate that these were the samples for statistical analysis, and to avoid confusion with other sample numbers that arose (e.g. 331, 532).

These 54 specimens (2 pelites x 3 traverses x 3 locations x 3 samples = 54) were analysed once, in random order, and the results used in both analysis of variance and discriminant function analysis experiments. The results are tabulated in Appendix III, Table 1.

The analysis of variance method

The estimate of variance for a population is given by:

$$s^2 = \frac{\sum_{i=1}^{n} (x_i - \bar{x})^2}{(n - 1)}$$

where x is the mean of n individual measurements, x_i. This estimate can be considered as being two parts, the sum of squares of deviations of individuals from the mean ("sum of squares"), and a number one less than the number of samples used in the estimate ("number of degrees of freedom"). In analysis of variance these two values are calculated for each of the sources of variation to be examined, each source being isolated as shown in the following example:

Consider the case of five measurements of Al_2O_3 content on each of two samples of rock (Table 3.1, columns 1a and 1b). Variation in this case can be assigned to two possible sources, variation between the two samples, and variation between individual measures within the samples.

The total sum of squares can be found by subtracting the grand mean from each of the measurements, and squaring the result (Table 3.1, columns 2a and 2b) so that the total sum of squares = 129.44+128.83 = 258.27, with (10-1) = 9 degrees of freedom.

In order to isolate the between-samples effect the within-sample variation must be eliminated, which can be done by replacing each of

	1a	1b	2a	2b	3a	3b	4a	4b	5a	5b	6a	6b
	17.10	16.92	1.86	2.38	18.52	18.41	.003	.003	-1.42	-1.49	2.02	2.22
	10.20	20.68	68.30	4.91	18.52	18.41	.003	.003	-8.32	2.27	69.22	5.15
	19.30	26.00	.70	56.79	18.52	18.41	.003	.003	.78	7.59	.61	57.61
	20.10	10.39	2.68	65.19	18.52	18.41	.003	.003	1.58	-8.02	2.50	64.32
	25.90	18.05	55.29	.17	18.52	18.41	.003	.003	7.38	-.36	54.46	.13
Total	92.60	92.04	128.83	129.44			.015	.015			128.81	129.43
Mean	18.52	18.41										
Grand Total		184.64										
Grand Mean		18.464										

TABLE 3.1 Example of an analysis of variance calculation (See text for explanation)

the items by its own sample average (Table 3.1, columns 3a and 3b). The procedure for finding the between-samples sum of squares is then the same as for the total sum of squares, taking the square of the deviations of these new entries from the grand mean (Table 3.2, columns 4a and 4b), so that the between-samples sum of squares = 0.015 + 0.015 = 0.030, and degrees of freedom is one less than the number of samples on which the estimate is based, i.e. (2-1)=1.

It now only remains to find the within-sample sum of squares and degrees of freedom, which must involve the removal of the between-samples effect. This is done by subtracting from each of the original data items its own sample average (Table 3.2, columns 5a and 5b). These two columns have a grand mean of zero, and the sum of squares of deviations from this mean is simply the square of each entry in columns 5a and 5b, with results placed in columns 6a and 6b. The within-sample sum of squares is then 128.81 + 129.43 = 258.24.

To find the associated number of degrees of freedom, the argument is as follows: each sample consists of five items. For each sample the number of degrees of freedom within that sample will be one less than the number of items in that sample, i.e. 4. However, there are two such samples, so the total degrees of freedom within-samples is $2 \times 4 = 8$.

The results can now be tabulated in an analysis of variance table (Table 3.2). It can be seen that the total sum of squares has been broken down into two parts. In this model the null hypothesis is that the two sets of data are random samples from the same (normal) population, and this can be tested against Snedecor's F ratio for the variance estimates (the "mean square" for each source). The ratio of between-samples mean square to within-sample mean square is found and the

Source	Sum of Squares	Degrees of Freedom	Variance Estimate (Mean Square)
Between Samples	.030	1	.030
Within Samples	258.24	8	32.28
Total	258.27		

TABLE 3.2 Analysis of variance table for the example in Table 3.1

result compared to the tabulated F-statistic with 1 and 8 degrees of freedom. If the tabulated value is exceeded, then the hypothesis is rejected, and the means for the two samples vary more than the items within each sample. In this case the ratio is 0.0009, compared to the tabulated value of F at the 95% significance level of 5.32, so the hypothesis is accepted.

In practice the calculations involved can be reduced to much more rapid and convenient computational forms, but more insight into the meaning of the technique can be gained from the calculations as laid out here.

The mathematical structure of the example given can be summarised as follows:

$$X_{ij} = \bar{x} + a_j + b_{i(j)}$$

where each observation X_{ij} is made up from the population mean, as estimated by $\bar{x}$, a deviation attributable to variation between samples a_j, and a deviation attributable to variation between measures within samples $b_{i(j)}$.

In the subsequent study of the pelites the mathematical model employed is:

$$X_{ijk} = \bar{x} + T_i + L_{j(i)} + S_{k(ji)}$$

This means that any individual parameter for specimen ijk is made up from the mean value for the population (i.e. the whole pelite unit, estimated from the mean of the sample taken, $\bar{x}$), plus a variation T_i attributable to the variability between traverses, a variation $L_{j(i)}$ attributable to variation between locations on traverses, and a small scale variation $S_{k(ij)}$, the variation between individual specimens within each location

Source	Degrees of Freedom	Sum of Squares	Mean Square
Between Traverses	I-1	$\frac{\sum_i Y_{i..}^2}{JK} - \frac{Y_{...}^2}{IJK}$	MS_T
Between Locations Within Traverses	I(J-1)	$\frac{\sum_i \sum_j Y_{ij.}^2}{K} - \frac{\sum_i Y_{i..}^2}{JK}$	MS_L
Between Specimens Within Locations Within Traverses	IJ(K-1)	$\sum_i \sum_j \sum_k Y_{ijk}^{2jk} - \frac{\sum_i \sum_j Y_{ij.}^2}{K}$	MS_S
Total	IJK-1	$\sum_i \sum_j \sum_k Y_{ijk}^2 - \frac{\sum_i \sum_j Y_{ij.}^2}{K}$	

Variance Components

$$\hat{\sigma}_S^2 = MS_S \qquad \hat{\sigma}_L^2 = \frac{MS_L - MS_S}{K} \qquad \hat{\sigma}_T^2 = \frac{MS_T - MS_L}{KJ}$$

TABLE 3.3 Form of analysis of variance, and estimates of components of variance used in this study. Individual observations have the form $X_{ijk} = \bar{x} + T_i + L_{j(i)} + S_{k(ji)}$

The brackets around suffixes indicate that each variable is "nested" in the higher level, i.e. that traverses are made up of locations which are in turn made up of specimens.

The factors can be considered in terms of the scale and form of the variation:

Between specimens - 2m. This measures the small scale variation, and includes any variation not accounted for by other sources in the analysis, such as analytical error.

Between locations - 20m. This measures an effect operating across the strike, or upwards through the original sequence of beds in the unit.

Between traverses - 200m. This measures some effect along the strike, lateral variations within the unit.

Analytical error was not separately assessed, being included in the lowest level of variation. An estimate of analytical variation could have been obtained by making duplicate analyses of all the samples which would have allowed the between-analysis level of variation to be isolated, but lack of time prevented this.

In Table 3.3 are given the measures appropriate to the sampling design and mathematical model used in this study. The results obtained can be interrogated as follows:

1) F ratios tests on two hypotheses:

(i) $F = MS_L/MS_S$

The null hypothesis for this ratio is that the locations represent random samples from the same normal population. If this hypothesis is rejected, then the experiment has detected differences between the locations. If accepted, differences are absent, or undetectable because of variations in the lower, between-samples level, or from variations in the analytical technique.

(ii) $F = MS_T/MS_L$

The null hypothesis tested by this ratio is that variation among the traverse means is no greater than variation among location means. If rejected, then variation between the traverses is greater than at either the location or sample level, indicating a change along the strike. The F test of the hypothesis of equal means assumes homogeneity of variances within the levels tested. This assumption can be verified using Bartlett's test for homogeneity of the variances as a whole, or Cochran's test for isolating any variance value which seems to be extreme. The form of the tests is given in Table 3.4.

2) Components of variance can be derived from the mean square values for each level. The mean squares are estimates of variance at each level, and the components of variance are estimates of the population variance arising from each source. They can be used to indicate where the sampling design can be altered, to increase the amount of information available at a given level, or to simplify the sampling procedure.

3) Confidence intervals about the variable means can be evaluated from the estimates of population variance. The between-traverses mean square provides an estimate of population variance about the grand mean, $\hat{\sigma}^2 = \frac{MS_T}{27}$ (Anderson & Bancroft, 1952, p.326). Associated confidence limits are estimated by $\bar{\bar{X}} \pm t_{\alpha}\frac{\hat{\sigma}}{\sqrt{N}}$, where t is Student's t to desired significance level α and N is number of observations (3). These are confidence limits for sample size 27, taken at random.

Results of the analysis of variance for the Lochailort Pelitic Group

This is known to be an inhomogeneous stratigraphic unit in that minor psammitic bands occur within the dominantly pelitic and semi-pelitic unit (disregarding minor lithologies, calc silicates and

TABLE 3.4 Form of Bartlett's and Cochran's tests for homogeneity of variances (see text for explanation and tables 3.5 , 3.9 for results).

Bartlett's Test:

$$\chi^2 = \frac{2.303}{C} \left(\log \bar{s}^2 \sum (n_i - 1) - \sum_{i=1}^{k} ((n_i - 1) \log s_i^2) \right)$$

and $$C = \frac{1}{3(k-1)} \left[\sum \frac{1}{n_i - 1} - \frac{1}{k(n_i - 1)} \right]$$

where s_i^2 are the individual variances, i=1,2,..k , n_i is the number of terms used in calculating s_i^2 and $\bar{s}^2$ is the pooled estimate of variance. The statistic is distributed as χ^2 with k-1 degrees of freedom, and tests the null hypothesis $H_o : \sigma_1^2 = \sigma_2^2 = \ldots \sigma_k^2$, where σ_k^2 is the variance estimated by s_k^2.

Cochran's Test:

$$g = \frac{\max s_i^2}{\sum_{i=1}^{k} s_i^2}$$

Each variance estimate s_i^2 is based upon n variables, and the hypothesis $\sigma_1^2 = \sigma_2^2 = \ldots \sigma_k^2$ is accepted if $g \leq g_\alpha$, where g_α is given in tables for levels of significance α, and the tables are entered with n and k.

amphibolites, which are chemically and mineralogically distinct). For the data obtained standard deviations and skewness coefficients are very high for most of the variables, indicating that the variables are not normally distributed. Examination of the data shows that two of the items (231K and 232K) are in fact psammites, so that although the data is random in terms of the unit as a whole, and reflects the variation of the unit well, the data cannot be considered as being from a normal population. Bartlett's test for homogeneity of variances is failed by ten of the variables (Table 3.5) and the highest variance is found in locality 23.K for no fewer than fourteen of the variables. This inhomogeneity renders the results of any analysis of variance performed suspect, since the analytical technique involves simultaneous comparison of means and variances, and inhomogeneity of the variances confuses the comparison. To reduce the inhomogeneity, and thus in effect examine only the pelitic and semipelitic parts of the unit, 231K and 232K were treated as missing data items for the purposes of the analysis. These two analyses were replaced by the means of the other analyses in that locality - only one in this case, 233K. This procedure minimises error introduced into the analysis, the variance for that locality falling to zero, and the locality mean taking on a value closer to the over-all mean as the skewness for the data of the locality is reduced. The number of degrees of freedom associated with the between-samples level must also be reduced, but all the other computations and tests of significance remain the same, with little added error (Huitson, 1966, p.21). Results are given in Tables 4.1A and 4.1B.

Results of analysis of the original data set (Table 3.6) do in fact show that the greatest variation is at the between-localities level for SiO_2, Al_2O_3, iron as total Fe_2O_3, MgO, P_2O_5, Zr, Y and Rb. Despite the unfavourable data structure, this does seem to be a reflection of the

TABLE 3.5 Results of Bartlett's and Cochran's tests for homogeneity of variances of the Lochailort Pelitic Group locations. For form of tests see Table 3.4.

Variable	Original Data (27 specimens)		Data with interpolated values for 231K and 232K	
	Bartlett	Cochran	Bartlett	Cochran
SiO_2	xx	x 6	-	- 4
TiO_2	x	x 6	-	- 4
Al_2O_3	x	x 6	-	- 8
MnO	x	x 6	-	- 4
ΣFe_2O_3	-	- 6	-	- 5
MgO	-	- 6	-	- 5
CaO	-	- 6	-	- 7
Na_2O	-	- 6	-	- 3
K_2O	x	xx6	-	- 7
P_2O_5	-	- 1	-	- 1
Zr	xx	xx6	-	- 8
Y	x	xx6	x	xx4
Rb	x	x 6	-	- 8
Nb	-	- 6	-	- 8
Sr	-	- 3	-	- 3
Zn	-	- 4	-	- 4
Nd	-	- 6	-	- 1
Ce	-	- 8	-	- 8
Ba	xx	xx6	-	- 8
La	-	- 6	-	- 8

xx indicates failure at the 1% significance level
x .. .. 5% .. ..
- no significant inhomogeneity

Numbers show location with highest variance for that variable:
1= 11. ; 2=12. ; 3=13. ; 4=21. ; 5=22. ; 6=23. ; 7=31. ; 8=32. ; 9=33.

Variable	Mean Squares			F ratios	
	Traverses (MST)	Locations (MSL)	Specimens (MSS)	MST/MSL (2,6)	MSL/MSS (6,18)
SiO_2	17.4	22.3	7.17	.779	3.11**
TiO_2	.019	.035	.017	.529	2.06
Al_2O_3	1.65	5.08	.990	.324	5.14***
ΣFe_2O_3	2.70	3.80	1.27	.711	2.98**
MnO	.0002	.0010	.0004	.200	2.50*
MgO	.241	.170	.061	1.42	2.77**
CaO	.256	.426	.244	.601	1.75
Na_2O	.037	.312	.400	.120	.780
K_2O	.134	1.14	.728	.118	1.56
P_2O_5	.003	.0054	.0011	.630	4.91***
Zr	2284.7	10434.1	1192.5	.219	8.75***
Y	100.2	288.7	76.5	.347	3.77**
Rb	36.8	1063.7	381.0	.035	2.79**
Nb	.259	14.9	8.70	.017	1.72
Sr	2.48	2481.3	1685.9	.001	1.47
Zn	1522.4	934.6	344.7	1.63	2.71**
Nd	555.1	93.7	123.1	5.92**	.762
Ce	3264.7	1354.2	553.9	2.41	2.44*
Ba	53676.8	82694.3	36573.4	.649	2.26*
La	683.4	226.3	127.0	3.02	1.78

TABLE 3.6 Results of analysis of variance, Lochailort Pelitic Group, original data.

* F ratios significant at 10% level
** F ratios significant at 5% level
*** F ratios significant at 1% level

Variance Components			Coefficients of Variation (%)		
Traverses	Locations	Specimens	Traverses	Locations	Specimens
-.546	5.04	7.17	0	3.67	4.38
-.002	.006	.017	0	7.88	13.26
-.381	1.36	.990	0	6.29	5.36
-.122	.842	1.27	0	11.9	14.7
-.0001	.0002	.0004	0	11.9	16.8
.008	.036	.061	4.08	8.66	11.3
-.019	.061	.244	0	11.9	23.7
-.031	-.029	.400	0	0	24.3
-.111	.136	.728	0	10.9	25.4
-.0002	.0014	.0011	0	16.4	14.5
-905.5	3080.5	1192.5	0	24.4	15.2
-20.9	70.7	76.5	0	15.6	16.2
-114.1	227.6	381.0	0	10.5	19.5
-1.63	2.09	8.70	0	7.59	15.4
-275.4	265.1	1685.9	0	6.34	15.9
65.3	196.6	344.7	6.76	11.7	15.5
51.3	-9.78	123.1	16.2	0	25.1
212.3	266.8	553.9	12.4	13.9	20.0
-3224.2	15373.6	36573.4	0	16.6	25.6
50.8	33.1	127.0	14.6	11.8	7.86

TABLE 3.6 (cont.) Mean Squares = Sample variance estimates

Variance Components = Population variance estima es

Coefficients of variation = $\frac{\sqrt{(\text{Variance components})}}{\text{Population Mean}}$

(See text for details).

Variable	Mean Squares			F ratios	
	Traverses (MST)	Locations (MSL)	Specimens (MSS)	MST/MSL (2,6)	MSL/MSS (6,16)
SiO_2	.789	3.04	3.58	.259	.850
TiO_2	.002	.009	.010	.250	.889
Al_2O_3	.451	1.71	.524	.262	3.27**
ΣFe_2O_3	.194	.641	.938	.303	.683
MnO	.0001	.0004	.0003	.250	1.48
MgO	.045	.042	.037	1.06	1.11
CaO	.161	.406	.162	.396	2.51 *
Na_2O	.105	.360	.314	.291	1.14
K_2O	.377	1.37	.314	.274	4.37***
P_2O_5	.001	.002	.001	.522	2.19 *
Zr	2366.3	10571.0	328.7	.224	32.16***
Y	35.7	207.0	81.4	.172	2.54 *
Rb	87.1	1048.9	200.0	.083	5.24***
Nb	8.04	3.30	7.17	2.44	.460
Sr	31.26	2534.2	1697.0	.012	1.49
Zn	521.4	257.1	301.5	2.05	.853
Nd	788.6	236.7	104.3	3.33	2.27
Ce	4815.4	2311.0	557.8	2.08	4.14**
Ba	102733.6	114530.0	16677.0	.897	6.87***
La	878.9	359.2	132.7	2.45	2.71 *

TABLE 3.7 Results of analysis of variance, Lochailort Pelitic Group, with interpolated values for specimens 231K and 232K.

* - F ratio significant at 10% level
** - F ratio significant at 5% level
*** - F ratio significant at 1% level

Variance Components			Coefficients of Variation (%)		
Traverses	Locations	Specimens	Traverses	Locations	Specimens
-.250	-.179	3.58	0	0	3.13
-.0007	-.0004	.010	0	0	9.78
-.140	.397	.524	0	3.34	3.84
-.050	-.099	.938	0	0	12.2
-.00003	.00004	.0003	0	5.20	13.5
.0003	.0014	.037	.77	1.67	8.62
-.027	.081	.162	0	13.6	19.2
-.028	.015	.314	0	4.78	21.8
-.111	.353	.314	0	23.1	16.5
-.0001	.0004	.001	0	8.66	13.9
-911.6	3414.1	328.7	0	25.6	7.95
-19.0	41.8	81.4	0	11.8	16.5
-106.9	283.0	200.0	0	11.4	9.62
.527	-1.29	7.17	3.70	0	13.7
-278.1	279.1	1697.0	0	6.52	16.1
30.0	-14.8	301.5	4.46	0	14.1
61.3	44.1	104.3	18.2	15.5	23.8
278.3	584.4	557.8	16.7	21.1	20.6
-1306.2	32617.5	16677.0	0	23.6	16.9
57.7	75.5	132.7	15.9	18.2	24.1

TABLE 3.7 (cont.) See text and Table 3.6 for details

TABLE 3.8 99% confidence limits for Lochailort Pelitic Group

(Sample size 27 items)

Variable	Original Data	Data with interpolated values for 231K and 232K
SiO_2	61.14±3.22	60.37± .69
TiO_2	.98± .11	1.02± .04
Al_2O_3	18.56± .99	18.84± .52
ΣFe_2O_3	7.56±1.27	7.91± .34
MnO	.12± .01	.12± .01
MgO	2.19± .38	2.25± .16
CaO	2.08± .39	2.10± .31
Na_2O	2.60± .15	2.57± .25
K_2O	3.36± .28	3.41± .48
P_2O_5	.23± .05	.24± .03
Zr	228± 37	228± 38
Y	54± 8	55± 5
Rb	144± 5	147± 7
Nb	19± 4	20± 2
Sr	257± 1	256± 4
Zn	120± 30	123± 18
Nd	44± 18	43± 22
Ce	118± 44	115± 54
Ba	748±179	766±248
La	49± 20	48± 23

known situation, where one locality is markedly different. Of the other elements, all show that the greatest variation is at the between-samples level, except for Nd, which shows significant differences at the 5% probability level between traverses, though again this may be due to the inadequacies of the data distribution.

Treating 231K and 232K as missing data changes the results somewhat. No inhomogeneities remain in the variances detectable by Bartlett's or Cochran's tests for any variable except Y (Table 3.5). The results of the analysis of variance show that Al_2O_3, CaO, K_2O, P_2O_5, Zr, Rb, Ce and Ba have significant differences at the between-localities level, all other variables having their greatest variances at the between-sample level.

The differences in Zr can probably be related to uneven distribution of detrital zircon vertically through the original sediments. P_2O_5 just exceeds the 10% probability value for F at the between-localities level, and this may be, like Zr, a reflection of original detrital mineral distribution, in this case apatite.

The variation in the distribution of Al_2O_3, K_2O, Rb, Ce and Ba would appear to indicate that a mineral such as K-feldspar, biotite or muscovite has an uneven distribution through the unit across the original bedding. Given that the unit is a mixed sequence of pelites and semi-pelites (the psammites having been eliminated in this analysis) the detection of vertical differences such as this is an indication of the adequacy of the analytical techniques employed.

Variation in CaO only just exceeds the 10% level, and may be considered in terms of its role either in apatite or as a constituent of K-feldspar.

Results of the analysis of variance for the Garnetiferous Pelite

In the field this unit appears to be more homogeneous in rock type than the Lochailort Pelitic Group, being mainly a highly garnetiferous pelite with subordinate semipelite, and only rare psammitic ribs. Despite this, the element distributions show very high skewnesses, and total iron, CaO, Na_2O, Zr, Rb and Nb all fail Bartlett's test for homogeneity of variances (Table 3.9). Two localities can be seen to have the highest variances for fifteen of the elements, localities 42.K and 63.K. Inspection of the analyses reveals that items 421K, 423K and 613K are the sources of these high variances, and treatment of these three points as missing data eliminates the variance inhomogeneity of most variables, although CaO and Na_2O remain inhomogeneous and skewed.

Analysis of variance for the original data (Table 3.10) shows that all variables except Sr have variations restricted to the between-samples level. Sr has a difference detected at the between-traverses level, indicating that variation along strike is a dominant source.

When three items (421K, 423K and 613K) are treated as missing data points Sr again shows a significant variation due to the between-traverses source (Table 3.11) so the along-strike variation would appear to be real, although its origin is uncertain. Of the remaining variables MgO, TiO_2 and P_2O_5 all show significant variation at the between-localities level. The significance level for P_2O_5 only just reaches the 10% value, which, as in the Lochailort Pelitic Group, may represent minor vertical fluctuations in the distribution of detrital apatite within the unit.

The variation in MgO appears real, since its data conform with all the assumptions of the technique, but the cause remains uncertain. It may be that MgO is a minor, but variable, constituent of one or more

TABLE 3.9 Results of Bartlett's and Cochran's tests for homogeneity of variances of the Garnetiferous Pelitec G locations. For form of tests see Table 3.4.

	Original Data (27 specimens)		Data with interpolated values for 421K, 423K and 613K.	
Variable	Bartlett	Cochran	Bartlett	Cochran
SiO_2	-	- 2	-	- 6
TiO_2	-	- 7	-	- 6
Al_2O_3	-	- 2	-	- 6
MnO	-	- 2	-	- 3
ΣFe_2O_3	xx	- 1	-	- 1
MgO	-	- 2	-	- 1
CaO	x	x 2	-	- 5
Na_2O	x	- 7	x	- 7
K_2O	x	- 2	-	- 5
P_2O_5	-	- 7	-	- 1
Zr	x	xx 2	-	- 5
Y	-	- 2	-	- 4
Rb	x	- 2	-	- 5
Nb	xx	xx 2	-	- 3
Sr	-	- 2	-	- 5
Zn	-	- 5	-	- 5
Nd	-	- 3	-	- 3
Ce	-	- 3	-	- 2
Ba	-	- 2	-	- 3
La	-	- 3	-	- 3

xx indicates failure at the 1% significance level
x .. .. 5% .. ..
- no significant inhomogeneity
Numbers indicate locations with highest variance for that variable:
1=41.; 2=42. ; 3=43. ; 4=51. ; 5=52. ; 6=53. ; 7=61. ; 8=62. ; 9=63.

Variable	Mean Squares			F ratios	
	Traverses (MST)	Locations (MSL)	Specimens (MSS)	MST/MSL (2,6)	MSL/MSS (6,18)
SiO_2	3.41	9.21	5.86	.370	1.57
TiO_2	.0015	.0045	.0029	.333	1.55
Al_2O_3	.406	2.16	.879	.187	2.46 *
ΣFe_2O_3	1.47	1.20	.900	1.22	1.33
MnO	.0002	.0004	.0003	.500	1.33
MgO	.084	.098	.038	.852	2.57 *
CaO	.037	.091	.157	.412	.579
Na_2O	.624	.211	.250	2.96	.844
K_2O	.258	.299	.293	.862	1.02
P_2O_5	.0011	.0037	.0014	.297	2.64 *
Zr	3367.6	1559.1	2086.0	2.16	.747
Y	9.59	97.2	75.3	.098	1.29
Rb	30.3	155.2	160.9	.195	.965
Nb	4.93	12.78	6.37	.386	2.01
Sr	2214.1	253.9	1775.3	8.72**	.143
Zn	144.4	197.7	144.3	.730	1.37
Nd	189.8	354.7	333.3	.535	1.06
Ce	306.7	1033.6	944.6	.297	1.09
Ba	2601.4	39391.8	20546.0	.066	1.92
La	108.6	429.9	292.7	.253	1.47

TABLE 3.10 Results of analysis of variance, Garnetiferous Pelite, original data.

* - F ratio significant at 10% level
** - F ratio significant at 5% level
*** - F ratio significant at 1% level

Variance Components			Coefficients of Variation(%)		
Traverses	Locations	Specimens	Traverses	Locations	Specimens
-.644	1.11	5.86	0	1.75	4.00
-.0003	.0005	.0029	0	2.34	5.63
-.195	.143	.879	0	2.05	5.09
.029	.100	.904	2.14	3.97	11.9
.00002	.00003	.0003	3.78	4.41	13.9
-.002	.020	.038	0	5.96	8.22
-.006	-.022	.157	0	0	15.7
.046	-.013	.250	7.65	0	17.8
-.005	.002	.293	0	1.27	15.4
-.0003	.0008	.0014	0	9.10	12.0
200.9	-175.6	2086.0	7.40	0	23.8
-9.73	7.27	75.3	0	7.32	23.6
-13.9	-1.89	160.9	0	0	10.4
-.870	2.14	6.37	0	8.74	15.1
217.8	-507.2	1775.3	14.8	0	13.6
-5.92	17.8	144.3	0	3.68	10.5
-18.3	7.16	333.3	0	8.42	57.9
-80.8	29.6	944.6	0	5.94	33.5
-4087.8	6281.9	20546.0	0	8.64	15.6
-35.7	45.7	292.7	0	18.9	47.8

TABLE 3.10 (cont.) See text and Table 3.6 for details.

Variable	Mean Squares			F ratios	
	Traverses (MST)	Locations (MSL)	Specimens (MSS)	MST/MSL (2,6)	MSL/MSS (6,15)
SiO_2	1.13	3.16	2.56	.779	1.24
TiO_2	.0001	.0041	.0009	.024	4.14**
Al_2O_3	.249	.840	.609	.296	1.38
ΣFe_2O_3	.431	1.20	.576	.360	2.08
MnO	.0002	.0003	.0003	.666	1.00
MgO	.254	.101	.015	2.52	6.52***
CaO	.121	.039	.088	3.13	.436
Na_2O	.635	.217	.291	2.93	.745
K_2O	.292	.181	.201	1.61	.902
P_2O_5	0.00	.002	.0008	0	2.78 *
Zr	533.4	542.6	775.0	.983	.700
Y	60.1	107.9	55.2	.557	1.96
Rb	91.8	41.3	74.6	2.22	.554
Nb	1.81	2.19	1.42	.830	1.54
Sr	1714.1	276.1	1690.0	6.42**	.158
Zn	15.4	231.7	92.2	.067	2.51*
Nd	228.1	380.6	356.8	.599	1.07
Ce	508.0	1148.2	1031.0	.442	1.11
Ba	29723.4	31167.2	14947.7	.954	2.09
La	135.8	460.5	323.6	.295	1.42

TABLE 3.11 Results of analysis of variance, Garnetiferous Pelite, with interpolated values for 421K,423K and 613K.

* - F ratios significant at 10% level
** - F ratios significant at 5% level
*** - F ratios significant at 1% level

Variance Components			Coefficients of Variation (%)		
Traverses	Locations	Specimens	Traverses	Locations	Specimens
-.225	.201	2.56	0	.751	2.68
-.0004	.001	.001	0	3.22	3.15
-.065	.077	.609	0	1.48	4.18
-.085	.206	.576	0	5.51	9.21
-.00001	0	.0003	0	0	13.8
.017	.028	.015	5.35	6.91	5.09
.009	-.017	.088	3.81	0	11.9
.047	-.025	.291	7.70	0	19.2
.012	-.007	.201	3.05	0	12.3
0	.0005	.0008	0	6.74	8.74
-1.02	-77.5	775.0	0	0	15.3
-5.30	17.6	55.2	0	11.9	21.1
5.61	-11.1	74.6	1.88	0	6.85
-.041	.254	1.42	0	3.12	7.37
160.8	-474.1	1690.0	4.09	0	13.2
-24.0	46.5	92.2	0	5.80	8.16
-16.9	7.93	356.8	0	9.32	62.5
-71.1	39.1	1031.0	0	7.05	36.2
-160.4	5406.5	14947.7	0	7.89	13.1
-36.1	45.6	323.6	0	19.5	52.0

TABLE 3.11 (cont.) See text and Table 3.6 for details

TABLE 3.12 99% Confidence limits for Garnetiferous Pelite

(Sample size 27 items)

Variable	Original Data	Data with interpolated values for 421K,423K and 613K
SiO_2	60.51± 1.42	59.68± .82
TiO_2	.96± .03	.97± .01
Al_2O_3	18.43± .49	18.68± .39
ΣFe_2O_3	7.97± .94	8.25± .51
MnO	.12± .01	.13± .01
MgO	2.37± .22	2.44± .39
CaO	2.53± .22	2.51± .27
Na_2O	2.80± .61	2.81± .62
K_2O	3.51± .39	3.64± .42
P_2O_5	.31± .03	.32± .02
Zr	192± 45	182± 18
Y	37± 2	35± 6
Rb	122± 4	126± 7
Nb	17± 2	16± 1
Sr	310± 36	310± 32
Zn	115± 9	118± 3
Nd	32± 11	30± 12
Ce	92± 14	89± 17
Ba	918± 40	932±133
La	36± 8	35± 9

of the minerals present, or that variation at the between-localities level for other elements has not been detected through inadequacies in the analytical techniques employed.

The irregular distribution of TiO_2 may be a consequence of the skewness of the data, although separation of cause and effect cannot be made with certainty in this sort of situation.

Zn does show variation at the between-localities level, just exceeding the 10% significance level, but the distribution of Zn is markedly skewed, with some variance inhomogeneity, so the result can only be regarded as suspect.

Conclusions

The sampling design employed proved successful within its limitations, indicating that on the whole the disparities between individual samples provide the largest source of variation. Further investigation to break down this between-sample variation could be made, splitting samples before crushing to examine very small scale (within-sample) differences, and performing multiple analyses on the split samples to assess variations contributed by the analytical techniques employed.

Even though the variations were mainly at the lowest level interrogated, the analytical methods did prove adequate in detecting variations at the between-localities level for a number of variables in the Lochailort Pelitic Group, indicating uneven distribution of minerals through the unit across the original bedding. For the variables which show this variation (Al_2O_3, CaO, K_2O, P_2O_5, Zr, Rb, Ce and Ba) the number of samples at the between-specimen within-locality level would appear to be sufficient, but for the other variables a higher number of samples from each locality could reduce the variance at the lowest

level, possibly to reveal variations from the higher levels which are masked in this sampling design. Variations detected are small, and would be unlikely to have been detected by other means, since the very slight differences in mineralogy would probably not be discovered by techniques such as point counting of thin sections, or by analysis of samples without such rigorous statistical treatment of the results.

From this study it would appear that individual samples cannot be taken as very useful estimators of the group mean in the discriminant analysis study. A mean based on at least three, and preferably more, specimens would be more representative of the rock groups under consideration.

This sort of study of chemical variation within larger units provides a valuable background to any future mineralogical study, in which an assumption of constant rock bulk chemical composition cannot be made without some estimate of the form and magnitude of any variation that might be present. In addition, knowledge of the internal variations of a rock unit must be available before any generalisations can be made about lateral variations within that unit on a much larger scale, over distances of tens or even hundreds of kilometers.

Chapter 4. DISCRIMINANT FUNCTION EXPERIMENT

Introduction

One of the commonest problems in geology is that of distinguishing between two or more populations of objects (e.g. rock types, minerals, fossils) using observed, though not necessarily quantifiable, characters (e.g. colour, hardness, refractive index). Unknown samples may then be assigned to one of the defined populations on the basis of these characters, using them either singly or in combination. The linear discriminant function provides a numerical criterion which can be used in assigning unknown samples, the function being derived from measured characters for samples ("training groups") from the defined populations.

The method has already found use in geology in discriminating between different sedimentary environments, using both chemical composition of the sediments (Potter et al., 1963, Middleton 1962) and textural parameters (Huang et al. 1974, Tillman 1973), and is of particular value in economic geology, applied as a means of distinguishing barren from productive materials (Griffiths 1957, Emery & Griffiths 1954, Wood 1961).

In this study an attempt has been made to produce a discriminant function based on chemical composition between two major pelitic units in the Moine of the Morar area, the Lochailort Pelitic Group (as defined by Powell 1964), and the Garnetiferous Pelite of the Morar Striped and Pelitic Group (Unit 2b of Richey & Kennedy, 1939). This follows a suggestion by Johnstone et al. (1969, p.178) that in considering the Moine succession of Scotland geochemical similarities or differences between widespread pelitic units might be useful in helping to solve correlation problems. In the Morar area the stratigraphic succession is well established, and folding causes the pelites studied to outcrop repeatedly across the area, at differing metamorphic grades. (Fig. 4.1).

The samples taken as training groups for the two units were the 54 specimens collected and used in the analysis of variance experiment. Each of these was analysed by rapid XRF methods for twenty elements (ten major and ten trace constituents). Discriminant analysis was initially made on all twenty elements, but later concentrated on sixteen variables only (ten major and six trace elements) which were the quickest and simplest to determine.

As tests of the efficiency of the derived discriminant functions, a total of 45 random samples were taken from stratigraphically equivalent pelites over the area (Figure 4.1), and the functions used to try and assign them to their correct groups. For the Garnetiferous Pelite, samples were taken from its extension to the north in Morar Bay and to the south of the Sound of Arisaig around Glenuig and Smearisary, these outcrops all being at upper greenschist facies metamorphic grade. To the east, the Glen Mama Pelitic Group (lower amphibolite facies) and the Arieniskill Pelitic Group (sillimanite grade) were sampled as the equivalents of the Garnetiferous Pelite (Powell, 1964). The Lochailort Pelite was sampled along the strike north and south of the training group area (all lying at kyanite grade), and in its equivalents to the east around Ranochan, called for convenience the East Ranochan Pelite and the West Ranochan Pelite, and both at upper sillimanite grade. This widespread random sample was used to assess the usefulness of the functions as an elementary form of "chemical stratigraphy", and that the variation in metamorphic grade did not have any disruptive effects upon the validity of the functions.

In addition, 4 samples were taken from the Basal Pelite of the Morar Moine succession in its outcrop along Beasdale Burn, and 8 from a pelite lying above the Lochailort Pelite in the succession and called

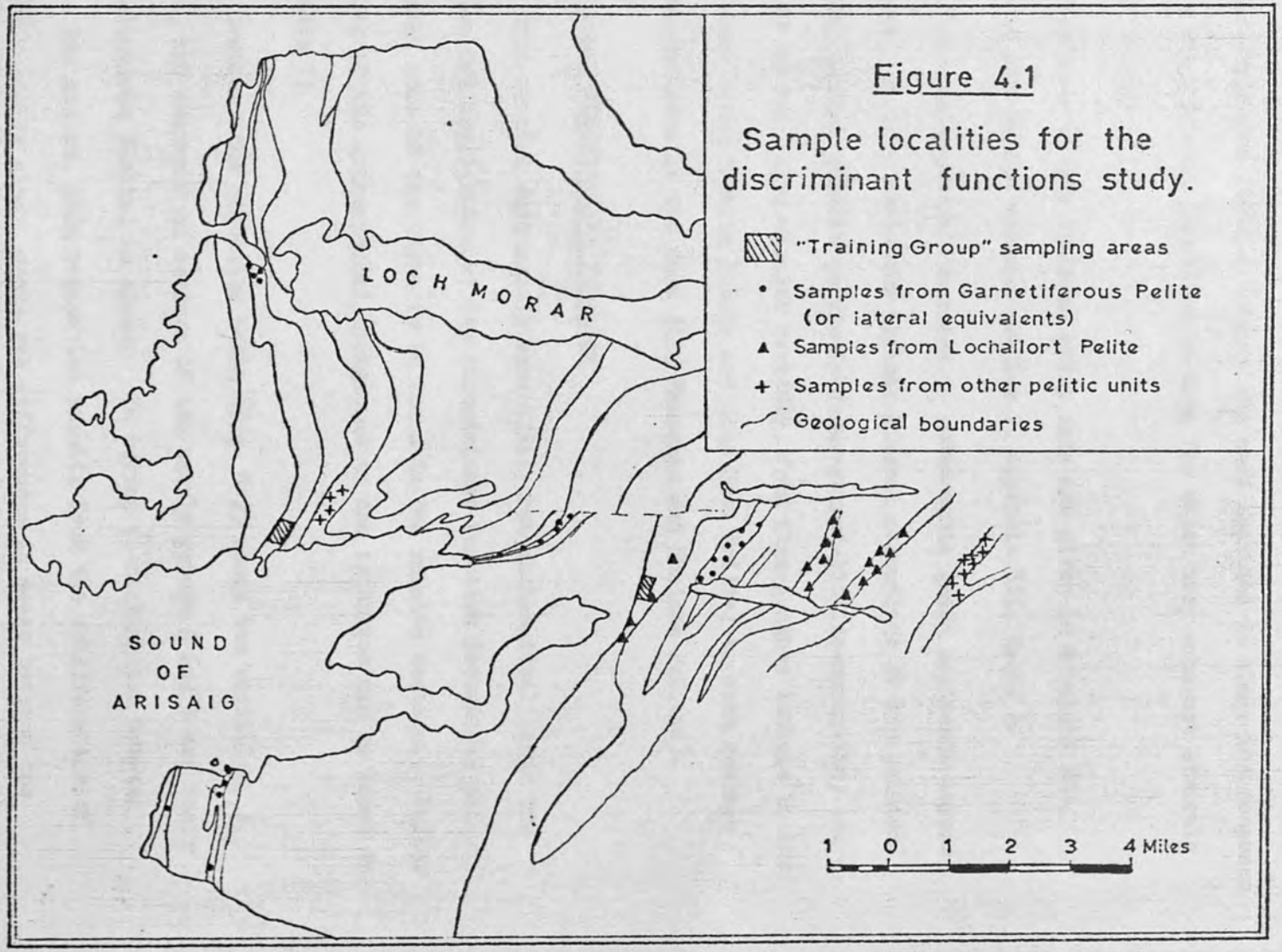

Figure 4.1

Sample localities for the discriminant functions study.

"Training Group" sampling areas

Samples from Garnetiferous Pelite (or lateral equivalents)

Samples from Lochailort Pelite

Samples from other pelitic units

Geological boundaries

here the Mhuidhe Pelite after its area of occurrence. These two pelites are known not to be equivalent to either the Lochailort or the Garnetiferous Pelitic Groups, and were included to study the response of the discriminant functions to data for which they were not strictly valid.

Analyses of the training group data are given in Appendix III, Table 1, and of the unknown samples in Appendix III, Table 2.

There is a general increase in metamorphic grade eastwards across the area, so that while the typical mineral assemblage of the pelites and semipelites remains quartz-feldspar-garnet-biotite-muscovite, the texture of the rocks changes markedly, from fine-grained schists in the west (the Garnetiferous Pelite and Glen Mama Pelite) to much coarser banded gneisses in the east (the Ranochan and Mhuidhe Pelites).

The linear discriminant function

This section outlines in essentially non-mathematical terms the meaning and application of the discriminant function technique, and explains some of the terms to be found in the results section. Fuller details of the mathematical background to the technique can be found in Appendix II.

Consider the situation shown (Fig. 4.2) where two variables, X_1 and X_2 are measured on members of two sample groups A and B and their distributions plotted as shown. In trying to distinguish between these two groups, poor separation results from the consideration of either variable alone, since the differences in means between the groups are small and the overlaps of the ranges large. However, a third variable axis Z can be drawn, which gives very good separation of the two groups by consideration of X_1 and X_2 together. For a simple two-variable case such as this, Z can be derived empirically,

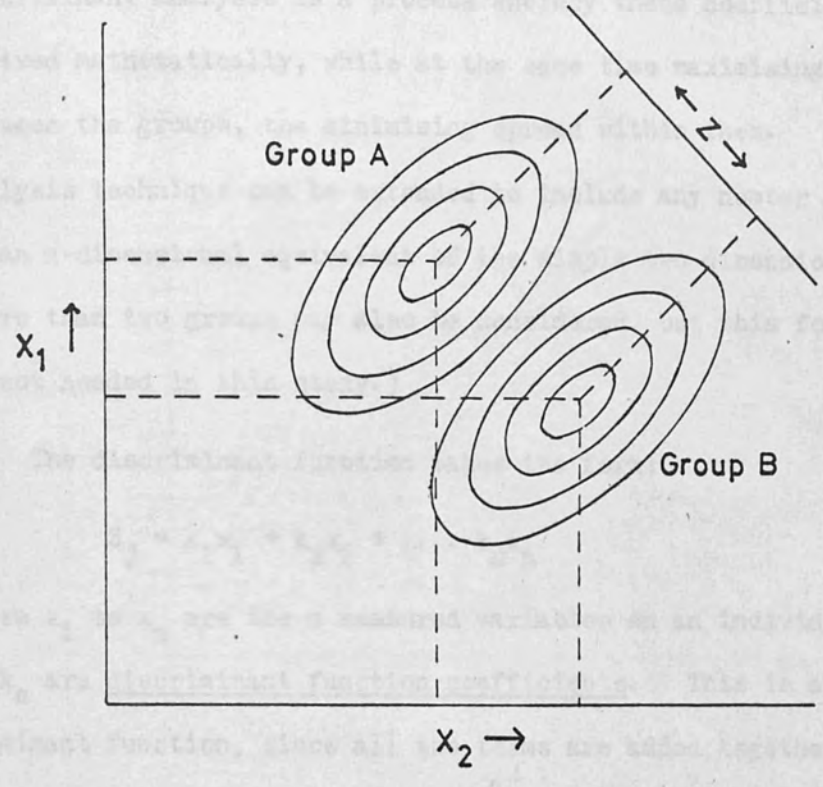

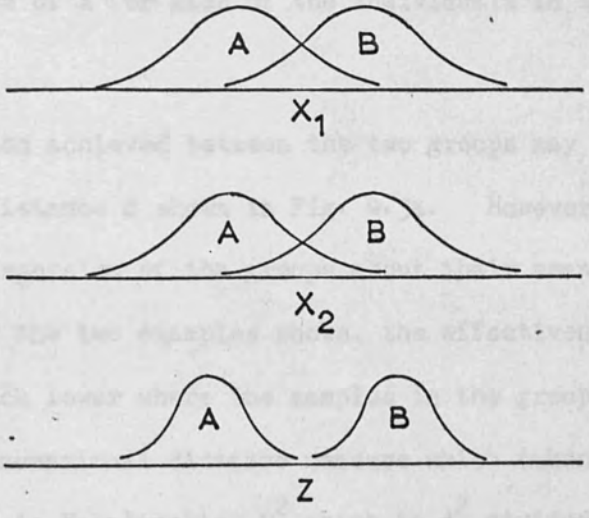

Figure 4.2 Relation between two variables, X_1 and X_2, and linear discriminant, Z, for two groups, A and B.

and the coefficients for the co-ordinates of Z found graphically. Discriminant analysis is a process whereby these coefficients can be derived mathematically, while at the same time maximising separation between the groups, the minimising spread within them. Further, the analysis technique can be extended to include any number of variables in an n-dimensional equivalent of the simple two-dimensional problem. (More than two groups may also be considered, but this form of analysis is not needed in this study.)

The discriminant function takes the form:

$$Z_j = k_1x_1 + k_2x_2 + \dots k_nx_n$$

where x_1 to x_n are the n measured variables on an individual, j, and k_1 to k_n are discriminant function coefficients. This is a linear discriminant function, since all the terms are added together to yield a single number z_j, the discriminant score for individual j. The mathematical analysis finds the values of the discriminant function coefficients using the n values of x for each of the individuals in the two sample training groups.

The separation achieved between the two groups may be measured by calculating the distance d shown in Fig. 4.3a. However, d takes no account of the dispersion of the groups about their means, so although d is the same for the two examples shown, the effectiveness of the discrimination is much lower where the samples in the group are more scattered. A conventional distance measure which takes account of sample dispersion is Mahalanobis' D^2 which is d^2 divided by the average dispersion of the items. The smaller the sample dispersion, the larger D^2 becomes so that in Fig. 4.3 D^2 in situation (a) is much larger than in situation (b).

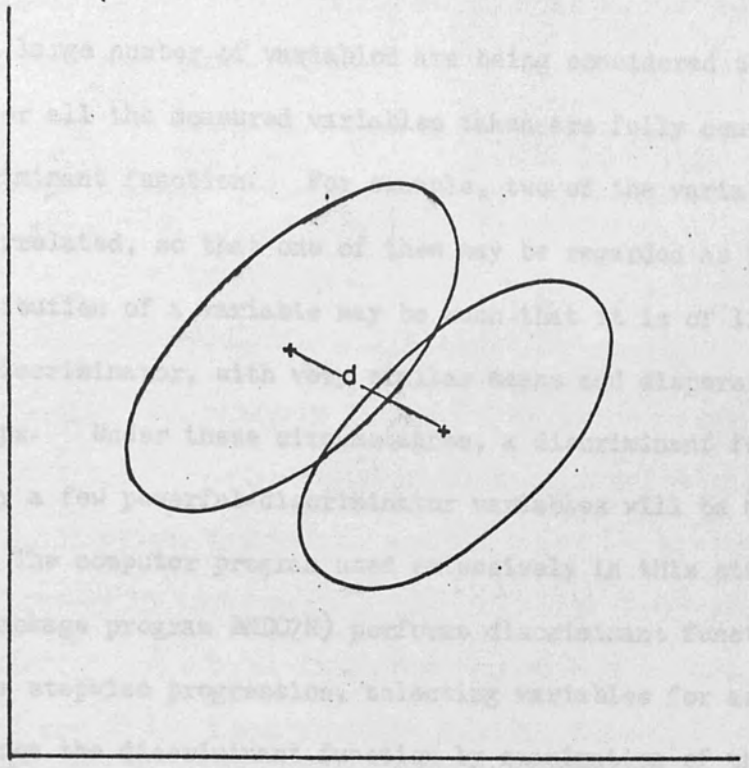

4.3a

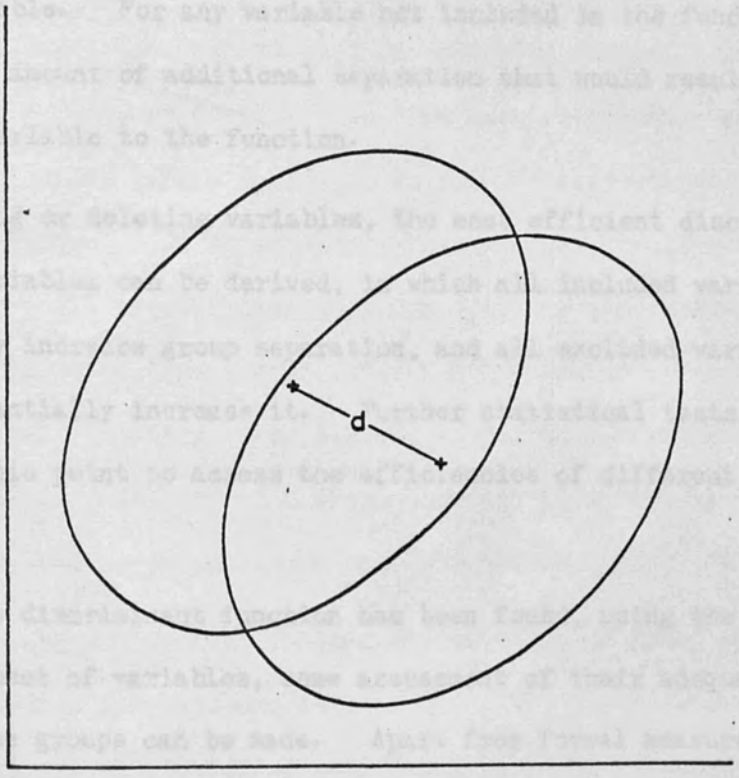

4.3b

Figure 4.3 Inadequacy of d as a measure of group separation (see text for details)

Where a large number of variables are being considered the problem arises whether all the measured variables taken are fully contributing to the discriminant function. For example, two of the variables may be highly correlated, so that one of them may be regarded as redundant; or the distribution of a variable may be such that it is of little value as a discriminator, with very similar means and dispersions for the two groups. Under these circumstances, a discriminant function based on only a few powerful discriminator variables will be more efficient. The computer program used extensively in this study (UCLA Biomedical Package program BMD07M) performs discriminant function analysis by a stepwise progression, selecting variables for addition to, or removal from the discriminant function by examination of their associated F-statistic. For each variable included in the discriminant function F is a measure of the amount of group separation attributable to that variable. For any variable not included in the function F measures the amount of additional separation that would result from adding the variable to the function.

By adding or deleting variables, the most efficient discriminator subset of variables can be derived, in which all included variables substantially increase group separation, and all excluded variables cannot substantially increase it. Further statistical tests can be applied at this point to assess the efficiencies of different sized subsets.

Once the discriminant function has been found, using the most efficient subset of variables, some assessment of their adequacy in separating the groups can be made. Apart from formal measures of statistical significance a simple method is to treat the items used in the analysis as unknowns, and then use the derived discriminant function to assign each in turn to that group to which it is closest. This is

done by calculating Z for each item and considering D^2 for each item from the centre of each group. The group centre to which the item is nearest is the group to which that item is assigned. The percentage of items correctly assigned indicates the power of the discriminant function.

Results of the discriminant function analysis

Twenty elements were analysed for in the 27 samples from each of the units. Of these twenty elements, ten are major constituents, expressed as oxide weight per cents., and the other ten are trace constituents, expressed in parts per million. The ten major element oxides (SiO_2,TiO_2,Al_2O_3, total iron as Fe_2O_3, MnO, MgO, CaO, Na_2O, K_2O, P_2O_5) and six of the trace elements (Nb, Zr, Rb, Sr, Y, Zn) are all analysed using a silver-target X-ray tube in two pre-set programs totalling some $3\frac{1}{2}$ hours running time (full details of analytical conditions are given in the chapter on sample preparation). The other four trace elements (Ba, La, Nd, Ce) are analysed using a tungsten-target tube, needing 2 hours of machine time, and requiring prior analysis of major element oxides before full mass absorption corrections can be made to the results. In consequence, the data was considered under two groupings - all twenty elements taken together (the largest and costliest in terms of time and effort), and the sixteen elements which conveniently fall together, i.e. ten majors and six Nb-Zr group trace elements. In addition, the ten major elements alone and the six Nb-Zr traces alone were considered, as independent sets of data.

For all twenty elements, initial calculations of mean, variance, standard deviation and skewness were made for the two groups. When all 27 samples were included for each unit, skewness values were very high, indicating that assumptions of normality in the distributions of most variables were unrealistic. On inspection, two of the data

TABLE 4.1A

Means, standard deviations and skewness coefficients for samples of the Garnetiferous Pelite. Original sample size 27 items, 3 of which were removed to reduce skewness in the data, giving a sample of 24 items.

	27 items			24 items		
Variable	Mean	Standard Deviation	Skewness	Mean	Standard Deviation	Skewness
SiO_2	60.51	2.54	1.16**	59.78	1.52	.10
TiO_2	.96	.06	-.99**	.97	.04	-.29
Al_2O_3	18.43	1.07	-.44	18.70	.78	.66
ΣFe_2O_3	7.97	1.01	.44	8.19	.82	-.35
MnO	.12	.02	-.42	.13	.02	-.57
MgO	2.37	.24	-.69*	2.41	.22	-.98*
CaO	2.53	.36	.98*	2.51	.28	-.43
Na_2O	2.80	.52	-.55	2.82	.54	-.63
K_2O	3.51	.54	-.93*	3.61	.44	-.48
P_2O_5	.31	.04	-.76*	.32	.03	-.73*
Zr	191	45.4	2.77**	183	26.1	.61
Y	37	8.7	.74*	36	7.8	.86*
Rb	122	12.2	-1.56**	125	7.8	-.94*
Nb	17	2.8	3.23***	16	1.3	-.19
Sr	310	38.2	.63	311	36.1	.69
Zn	115	12.5	-.97**	117	10.7	-1.21**
Nd	32	18.1	-.07	30	18.3	.05
Ce	92	30.3	-.18	90	30.9	-.07
Ba	918	153.3	-.65	936	137.5	-.25
La	36	17.6	.23	36	17.9	.35

* - greater than 5% significant
** -greater than 1% significant

TABLE 4.1B

Means, standard deviations and skewness coefficients for samples of the Lochailort Pelitic Group. Original sample size 27 items, 2 of which were removed to reduce skewness in the data, giving a sample of 25 items.

	27 items			25 items		
Variable	Mean	Standard Deviation	Skewness	Mean	Standard Deviation	Skewness
SiO_2	61.14	3.38	1.92**	60.33	1.79	.14
TiO_2	.98	.15	-1.43**	1.01	.09	-.21
Al_2O_3	18.56	1.40	-1.49**	18.87	.90	-.55
ΣFe_2O_3	7.65	1.40	-1.40**	7.97	.87	.21
MnO	.12	.02	-1.18**	.12	.02	.89*
MgO	2.19	.32	-1.65**	2.26	.20	-.60
CaO	2.08	.54	-.43	2.12	.47	.12
Na_2O	2.60	.59	.33	2.61	.54	.54
K_2O	3.36	.88	.44	3.33	.71	.09
P_2O_5	.23	.05	-1.20**	.24	.03	-.48
Zr	228	58.4	.93*	221	49.4	.33
Y	54	11.3	-.36	56	9.8	-.26
Rb	144	22.6	-.73*	146	19.7	-.25
Nb	19	3.1	-.73*	20	2.5	-.38
Sr	257	41.7	.26	257	41.9	.28
Zn	119	23.9	-1.06**	124	16.5	.05
Nd	44	12.2	-.55	45	11.8	-.55
Ce	118	30.8	-.29	120	30.6	-.47
Ba	748	220.3	.52	736	189.9	.08
La	49	13.9	-.35	50	13.7	-.52

* - greater than 5% significant

** - greater than 1% significant

points in the Lochailort Pelitic Group, and three data points in the Garnetiferous Pelite caused most of the skewness in each group and removal of these points gave good approximations to unskewed distributions for the two groups for the remaining samples. Since approximation to normality is a necessary assumption for discriminant function analysis, the two reduced groups were compared to each other, as well as attempting discrimination on the original full sample groups. Skewness values were also calculated for logarithm values of the trace elements, both for the original and reduced groups. No improvement in skewness values were obtained, so these values were not considered further.

The results are therefore considered under the following groupings:

1) Two sample groups, 27 items in each group.
   a) 16 variables
   b) 20 variables
   c) 10 major element oxides
   d) 6 Nb-Zr trace elements

2) Two groups of sample size 25 (L.P.G.) and 24 (G.P.)
   a) 16 variables
   b) 20 variables
   c) 10 major element oxides
   d) 6 Nb-Zr trace elements

Results

1) Two groups, 27 samples in each group

(a) 16 variables (10 major element oxides, 6 Nb-Zr group trace elements). The data used in this case does not fit the mathematical requirements of the method well, because of skewness produced by outlying data points. However, the over-all variation of the groups is better represented, so the use of this data is justifiable in geological rather than mathematical terms.

Figure 4.4 shows graphically the increase in D^2 for the discriminant subset as variables are added to it, and results are tabulated in Table 4.2. The significant steps are outlined below:

Step 1 - P_2O_5 is taken into the discriminant subset as the most significant variable. Using P_2O_5 alone as a discriminator 45 of the 54 items can be assigned to their correct groups. Misclassification probability given by D/2 is greater than 10%. F statistic significantly much higher than 99.95%.

Step 2 - Zn added to the subset. Only 4 of the original 54 are misclassified using these two variables. D/2 indicates probability of misclassification about 5%

Step 3 - Rb added - only 2 now misclassified.

Step 4 - K_2O added - all the original data items can now be assigned to their correct groups, and probability of misclassification has dropped to less than 1%.

Step 5 - Y added to the subset. Misclassification probability now less than 0.5%.

Step 6 - Zn removed from the discriminator subset, as its contribution to the group separation has dropped to a very low level. (Zn is only introduced again into the discriminant subset at step 17, as the 15th variable to be taken.) At this point the F statistic for separation significance rises sharply, but D^2 is little changed, despite there being fewer variables in the subset. Of the unknown samples, only three are incorrectly assigned on the basis of the discriminant function at this point (498, 556 & 558 - these three rocks have unusual compositions and are consistently misclassified by different discriminant functions).

TABLE 4.2

Results of stepwise discriminant function analysis on data from the Lochailort Pelitic Group (27 items in sample) and the Garnetiferous Pelite (27 items in sample). At each step is given the variable added to the discriminant function, and the associated F statistic and value of Mahalanobis' D^2 (see text for fuller explanation)

Number of Variables in function	Variable added at this step	F ratio	Mahalanobis' D^2
1	P_2O_5	44.1	3.27
2	Zn	61.6	9.31
3	Rb	56.6	13.08
4	K_2O	77.4	24.35
5	Y	75.6	30.33
4	Zn removed	96.5	30.33
5	Nb	90.4	36.27
6	MnO	80.4	39.55
7	CaO	71.3	41.80
8	Na_2O	63.4	43.39
9	Sr	59.3	46.75
10	Zr	55.8	49.99
11	TiO_2	50.9	51.38
12	SiO_2	46.8	52.79
13	MgO	42.4	53.05
14	ΣFe_2O_3	38.5	53.27
15	Zn	35.1	53.41
16	Al_2O_3	32.1	53.41

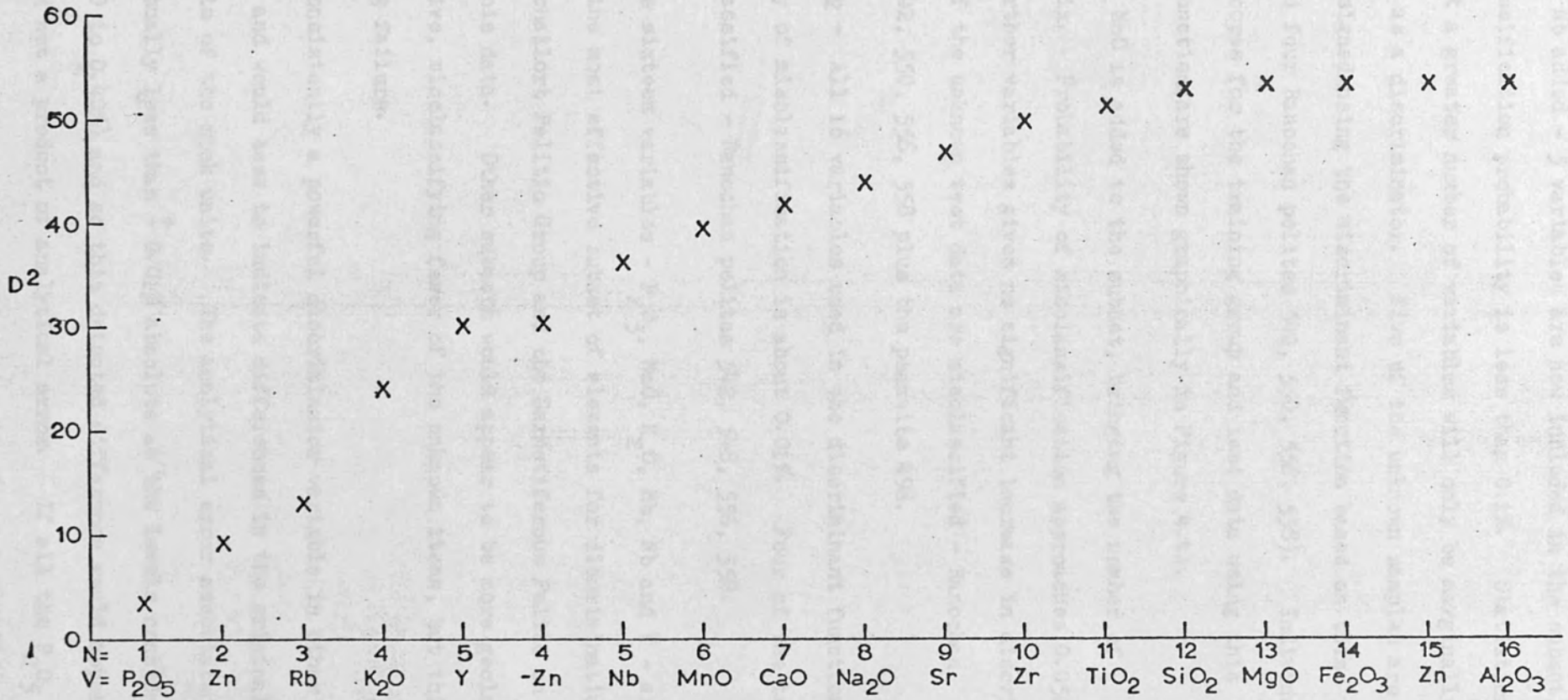

Figure 4.4 Changes in Mahalanobis' D^2 for subsets of N variables from 16, total sample size 54. Data from Table 4.2 . V = variable added to (or subtracted from) subset.

Step 7 - Nb added - 5 variables are now included in the subset, and the misclassification probability is less than 0.1%. Statistical tests show that a greater number of variables will only be marginally more efficient as a discriminator. Five of the unknown samples are incorrectly assigned using the discriminant function based on this subset (353 and four Ranochan pelites 542, 550, 556, 558). Individual discriminant scores for the training group and test data using this discriminant function are shown graphically in Figure 4.4A.

Step 8 - MnO is added to the subset, bringing the number of variables to six. Probability of misclassification approaches 0.05%. Addition of further variables gives no significant increase in discrimination. Five of the unknown test data are misclassified - Ranochan pelites 541, 542, 550, 556, 558 plus the psammite 498.

Final step - All 16 variables used in the discriminant function, and probability of misclassification is about 0.01%. Four of the test data are misclassified - Ranochan pelites 542, 548, 556, 558.

Six of the sixteen variables - P_2O_5, MnO, K_2O, Rb, Nb and Y - are statistically the most effective subset of elements for discrimination between the Lochailort Pelitic Group and the Garnetiferous Pelite on the basis of this data. Other subsets would appear to be more geologically effective, misclassifying fewer of the unknown items, but this may be sampling failure.

P_2O_5 is consistently a powerful discriminator variable in other data groupings and would seem to indicate differences in the original apatite contents of the rock units. The analytical error associated with P_2O_5 is usually less than $\pm$ 0.01% absolute at the levels considered here (i.e. 0.10 to 0.40%) and so this detected difference would appear to be real, and not a product of analytical error. If all the P_2O_5 is held in apatite, then the mean apatite content of the Garnetiferous

Figure 4.4A Individual discriminant scores for subset of 5 best variables from 16; training group sample sizes 27(Lochailort Pelite) and 27(Garnetiferous Pelite). The discriminant function used is:-

$$Z = .42Y + .683\ Rb - 1.01\ Nb - 10.85\ K_2O - 179.1\ P_2O_5$$

Z_g is the mean discriminant score of the Garnetiferous Pelite training group sample, and Z_l that for the Lochailort Pelite.

▼ indicates a sample group mean discriminant score. Scores to the left of the discriminant boundary, Z_0 , show similarity to the Garnetiferous Pelite, those to the right show similarity to the Lochailort Pelite.

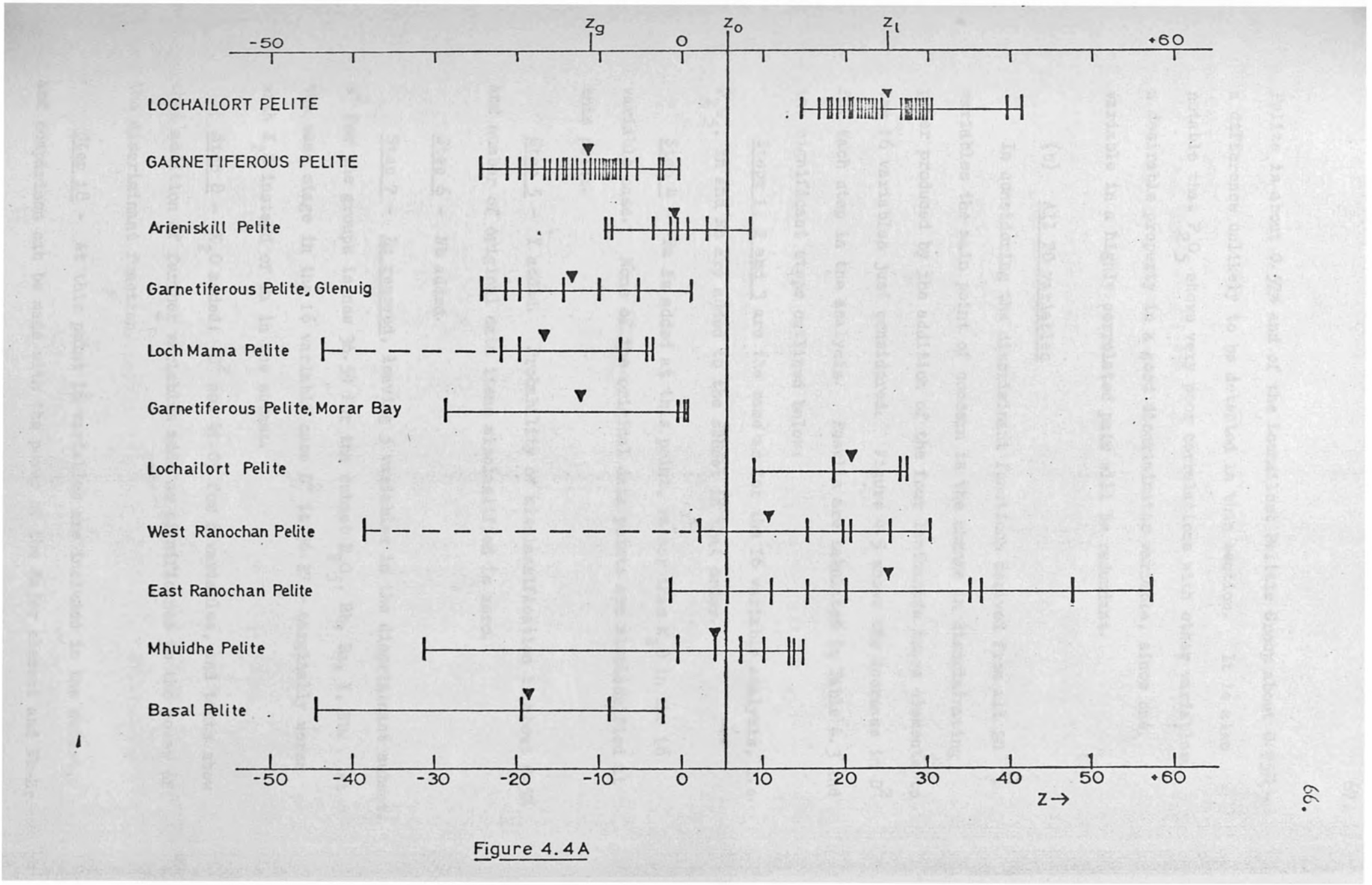
Z_g
Z_o
Z_l
-50
0
+60
LOCHAILORT PELITE
GARNETIFEROUS PELITE
Arieniskill Pelite
Garnetiferous Pelite, Glenuig
Loch Mama Pelite
Garnetiferous Pelite, Morar Bay
Lochailort Pelite
West Ranochan Pelite
East Ranochan Pelite
Mhuidhe Pelite
Basal Pelite
-50
-40
-30
-20
-10
0
10
20
30
40
50
+60
Z→

Figure 4.4A

Pelite is about 0.57% and of the Lochailort Pelitic Group about 0.75% - a difference unlikely to be detected in thin section. It is also notable that P_2O_5 shows very poor correlations with other variables, a desirable property in a good discriminator variable, since one variable in a highly correlated pair will be redundant.

(b) All 20 variables

In considering the discriminant functions derived from all 20 variables the main point of concern is the change in discriminating power produced by the addition of the four lanthanide trace elements to the 16 variables just considered. Figure 4.5 shows the increase in D^2 for each step in the analysis. Results are tabulated in Table 4.3 and the significant steps outlined below:

Steps 1, 2 and 3 are the same as for the 16 variable analysis, i.e. P_2O_5, Zn and Rb are added to the subset in that order.

Step 4 - Ba is added at this point, rather than K_2O in the 16 variable case. None of the original data points are misclassified at this point.

Step 5 - Y added. Probability of misclassification is about 0.5% and number of original data items misclassified is zero.

Step 6 - Nb added.

Step 7 - Zn removed, leaving 5 variables in the discriminant subset. D^2 for the groups is now 36.54 for the subset P_2O_5, Rb, Ba, Y, Nb. At the same stage in the 16 variable case D^2 is 36.27 - marginally worse with K_2O instead of Ba in the subset.

Step 8 - K_2O added: D^2 now 41.09 for 6 variables, and tests show that addition of further variables adds no significance to the power of the discriminant function.

Step 18 - At this point 16 variables are included in the subset, and comparison can be made with the power of the Major element and Nb-Zr

TABLE 4.3

Results of stepwise linear discriminant function analysis on data from The Garnetiferous Pelite (27 items in sample) and the Lochailort Pelitic Group (27 items in sample). At each step is given the variable added to the discriminant function, and the associated F statistic and value of Mahalanobis' D^2 (see text for explanation of terms)

Number of variables in function	Variable added at this step	F ratio	Mahalanobis' D^2
1	P_2O_5	44.1	3.27
2	Zn	61.6	9.31
3	Rb	56.6	13.08
4	Ba	83.7	26.30
5	Y	77.4	31.05
6	Nb	74.3	36.54
5	Zn removed	91.1	36.54
6	K_2O	83.6	41.09
7	MnO	74.6	43.70
8	CaO	67.5	46.25
9	Zr	61.2	48.24
10	Sr	54.8	49.12
11	Na_2O	52.1	52.59
12	ΣFe_2O_3	47.9	54.05
13	Nd	44.1	55.21
14	MgO	40.1	55.48
15	SiO_2	37.1	56.47
16	TiO_2	34.1	56.91
17	Ce	31.4	57.10
18	La	28.9	57.34
19	Al_2O_3	26.7	57.47
20	Zn	24.6	57.51

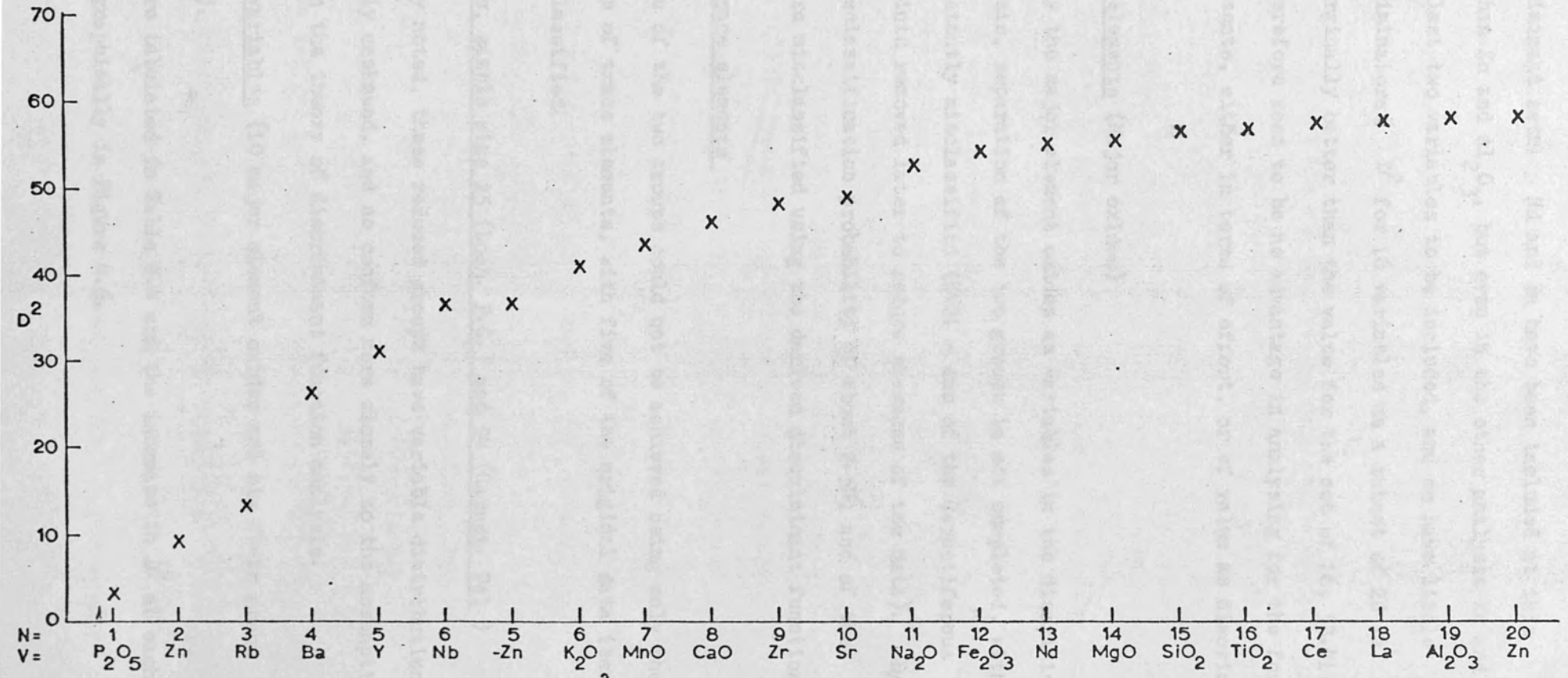

Figure 4.5 Changes in Mahalanobis' D^2 for subsets of N variables from 20, total sample size 54.(from Table 4.3)

group as discriminant sets. Nd and Ba have been included at this point rather than Zn and Al_2O_3, but even in the other analysis Zn and Al_2O_3 are the last two variables to be included, and so have little value as discriminators. D^2 for 16 variables as a subset of 20 is 56.91, only marginally better than the value for the set of 16, 53.41. There would therefore seem to be no advantage in analysing for the four lanthanide elements, either in terms of effort, or of value as discriminators.

(c) 10 elements (Major oxides)

Using only the major element oxides as variables in the discriminant function analysis, separation of the two groups is not completed, with one item consistently misclassified (K421 - one of the Garnetiferous Pelite data points removed later to reduce skewness of the data). D/2 indicates a misclassification probability of about 2.5%, and of the unknowns, 13 are misclassified using the derived discriminant function.

(d) 6 trace elements

Separation of the two groups could not be achieved using only the six Nb-Zr group of trace elements, with five of the original data items remaining misclassified.

2) Two groups, sample size 25 (Loch. P.G.) and 24 (Garnet. Pel.)

As already noted, these reduced groups have variable distributions which are mostly unskewed, and so conform more closely to the assumptions of normality in the theory of discriminant function analysis.

(a) 16 variables (10 major element oxides and six Nb-Zr group trace elements).

Results are tabulated in Table 4.4 and the increase in D^2 at each step is shown graphically in Figure 4.6.

Step 1 - P_2O_5 taken into subset as the single most powerful discriminant variable. Only 5 of the 49 data items are misclassified on the basis of P_2O_5 content alone. Probability of misclassification slightly greater than 10%.

Step 2 - Y added, and all the original 40 data points can be correctly assigned on these two variables alone. D/2 indicates misclassification probability of under 2.5%.

Step 3 - MgO added to subset.

Step 4 - Rb added to subset. Misclassification probability less than 0.5%.

Step 5 - K_2O taken into the subset. 4 of the first 5 variables are the same as for the groups based on 54 data points. Misclassification probability is less than 0.05%, but of the test data six are wrongly assigned, 353 (Ar.P.G.) and 5 Ranochan pelites, although the mean score of the Ranochan pelites is correctly assigned and close to the Lochailort Pelite group mean score. F tests on additional variables show that six variables will discriminate marginally better than these five, and that discrimination will increase to nine variables and beyond. Discriminant scores for the training groups and the test data at this point are shown graphically in Figure 4.6A.

Step 9 - Iron as total Fe_2O_3 is added to the subset (MnO, TiO_2, Sr have been included). D/2 indicates misclassification probability is much less than 0.01%. Of the test data, 352 (Ar.P.G.) and 8 of the Ranochan area pelites are incorrectly assigned, although again the mean discriminant score for the Ranochan area pelites is correctly close to the Lochailort Pelite mean score, F tests show that these 9 variables provide the best discriminant and that nothing is gained by adding further variables, although fewer will cause a reduction in the power of the discriminant.

TABLE 4.4

Results of stepwise linear discriminant function analysis on data from the Garnetiferous Pelite (24 items in sample) and the Lochailort Pelitic Group (25 items in sample). At each step is given the variable added to the discriminant function, and the associated F statistic and value of Mahalanobis' D^2 (see text for explanation of terms)

Number of variables in function	Variable added at this step	F ratio	Mahalanobis' D^2
1	P_2O_5	76.9	6.28
2	Y	92.5	15.43
3	MgO	93.1	23.81
4	Rb	78.1	27.25
5	K_2O	100.8	44.97
6	MnO	90.3	49.52
7	TiO_2	87.9	57.60
8	Sr	85.5	65.63
9	ΣFe_2O_3	87.8	77.79
10	Zr	81.6	82.45
11	Al_2O_3	76.1	86.87
12	CaO	69.9	89.56
13	Na_2O	63.2	90.13
14	SiO_2	57.3	90.54
15	Nb	52.0	90.73
16	Zn	47.3	90.87

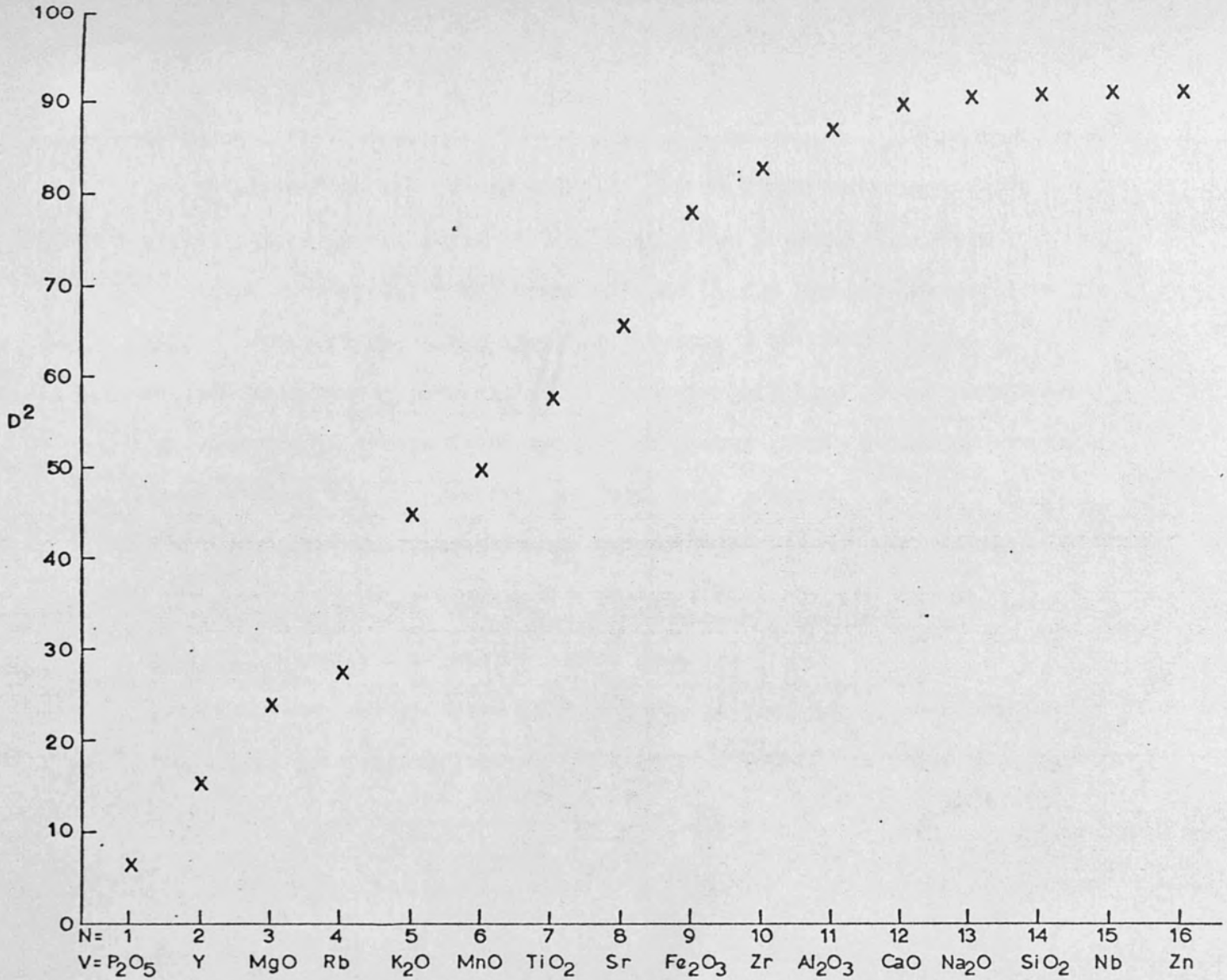

Figure 4.6 Changes in Mahalanobis' D^2 for subsets of N variables from 16, total sample size 49. Data from Table 4.4

Figure 4.6A Individual discriminant scores for subset of 5 best variables from 16; training group sample sizes 25(Lochailort Pelite) and 24(Garnetiferous Pelite). The discriminant function used is:-

$$Z = 18.42\ MgO - 12.91\ K_2O - 267.45\ P_2O_5 + .51\ Y + .57\ Rb$$

Z_g is the mean discriminant score of the Garnetiferous Pelite training group sample, and Z_1 that for the Lochailort Pelite.

▼ indicates a sample group mean discriminant score. Scores to the left of the discriminant boundary, Z_0 , show similarity to the Garnetiferous Pelite, those to the right similarity to the Lochailort Pelite.

Using this discriminant function, two of the samples removed from the Garnetiferous Pelite training group, 423K and 613K fall into the field of the Lochailort Pelite training group, having discriminant scores of 28.4 and 55.6 respectively. The samples removed from the training groups are marked by X .

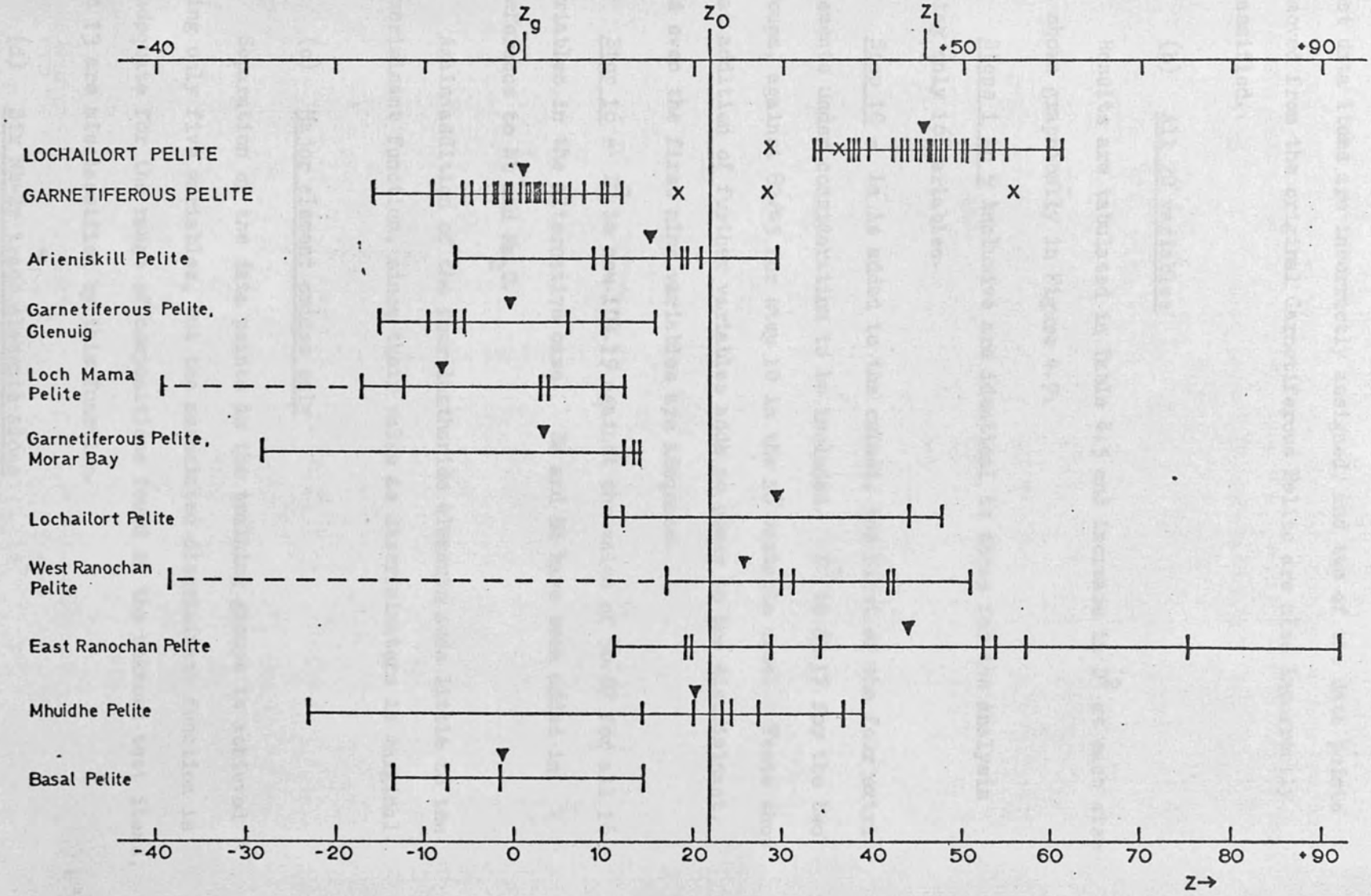
Z_g
Z_o
Z_l
-40
0
+50
+90
LOCHAILORT PELITE
GARNETIFEROUS PELITE
Arieniskill Pelite
Garnetiferous Pelite, Glenuig
Loch Mama Pelite
Garnetiferous Pelite, Morar Bay
Lochailort Pelite
West Ranochan Pelite
East Ranochan Pelite
Mhuidhe Pelite
Basal Pelite
-40 -30 -20 -10 0 10 20 30 40 50 60 70 80 +90
Z→

Figure 4.6A

Step 16 - All variables included in the function. Ten of the test data items are incorrectly assigned, and two of the data points removed from the original Garnetiferous Pelite are also incorrectly classified.

(b) All 20 variables

Results are tabulated in Table 4.5 and increase in D^2 at each step is shown graphically in Figure 4.7.

Steps 1 to 9 inclusive are identical to those for the analysis using only 16 variables.

Step 10 - La is added to the subset, the first of the four extra elements under consideration to be included. D^2 is 83.17 for the two groups, against 82.45 for step 10 in the 16 variable case. Tests show that addition of further variables adds no power to the discriminant, and even the first nine variables are adequate.

Step 16 - D^2 is now 104.19 against the value of 90.87 for all 16 variables in the alternative case. Ba and Nd have been added in preference to Nb and Na_2O.

Again addition of the four lanthanide elements adds little to the discriminant function, since their value as discriminators is marginal.

(c) Major element oxides only

Separation of the data points in the training groups is achieved using only five variables, but the associated discriminant function is inadequate for the range of compositions found in the unknown test items, and 13 are misclassified by this function.

(d) Six Nb-Zr trace elements alone

These six variables alone cannot produce an adequate discriminant for the training groups, separation of the two groups remaining incomplete after addition of all six elements to the discriminant function.

TABLE 4.5

Results of stepwise linear discriminant function analysis on data from the Garnetiferous Pelite (24 items in sample) and the Lochailort Pelitic Group (25 items in sample). At each step is given the variable added to the discriminant function, and the associated F statistic and value of Mahalanobis' D^2. (see text for explanation of terms)

Number of variables in function	Variable added at this step	F ratio	Mahalanobis' D^2
1	P_2O_5	76.9	6.28
2	Y	92.5	15.43
3	MgO	93.1	23.81
4	Rb	78.1	27.25
5	K_2O	100.8	44.97
6	MnO	90.3	49.52
7	TiO_2	87.9	57.60
8	Sr	85.5	65.63
9	ΣFe_2O_3	87.8	77.78
10	La	82.3	83.17
11	Zr	79.6	90.88
12	Ba	75.8	96.96
13	CaO	69.9	99.61
14	Al_2O_3	64.9	102.62
15	SiO_2	59.4	103.69
16	Nd	54.2	104.19
17	Ce	49.8	104.89
18	Nb	45.6	105.05
19	Na_2O	41.9	105.25
20	Zn	38.4	105.39

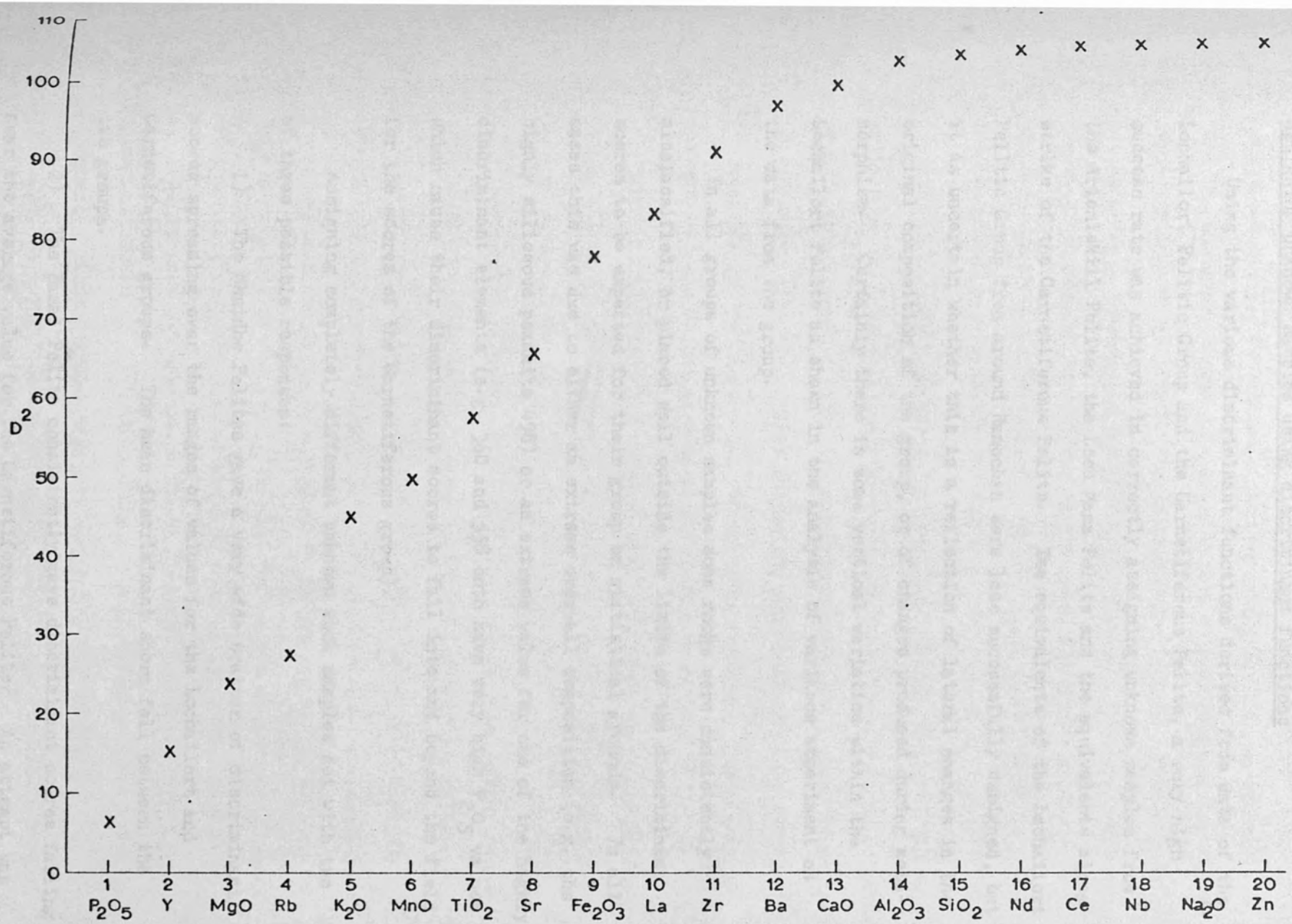

Figure 4.7 Changes in Mahalanobis' D^2 for subsets of N variables from 20, total sample size 49.
(Data from Table 4.5)

Assigning unknown samples using discriminant functions

Using the various discriminant functions derived from data of the Lochailort Pelitic Group and the Garnetiferous Pelite, a very high success rate was achieved in correctly assigning unknown samples from the Arieniskill Pelite, the Loch Mama Pelite and the equivalents along strike of the Garnetiferous Pelite. The equivalents of the Lochailort Pelitic Group from around Ranochan were less successfully assigned, but it is uncertain whether this is a reflection of lateral changes in the original composition of the group, or of changes produced during metamorphism. Certainly there is some vertical variation within the Lochailort Pelite as shown in the analysis of variance experiment on the data from the group.

In all groups of unknown samples some rocks were consistently misclassified, or placed well outside the limits of the discriminant scores to be expected for their group on statistical grounds. In all cases this was due to either an extreme over-all composition (e.g. the highly siliceous psammite 498) or an extreme value for one of the highly discriminant elements (e.g. 360 and 558 both have very high P_2O_5 values which cause their discriminant scores to fall into and beyond the field for the scores of the Garnetiferous group).

Assigning completely different unknown rock samples met with two of three possible responses:

1) The Mhuidhe Pelites gave a very wide scatter of discriminant scores spreading over the ranges of values for the Lochailort and Garnetiferous groups. The mean discriminant score fell between the two groups.

2) The Basal Pelite consistently gave discriminant scores falling near the average value for the Garnetiferous Pelite. An attempt was

made at stepwise discriminant function analysis between the four Basal Pelite samples and 27 samples of the Garnetiferous Pelite, and separation was achieved, though to a lower degree of significance than for the Lochailort-Garnetiferous Pelite separation (partly a consequence of the very small sample size for the Basal Pelite). However, the best discriminator by far for separating the Basal and Garnetiferous Pelites was shown to be Sr, an element of very low discriminant power between the Lochailort and Garnetiferous Pelites.

3) The other possibility in assigning unknowns which belong to neither of the original sample groups is probably the clearest indicator of this relationship. That is, when the unknown items give discriminant scores which fall in a cluster beyond the ranges of the scores for the two training groups, indicating compositions different from either of the original groups (as already seen for samples 498 and 360).

Although the first and third alternatives given above automatically arouse suspicion that something is wrong, the example of the Basal Pelite underlines the major difficulty in trying to use discriminant functions in the way attempted here. The unknowns must belong to one of the groups for which the discriminant function has been calculated, or spurious conclusions can be drawn. This is particularly so when only two groups are considered, since assignment of individual unknown items can only really be to one group or the other, not to neither. This uncertainty can be partly resolved by the use of stepwise discriminant analysis between the group of unknown items and the nearest original group. If separation can be achieved by using a different subset of variables, then the unknown and original groups are probably different. This has been shown in separating the Mhuidhe pelites from both the Lochailort and Garnetiferous Pelites, confirming their

lack of affinity to either; in separating the Basal Pelite and Garnetiferous Pelite; and in separating the equivalents of the Lochailort Pelite of the Ranochan area from the Garnetiferous Pelite. Should separation of the original and unknown groups prove impossible or uncertain, then the two groups can only be considered to be equivalent, lacking further evidence. For example, the two groups of pelites from around Ranochan cannot be adequately separated from each other or from their known equivalent, the Lochailort Pelite.

The last example is interesting in that the known equivalents of the Lochailort Pelite from the Ranochan area do not as individuals give discriminant scores very close to the mean for the Lochailort Group, whereas the mean score for the Ranochan groups is very close to the Lochailort mean score. This is probably due to the fact that individual specimens do not and cannot reflect the variation of the unit sampled, and the mean of several scattered random samples is more truly representative of the unit as a whole, and more reliance can be placed on the discriminant score produced from this mean value. This conclusion was also reached from the analysis of variance study on the training group data. Where large sample sizes are possible for the unknown groups, a sampling design which again allowed analysis of variance on the unknowns would be very desirable.

Application of the discriminant functions beyond the Morar area

Unfortunately, the vast majority of published analyses for Moine rocks give only major element oxide determinations, and this study has shown that for the two pelitic units considered major elements alone do not provide a decisive discriminant function.

However, Winchester (1974b) quoted 26 new analyses of pelites from the Meall an t-Sithe Pelite of Fannich Forest, and for 5 of these has also determined trace elements Sr, Rb, Zr, Nb and Ni. This data can thus be used in the function based on a subset of six variables for the original 54 items in this study (i.e. the function $126.89MnO-10.19K_2O-220.76P_2O_5+ .48Y+.70Rb-1.32Nb$).

Even though Y has not been determined, making the assumption that the value of Y in the Meall an t-Sithe Pelite is equal to the grand mean value of Y for the Lochailort and Garnetiferous Pelites introduces no bias, and allows the function to be used. The discriminant score thus achieved by the mean of the Meall an t-Sithe data is 36.921 which lies very close to the mean score for the Lochailort Pelite data of 32.222, and is far from the mean score of -7.322 for the Garnetiferous Pelite. So on the basis of this discriminant function, the Meall an t-Sithe would be said to be equivalent to the Lochailort Pelitic Group. This in fact is the correlation suggested by Johnstone et al. (1969, Table I), so that the discriminant function gives the correct correlation in this case.

Making the assumption that the Y content of the Meall an t-Sithe Pelite is zero still produces a discriminant score lying within the range of the Lochailort Pelitic Group, and only a very high Y content (90 ppm or more) would place the score beyond the range of the Lochailort Pelite scores.

This result is very encouraging, but is based on a comparatively small sample from a restricted area, and the validity of the discriminant function will only be fully assessed by obtaining much more data from a much wider area, which would also allow any large-scale regional variation in the larger pelitic units of the Moine succession to be considered.

Conclusions

The aim of this study was to assess the value of the discriminant function technique in the classification of pelitic units on a large scale, using chemical data obtained by rapid XRF techniques. As few as six elements or their oxides (MnO, K_2O, P_2O_5, Rb, Nb, Y) can be used to provide a good index with which to classify "unknown" data to a high degree of certainty, for the two units sampled and their equivalents. The discriminant function based on these six elements, from a total sample size of 54 is as follows:

$$Z = 126.89\ MnO - 10.19K_2O - 220.76P_2O_5 + .48Y + .70Rb - 1.32Nb$$

For the Lochailort Pelite this gives a mean Z value of 32.22, and for the Garnetiferous Pelite a value of -7.32, with the boundary between the two groups at a Z value of 12.45.

The two units studied are considered to be integral parts of the Morar Succession but of different age by Powell (1964, 1974) while Tanner et al. (1970) regard the Lochailort Pelite as part of the Glenfinnan Division, which is largely allochthonous over much of its outcrop. This study has shown that these two pelites appear to be chemically distinct, and if this implies necessarily an age difference, it provides additional support to the contention that the Lochailort Pelitic Group connects stratigraphically the Morar Succession with the Glenfinnan assemblage. Much of the Glenfinnan Division could still, however, be infolded Morar Succession, and this form of discriminant function could well be useful in identifying such relationships.

One of the biggest difficulties inherent in the method is the necessity of knowing that the unknowns do actually belong to one or other of the groups sampled. This can be overcome to some extent by

treating the unknown samples from a unit as another training group, and applying discriminant analysis to try and separate this new group from the original groups. If separation from one of the original groups cannot be satisfactorily achieved, there can be no grounds for believing the unknown unit to be different from that group, in the absence of further evidence.

That this type of "chemical stratigraphy" may be both valid and useful beyond the Morar area has been demonstrated with the data from the Meall an t-Sithe Pelite of the Fannich Forest area. However, the limitation of the method still remains that any unknown pelite should be equivalent to one of the pelites already involved in the discriminant function. On the basis of the few samples taken, it appears that the Basal Pelite of the Morar Succession cannot be distinguished from the Garnetiferous Pelite, using the discriminant function given above; much further work would be necessary to chemically typify all the major pelitic units of the Moine succession before any "unknown" pelite could be tested without any suspicions as to its correct stratigraphic position. This is rarely the case, however, so that even the simple discriminant provided by this study may be usable, if the results are treated with due caution.

Choice of the best discriminant subset for two groups remains a problem. Although statistical measures may indicate that one subset is the best for the original training data, another subset may prove better in actually assigning unknown items. This clash between the demands of the formal statistical model and geological practicality is

again seen in the choice of the original training groups. In this case the two groups of 27 items each, while not forming the best sample in statistical terms, is certainly more appropriate to the geological situation, in that the higher sample size is more truly representative of the variation of the unit. Reducing the sample size to reduce the skewness of the data distribution causes only a limited part of the unit to be represented. Since the more psammitic rocks are the cause of the skewness in this case, the reduced samples are only truly representative of the more pelitic members of the stratigraphic unit. Any discriminant function based on this limited sample cannot be expected to deal correctly with unknown items of psammitic composition, and this is seen in the failure of the discriminant function derived from only 49 items to cope with the variety of compositions in the random test samples.

Another detail, pointed out in the analysis of variance study and encountered again in this, is that the unknown items do not individually provide good estimators of the mean of the unknown unit sampled. This is shown in this case by individual discriminant scores scattering widely about the mean score for the correct group, in some cases being misclassified, whereas the mean score for the unknown unit is properly classified. A large number of samples from any unknown unit should be taken, and while this may seem extravagant in terms of analytical time and cost, if the unit is thought to belong to one of a number of groups which have already undergone discriminant analysis, the initial analyses of the unknowns need only be for those elements which have been shown to have discriminant significance.

Chapter 5. CALC SILICATES AND METAMORPHIC HISTORY

Introduction

The calc silicates occur as laterally impersistent thin bands or lenses, conformable with bedding, and from 2 to 20cm wide, while varying in length from under 1 to more than 10m. They are characterised mineralogically by the presence of quartz and garnet plus one or more of the minerals calcite, biotite, amphibole, pyroxene, zoisite, clinozoisite and usually a plagioclase feldspar. Their colour reflects this variation in mineralogy but they are typically white or green, with pink garnet porphyroblasts and show a very characteristic brownish careous surface where weathered. Their stratigraphic distribution is variable (Richey and Kennedy 1939, Powell 1964, Tanner 1971, Ramsay and Spring 1962) but they are most commonly found in the Arieniskill and Lochailort Pelitic Groups and their lithostratigraphic equivalents, and in the lowest and highest parts of the Ardnish Psammite (
Their sedimentary origin can be demonstrated in many places along the west coast of Morar, where low grades of metamorphism and relatively weak deformation have allowed calc silicates to retain traces of current bedding structures. Here calc silicates may also be found which when traced laterally gradually change in composition, passing into calcareous psammites and thinning out. This type of structure conforms with their probable mode of origin as thin calcareous marls in sequences of silts and shallow water sandstones (Butler, 1965, pp 193-194), or as argillaceous calcareous sandstones (Flett, 1923, p.55).

The chemistry and mineralogy of calc silicate bands in the Morar area were studied in detail because they can be used as quite precise indicators of metamorphic grade; their chemistry controlling their mineralogical response to metamorphism in a predictable fashion.

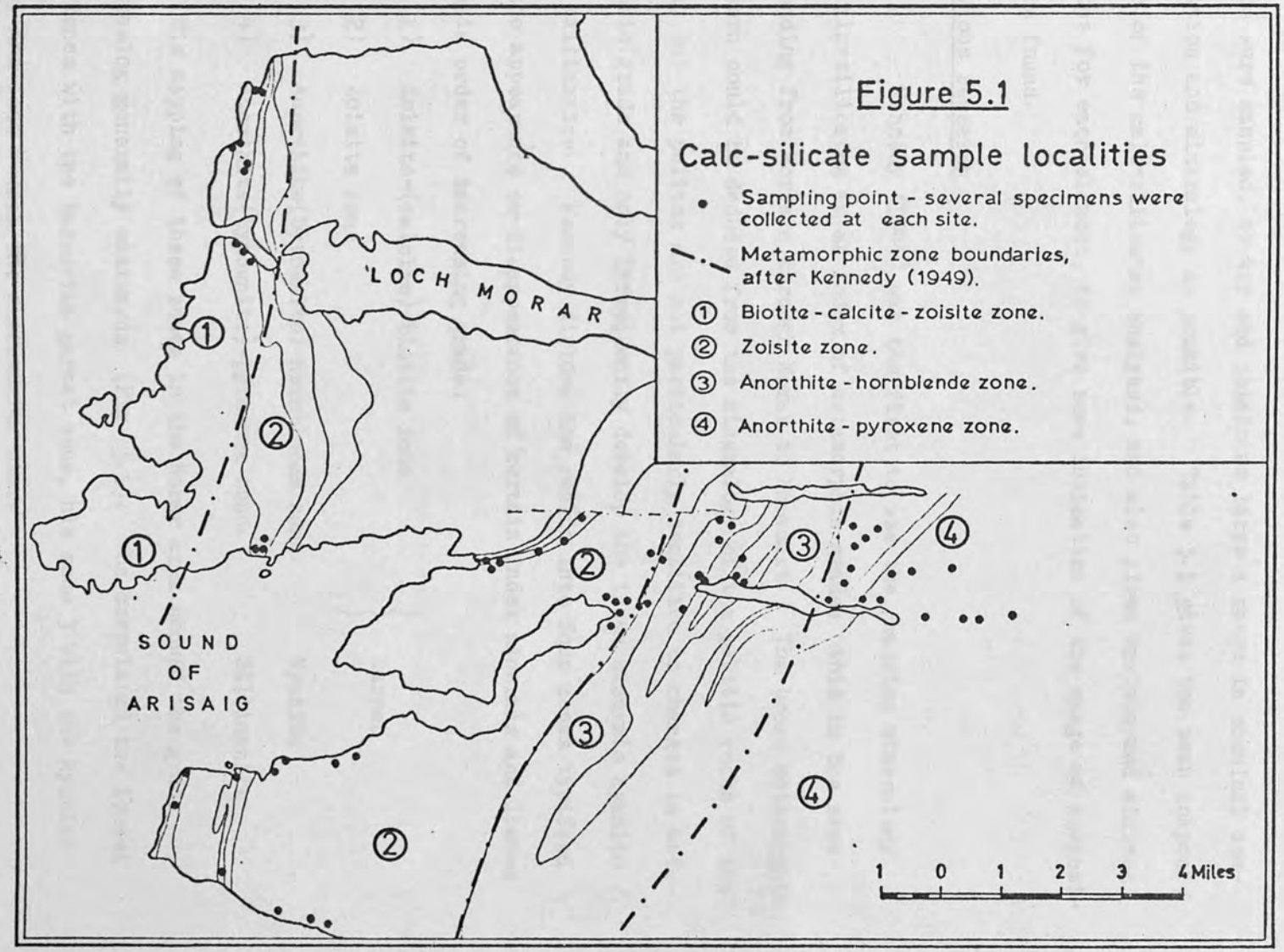
Figure 5.1
Calc-silicate sample localities
Sampling point - several specimens were collected at each site.
Metamorphic zone boundaries, after Kennedy (1949).
① Biotite - calcite - zoisite zone.
② Zoisite zone.
③ Anorthite - hornblende zone.
④ Anorthite - pyroxene zone.
'LOCH MORAR
SOUND OF ARISAIG
1 0 1 2 3 4 Miles

A total of 195 calc-silicate samples were collected, of which 106 were analysed for ten major elements and six trace elements (Nb, Zr, Y, Rb, Sr and Zn) and for 33 of which estimates of Ce and Ba content were also made. At each collection point (Fig. 5.1) several calc-silicate bands were sampled, to try and obtain as large a range in chemical composition and mineralogy as possible. Table 5.1 gives the mean composition of the calc-silicates analysed, and also gives maximum and minimum values for each element, to give some indication of the range of compositions found.

Previous research

Kennedy (1949) was the first to use the changing mineralogy of calc-silicates as an index of metamorphic grade; this in the area extending from Morvern through Morar to Knoydart. The broad metamorphic pattern could be deduced from the mineralogy of the pelitic rocks of the area, but the pelites are not particularly sensitive to changes in metamorphic grade and only infrequently develop the index minerals kyanite and sillimanite. Kennedy divided the region into four zones typified by the appearance or disappearance of certain index minerals and listed here in order of increasing grade:

1)	Zoisite-(calcite)-biotite zone	Garnet
2)	Zoisite zone	
3)	Anorthite(bytownite)-hornblende zone.	Kyanite
4)	Anorthite(bytownite)-pyroxene zone.	Sillimanite

His mapping of these zones in the Morar area showed the grade increasing generally eastwards (Fig. 5.1). He correlated the lowest two zones with the Barrovian garnet zone, his zone 3 with the kyanite zone, and zone 4 with the sillimanite zone.

	Mean	Minimum	Maximum
SiO_2	70.37	54.45	86.57
TiO_2	.48	.10	1.74
Al_2O_3	14.18	6.40	21.29
ΣFe_2O_3	2.75	.66	6.27
MnO	.26	.02	.58
MgO	.65	.03	1.78
CaO	6.57	1.77	14.89
Na_2O	2.11	.31	6.34
K_2O	.94	.10	5.14
P_2O_5	.22	0.00	.62
Zr	223	36	807
Y	35	7	107
Rb	46	0	535
Nb	13	1	41
Sr	306	89	935
Zn	18	0	70

TABLE 5.1 Mean analysis of 103 calc-silicates quoted, with maxima and minima.

Winchester (1970,1972) following Atherton (1965) pointed out that mineral reactions are as much dependent on the bulk chemistry of the host rock as on the prevailing P-T conditions, and concluded that in calc-silicates of the Fannich Forest area, the CaO/Al_2O_3 ratio could be used as an indicator of similarity between calc silicates with respect to a reaction in which biotite was replacing hornblende. He concluded that the lower the critical CaO/Al_2O_3 ratio at which the reaction could proceed, the higher the prevailing metamorphic grade. On the basis of this assumption he could draw "chemical isograds", connecting points showing the same reaction at the same CaO/Al_2O_3 ratio, thus outlining areas of higher and lower metamorphic grade.

Although the Fannich area only underwent metamorphism characteristic of Kennedy's lower two zones, Winchester went on (1973,1974a) to extend his theory to cover the higher zones, and to attempt a map showing the pattern of regional metamorphism for the whole of the Moine outcrop in the Scottish Caledonides.

The essential relationships between mineralogy, grade and critical CaO/Al_2O_3 ratio were summarised diagramatically (Fig. 5.2, after Winchester 1974a, Fig.1), using the index minerals biotite, hornblende, pyroxene and plagioclase feldspars.

The diagram shows the mineralogical reactions by which three metamorphic isograds are defined:

1) Kyanite isograd is defined by the first appearance of hornblende in calc silicates with a CaO/Al_2O_3 ratio of 0.4 or less.

2) Bytownite isograd defined by the first appearance of bytownite in calc silicates with CaO/Al_2O_3 ratio of 1.0 or less, according to the reaction:

$$\underset{\text{Hornblende}}{2Ca_2(Mg,Fe)_3Al_4Si_6O_{22}(OH)_2} = \underset{\text{Anorthite}}{CaAl_2Si_2O_8} + \underset{\text{Calcic Almandine}}{2(Mg,Fe)_3Al_2Si_3O_{12}.1Ca_3Al_2Si_3O_{12}} + \underset{\text{Quartz}}{SiO_2} + H_2O \qquad (5.1)$$

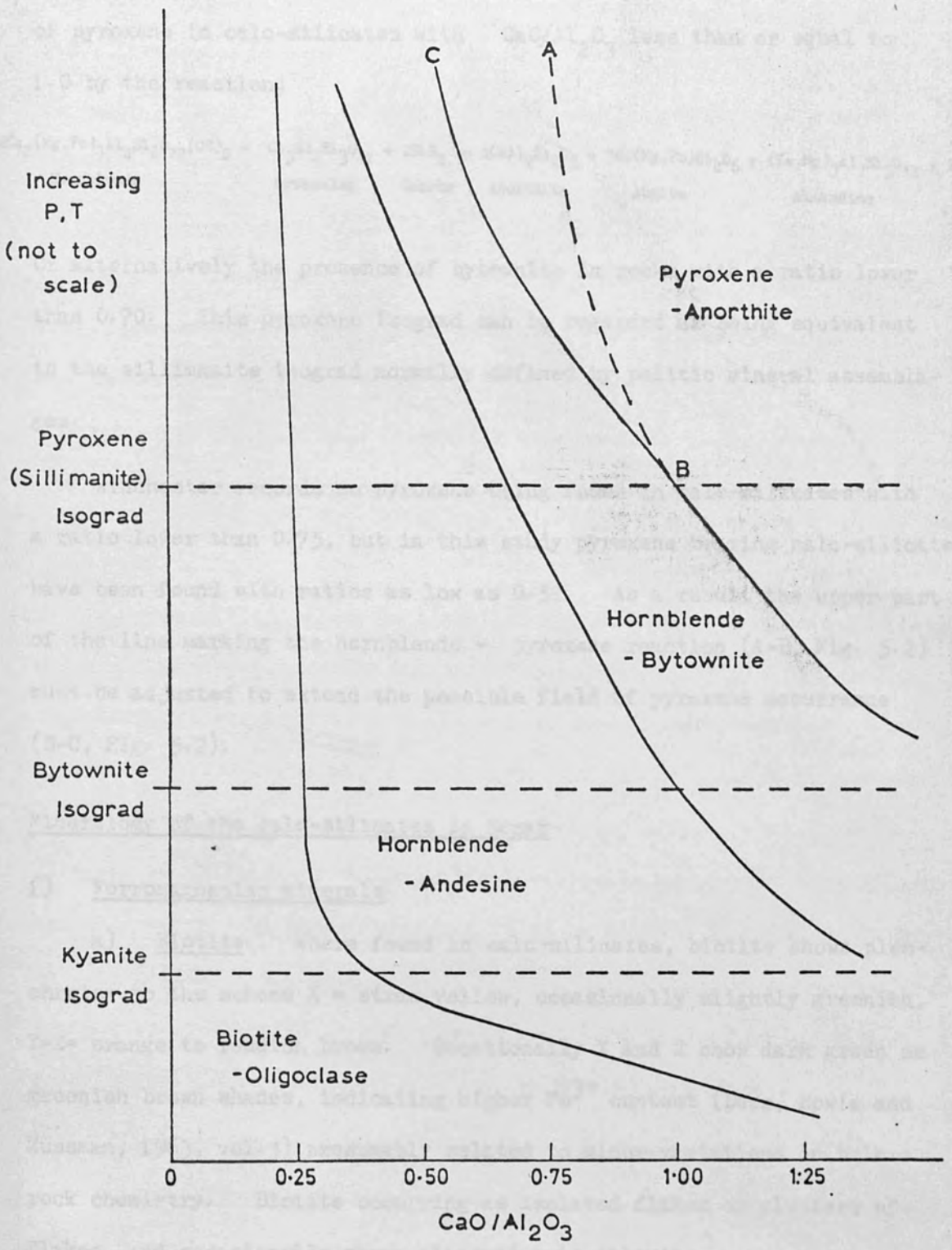

Figure 5.2 Schematic PT-composition plot of stability fields of biotite, hornblende, pyroxene and plagioclase feldspar in calc-silicate rocks. (Modified after Winchester, 1974a)

3) Pyroxene isograd is defined either by the first appearance of pyroxene in calc-silicates with CaO/Al_2O_3 less than or equal to 1.0 by the reaction:

$$\underset{\text{Hornblende}}{2Ca_2(Mg,Fe)_3Al_4Si_6O_{22}(OH)_2} + \underset{\text{Grossular}}{Ca_3Al_2Si_3O_{12}} + \underset{\text{Quartz}}{2SiO_2} = \underset{\text{Anorthite}}{4CaAl_2Si_2O_8} + \underset{\text{Augite}}{3Ca(Mg,Fe)Si_2O_6} + \underset{\text{Almandine}}{(Fe,Mg)_3Al_2Si_3O_{12}} + 2H_2O$$

Or alternatively the presence of bytownite in rocks with a ratio lower than 0.70. This pyroxene isograd can be regarded as being equivalent to the sillimanite isograd normally defined by pelitic mineral assemblages.

Winchester records no pyroxene being found in calc-silicates with a ratio lower than 0.75, but in this study pyroxene bearing calc-silicates have been found with ratios as low as 0.52. As a result the upper part of the line marking the hornblende - pyroxene reaction (A-B, Fig. 5.2) must be adjusted to extend the possible field of pyroxene occurrence (B-C, Fig. 5.2).

Mineralogy of the calc-silicates in Morar

1) Ferromagnesian minerals

a) Biotite. Where found in calc-silicates, biotite shows pleochroism to the scheme X = straw yellow, occasionally slightly greenish, Y=Z= orange to reddish brown. Occationally Y and Z show dark green or greenish brown shades, indicating higher Fe^{3+} content (Deer, Howie and Zussman, 1963, vol.3) presumably related to minor variations in bulk rock chemistry. Biotite occurring as isolated flakes or clusters of flakes, and occasionally shows alteration to chlorite.

b) Amphibole. The amphibole in calc-silicates is typically hornblende with X= pale yellow to colourless, Y= pale green, Z= dark green pleochroism. It occurs as ragged xenoblastic poikiloblastic

crystals, or more rarely as idioblastic inclusion free blades, in which form it is usually aligned with c axis parallel to the bedding schistosity. Where amphibole is seen replacing pyroxene, it takes the form of small pale green slightly pleochroic needles, possibly of a more tremolitic composition.

c) Pyroxene is found in calc-silicates only in the extreme east of the area, around the eastern end of Loch Eilt (Fig. 5.1). It forms small, ragged, colourless grains with good cleavage inclined at about 40° in extinction; it is biaxial (+) with a 2V of about 40°. Almost invariably alteration to a tremolitic amphibole is taking place, and the pyroxene may only be present as minute remnants in a fibrous amphibole mass.

2) Feldspars. Plagioclase is almost always found in the calc-silicates, only 4 of the samples taken lacking plagioclase entirely. It occurs both as small grains in the matrix and as larger porphyroblasts. Alteration is very common, but the number of grains showing alteration tends to increase eastwards, at the same time the type of alteration changing in character from clay-mineral-sericite aggregates to muscovite and clinozoisite breakdown products. It is notable that the feldspars in calc silicates may show alteration when the feldspars in the surrounding pelite or psammite do not, possibly reflecting the higher and more readily available H_2O and CO_2 content of the calc-silicates.

Anorthite determinations, where possible, were made by the Michel-Levy method, which tends to give a minimum estimate of anorthite content unless a correctly oriented grain has been measured.

Along the west coast the feldspars are often very small, lightly altered and poorly twinned, but the refractive index (estimated by the

Becke line method) and sign determinations were used for approximate estimates. In the extreme east of the area, although good albite twinning allowed determinations of anorthite content to be made in many cases, many of the feldspar grains showed no twinning. These however have very high relief, indicating extremely anorthite rich compositions.

Many of the feldspars show strained extinction or zoning, and in the area east of Lochailort particularly, the feldspars have an outer rim of less calcic composition then the centre.

K-feldspar was not found in any of the calc silicates. The K_2O content is low, usually 0.5-1.0%, and any K_2O is presumably held in biotite, or in muscovite in the more potash rich calc silicates.

3) Garnet occurs either as small aggregates of small grains or larger porphyroblasts, is invariably xenoblastic and full of inclusions (usually of quartz, but also of plagioclase, clinozoisite, sphene and calcite). In hand specimen the garnet forms distinct pinkish brown patches, or nodules on weathered surfaces, and in thin section shows a slight yellow tinge.

4) Epidote minerals

a) Zoisite is the index mineral for Kennedy's lowest two zones, and occurs in calc silicates throughout the western part of the region. Elongated straight-sided needles or blades are the commonest form, but stout prismatic crystals are also found. Where elongated, the long axes of crystals tend to lie in the plane of the bedding schistosity.

Interference colours are low first-order greys, sometimes with an anomalous brown tinge. Kennedy identified the zoisites as the β form, suggested to be the iron-free form of zoisite by Myer (1966), although originally α-zoisite was regarded as the iron-free orthorhombic epidote mineral.

b) Clinozoisite is found in calc-silicates throughout the area, as intergrowths with amphibole or zoisite, as grains in altered plagioclase feldspar, and as irregular xenoblastic intergranular aggregates. Interference colours are anomalous first order blues and yellows. Distinguishing between zoisite and clinozoisite is difficult, the only truly diagnostic feature in thin section being the inclined extinction to cleavage in the prism section of clinozoisite, whereas orthorhombic zoisite gives straight extinction. Where this test has been possible, the anomalous interference colours have been as described, blue in clinozoisite and brown in zoisite, and this difference has been accepted as diagnostic within the rocks from this area.

5) Calcite is found mainly in the calc-silicates of the western part of the area, and in the east is found only in minor amounts as a product of feldspar or amphibole breakdown. Single large grains or aggregates of small grains are typical, often interfingering between other matrix grains. Small grains are occasionally seen as inclusions within garnet, particularly in the calc-silicates within the west coast area.

Accessory minerals include sphene, apatite, opaque iron oxides, epidote proper and muscovite. Muscovite is found both as a product of feldspar breakdown and as flakes within the matrix of calc-silicates with a K_2O content higher than about 1%.

Metamorphic history from calc-silicate evidence

The three ferromagnesian minerals found in calc-silicates, biotite, amphibole and pyroxene are each stable at progressively increasing metamorphic grade. The points at which reactions occur with biotite breaking down to form amphibole and amphibole to form pyroxene, depends also on the bulk chemistry of the rock (Atherton, 1965), and the ratio CaO/Al_2O_3 can be used as a convenient index of similarity between calc-

silicates for reactions involving these minerals (Winchester 1972, 1974a). Taking a number of calc-silicates from a small locality, the CaO/Al_2O_3 ratio above which a reaction will occur can be determined from an examination of the ferromagnesian minerals present and their relationships. As an example, consider an ideal situation where the reaction biotite - hornblende takes place at a CaO/Al_2O_3 ratio of 0.5 and above. In calc-silicates with a ratio less than 0.5 biotite only should be found, in those above 0.5 amphibole only should be found, and in those with ratios about 0.5 amphibole and biotite should occur together. The direction of the reaction can be deduced from the relationships of the two minerals, in this case amphibole replacing biotite. Situations this clear cut are inevitably extremely unusual, as minor variations in H_2O, CO_2 and alkali content may affect the reaction, but an estimate of the critical CaO/Al_2O_3 ratio can often be made if the range of ratios found includes the critical ratio. At a higher metamorphic grade, the ratio at which this reaction could occur will be lower than 0.5, but at lower levels of metamorphism the reaction may only be possible in those calc-silicates with a much higher amount of CaO in relation to Al_2O_3.

Using this model it is possible to make estimates of the peak metamorphic grade for a number of localities, given suitable samples, and thus to build up a picture of the metamorphic pattern over a larger area. It has also proved possible in this study, from a consideration of the replacement textures, to assess the level of metamorphism not only in an early prograde event, but also the degree of metamorphism attributable to a later, retrogressive episode.

One of the major problems in this study lay in the restricted range of CaO/Al_2O_3 ratios found in the calc-silicates analysed. Only 4 of the 106 analysed showed CaO/Al_2O_3 ratios in excess of 0.75, and this inevitably restricted the degree of detail which could be resolved in the metamorphic patterns observed.

Evidence available from the pelites in the area was used to supplement that from the calc-silicates, mainly in the location of the kyanite and sillimanite zones of metamorphism. The region can be conveniently considered in two parts, the area west of Lochailort, in which only a limited number of samples were collected, and the more closely sampled area extending east from Lochailort to the eastern end of Loch Eilt.

1) West coast to Lochailort

Kennedy (1949) used a breakdown reaction of biotite to mark the upper limit of his lowest zone, the biotite-calcite-zoisite zone, quoting the reaction:

biotite + calcite (zoisite) → hornblende (5.3)

This lowest zone covers only the extreme west coast of Morar, west of a line from Mallaig to Arisaig (Fig. 5.3). However, of the 24 samples taken within the higher zoisite (biotite free) zone all contained biotite, and only one showed amphibole replacing biotite (DP 127). It is significant that the amphibole-bearing calc-silicate has the highest CaO/Al_2O_3 ratio (0.642), so that reaction could probably not occur in the other calc-silicates. Winchester (1972) indicated that for calc-silicates in this zone in the Fannich area the biotite - hornblende reaction only occurred at ratios exceeding 1.0 at the lower grade and at ratios in excess of 0.5 at the higher grade limit.

Within the biotite-calcite-zoisite zone, Kennedy indicated that the assemblage biotite-hornblende-zoisite-calcite-garnet was stable, and confirmation of this assemblage (NC309) indicated that the lowest

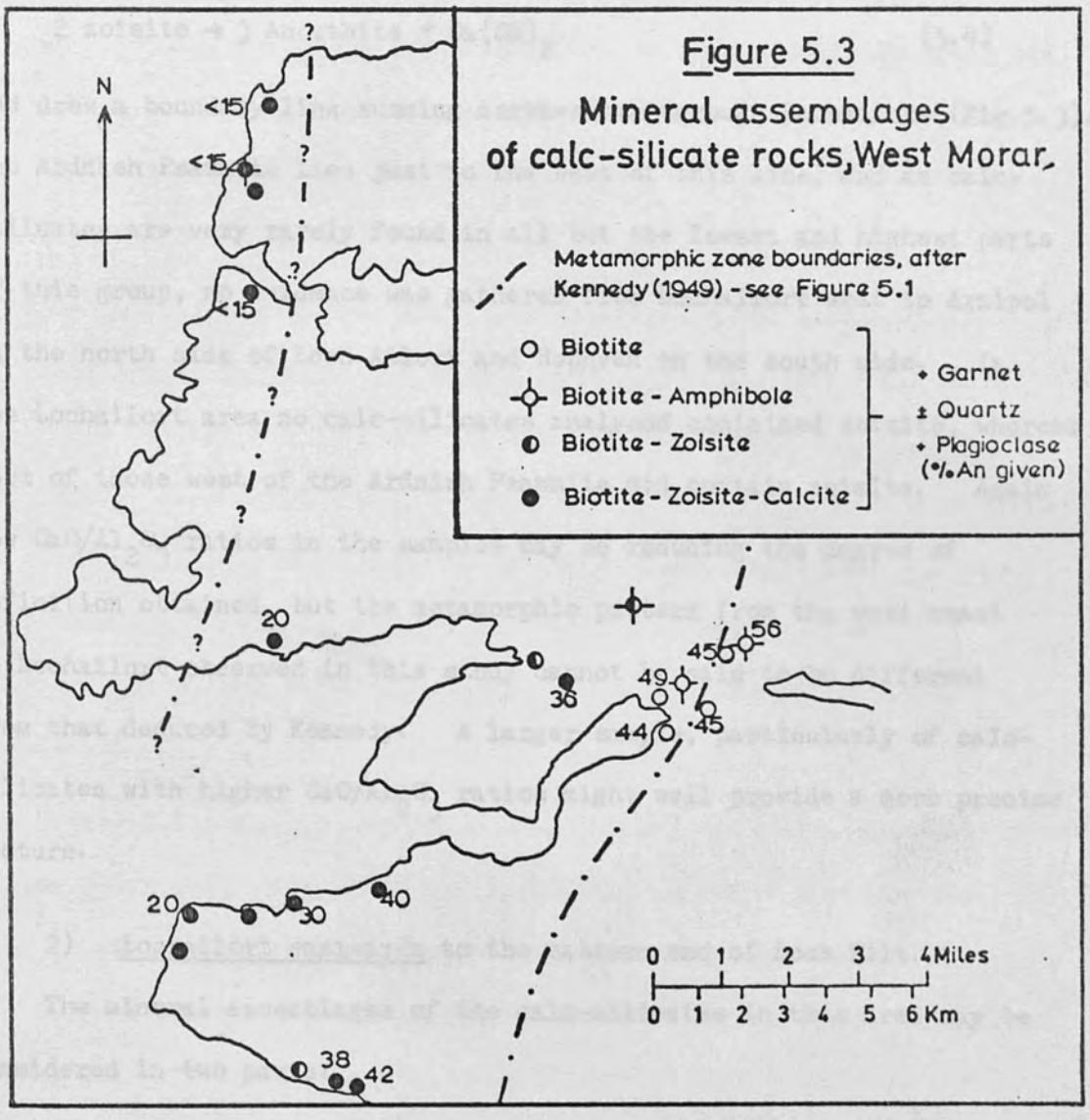

Figure 5.3

Mineral assemblages of calc-silicate rocks, West Morar.

zone lies within the highest part of the greenschist facies in the quartz-albite-epidote-almandine subfacies (Winkler, 1967).

Kennedy defined the upper limit of the zoisite zone by the reaction:

$$2 \text{ zoisite} \rightarrow 3 \text{ Anorthite} + Ca(OH)_2 \qquad (5.4)$$

and drew a boundary line running north-south through Lochailort (Fig. 5.3). The Ardnish Psammite lies just to the west of this line, and as calc-silicates are very rarely found in all but the lowest and highest parts of this group, no evidence was gathered from Lochailort west to Arnipol on the north side of Loch Ailort and Roshven on the south side. In the Lochailort area no calc-silicates analysed contained zoisite, whereas most of those west of the Ardnish Psammite did contain zoisite. Again low CaO/Al_2O_3 ratios in the samples may be reducing the degree of definition obtained, but the metamorphic pattern from the west coast to Lochailort observed in this study cannot be said to be different from that deduced by Kennedy. A larger sample, particularly of calc-silicates with higher CaO/Al_2O_3 ratios might well provide a more precise picture.

2) Lochailort eastwards to the eastern end of Loch Eilt.

The mineral assemblages of the calc-silicates in this area may be considered in two parts:

a) with respect to the evidence they provide for the grade of metamorphism achieved in the rocks during a prograde metamorphic event.

b) with respect to the evidence they provide for a later, retrogressive event.

a) First event

The western margin of the Lochailort Pelitic Group marks the approximate position of the upper limit of Kennedy's zoisite zone, but as already noted, no zoisite was found in the analysed calc-silicates from the area about the boundary. However, it is in this region that the metamorphism reached a level where the reaction involving breakdown of biotite to form hornblende can take place in calc-silicates of low CaO/Al_2O_3 ratio, and this reaction can be plotted in terms of decreasing critical ratio eastwards.

By Inverailort Bridge (Fig. 5.4) amphibole forms at the expense of biotite at a CaO/Al_2O_3 ratio of about 0.50, while less than 1km to the north east amphibole occurs in calc-silicates with ratios of 0.30 and less. Winchester (1974) regards those calc-silicates with a ratio of less than 0.3 as semipsammites rather than calc-silicates, but the specimens described here have all the chemical characteristics of calc-silicates, and certainly develop the appropriate mineral assemblages.

1½km to the north, and 300 metres higher, by Loch an Iasgair and on the south west ridge of Creag Bhan (Fig. 5.4) this eastward reduction in the critical ratio can again be detected, enabling "chemical isograds" to be drawn for the biotite-amphibole reaction in this area. These correspond in their trend (Fig. 5.4) both to Kennedy's zoisite zone upper boundary and to the western limit of a zone of regional migmatisation as defined by the Geological Survey (1" sheet 61, 1971).

The Isograd marking the ratio 0.40 for this reaction is also regarded by Winchester (1974) as the lower boundary of kyanite zone metamorphism, which would appear to be confirmed by the rare development

FIGURE 5.4

Mineral assemblages of calc-silicate rocks, eastern Morar

Figure 5.4.1 shows mineral assemblages and plagioclase feldspars attributed to the first metamorphic event in the area, while Figure 5.4.2 indicates the effect of the second metamorphic event upon the earlier assemblages. Each point represents up to 8 individual samples; garnet and quartz are always present, with additional mafic minerals as follows:

○ Stable mafic minerals		□ Unstable mafic minerals	
◐	Biotite	◨	Amphibole breaking down to chlorite or calcite + clinozoisite
◑	Amphibole	◪	Amphibole breaking down, biotite stable
⊕	Pyroxene	◨	Pyroxene breaking down to amphibole

Plagioclase compositions (%Anorthite) are given by the upper figures in Figure 5.4.1, and in Figure 5.4.2 A indicates alteration of feldspars while Z indicates that feldspars are zoned (rims are invariably less calcic than cores).

CaO/Al_2O_3 ratios (multiplied by 100 to eliminate decimal points) are given by the numbers in Figure 5.4.2, and the lower numbers of the pairs in Figure 5.4.1. For stable amphibole and pyroxene these values are the minimumfound in samples containing the minerals, while for biotite and unstable pyroxene or amphibole, the values are the maximum found. (See text for details)

—0·5— Critical CaO/Al_2O_3 ratio isograds for replacement of biotite by amphibole. 0.4 ratio is equivalent to lower limit of kyanite grade metamorphism, event 1. Kyanite found in pelite at locality (K)

—0·4— k —

— s — Western limit of sillimanite grade metamorphism, event 1. Sillimanite in pelites found at localities (S)

— · — Western margin of Pyroxene-Anorthite zone (Kennedy,1949)

— P — Western limit of transgressive pegmatites (Geol. Surv.)

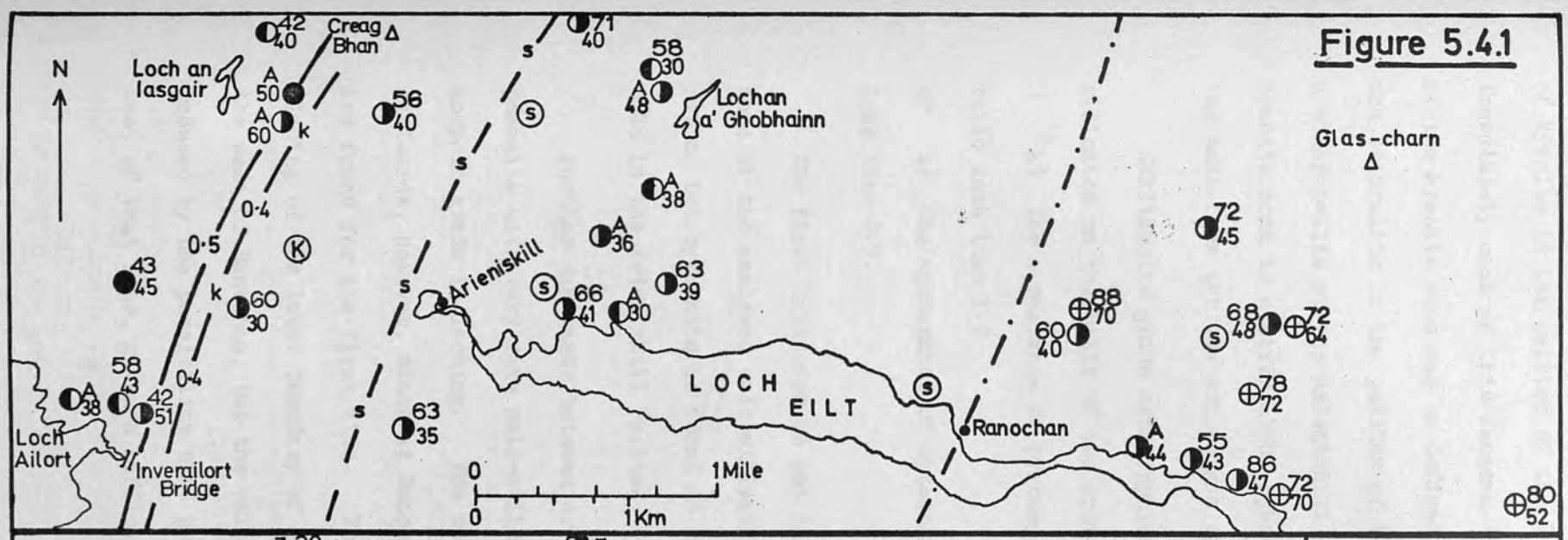
Figure 5.4.1
N
Loch an Iasgair
Creag Bhan
Lochan a' Ghobhainn
Glas-charn
Arieniskill
LOCH EILT
Ranochan
Loch Ailort
Inverailort Bridge
0·4
0·5
0-4
1Mile
1Km

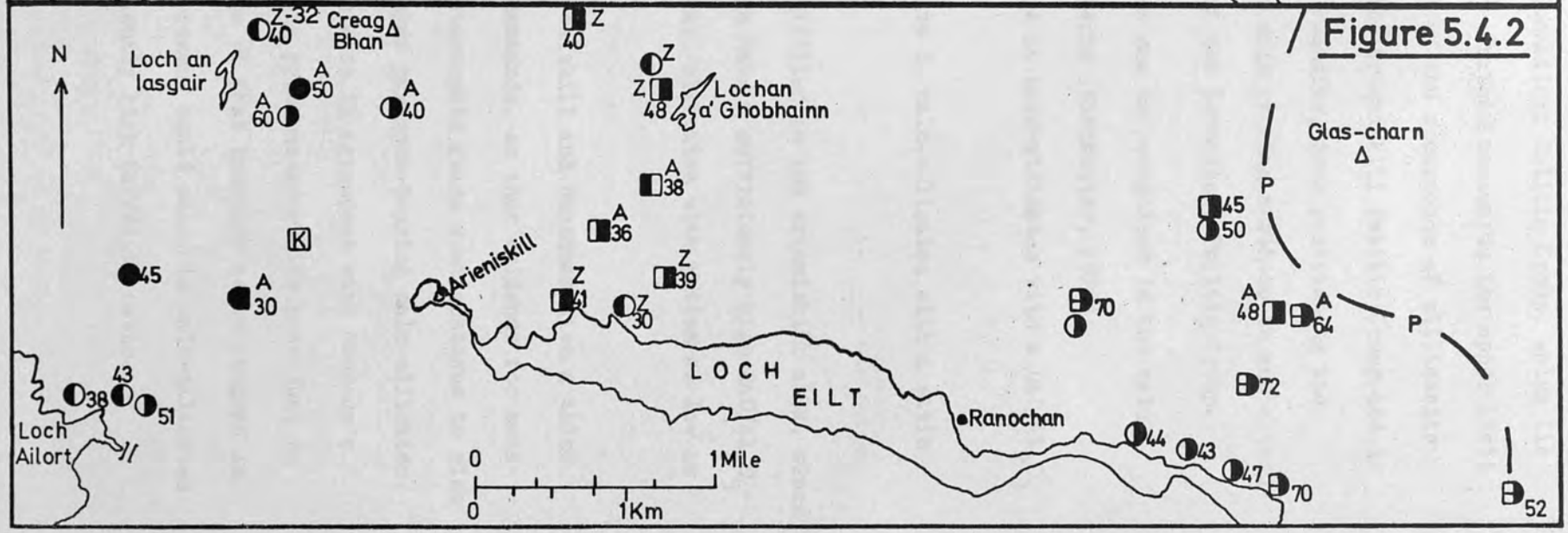
Figure 5.4.2
N
Loch an Iasgair
Creag Bhan
Lochan a' Ghobhainn
Glas-charn
Arieniskill
LOCH EILT
Ranochan
Loch Ailort
1Mile
1Km

of kyanite in the pelites of the Lochailort Pelitic Group, which lie immediately east of this isograd. Further eastwards the upper limit of the kyanite zone can be defined by the occurrence of sillimanite and staurolite in the pelites of the Arieniskill Pelitic Group and in a minor pelite of the Arieniskill Psammite, thus restricting the kyanite zone to a strip about $1\frac{1}{2}$km wide running north-south and extending east from the western margin of the Lochailort Pelitic Group.

Sillimanite grade metamorphism can be recognised in the calc-silicates on the basis of two criteria (Winchester, 1974):

a) The appearance of pyroxene in calc-silicates with a CaO/Al_2O_3 ratio less than 1.0

or b) The appearance of bytownite in calc-silicates with a ratio less than 0.7.

The first criterion is not fulfilled in the Arieniskill area, since none of the analysed calc-silicates have a sufficiently high CaO/Al_2O_3 ratio, but bytownite is found in calc-silicates with ratios as low as 0.48 in the Arieniskill Pelite.

Further eastwards between Arieniskill and Ranochan lies a thick psammite with very rare calc-silicate bands, so that evidence for metamorphic grade is lacking. The metamorphic grade must continue to rise eastwards, however, since at Ranochan pyroxene-bearing calc-silicates are found for the first time. This is in agreement with Kennedy's placing of the lower boundary of his pyroxene-anorthite zone just to the west of Ranochan, but the value of that boundary as an isograd is reduced by the possibility that pyroxene could occur in calc-silicates west of that line, given a sufficiently high CaO/Al_2O_3 ratio.

Winchester (1974) states that no Moine calc-silicates so far analysed with CaO/Al_2O_3 ratios of less than 0.75 have been found to contain pyroxene, but pyroxene is found by Ranochan in calc-silicates with a ratio of 0.70, and the critical ratio falls rapidly eastwards until 1km east of the end of Loch Eilt calc-silicates with a ratio as low as 0.52 are found to contain pyroxene. The effect of this on the hornblende - pyroxene reaction boundary in Figure 5.2 has already been noted, the line moving from A-B to B-C. Chemical isograds for the hornblende - pyroxene reaction could not be drawn with any degree of certainty, but would appear to run NNE-SSW like those defined at Lochailort.

Up to this point the metamorphic pattern indicated by Kennedy would seem to be valid, and the zones he drew are adequate estimators of the peak metamorphic grade achieved across the area. The location of the metamorphic maximum, and the point where grade starts to decline again must lie somewhere east of Loch Eilt, but will only be detectable by sampling further eastwards towards Glenfinnan.

b) Second event

Kennedy noted the presence of clinozoisite as a local development within the high grade assemblages, which he attributed to localised retrograde reaction. However, the calc-silicates everywhere east of Lochailort show textures indicating breakdown of amphibole, pyroxene, and feldspar also show reverse zoning, so that the retrogression would appear to be a more general event.

In the pyroxene-bearing calc-silicates, the pyroxene is invariably seen to be breaking down, usually to tremolitic amphibole needles, and in many cases the only pyroxene remaining is as minute fragments in aggregates of needle-like amphibole.

Often two generations of amphibole can be distinguished, large early formed hornblende fragments having margins frilled by later amphibole needles. In rare instances a complete sequence of events can be discerned, large hornblendes showing marginal breakdown to pyroxene (prograde), the pyroxene in turn reverting to acicular amphibole which also overgrows the early hornblende (retrograde pyroxene breakdown and regeneration of amphibole).

Amphibole breakdown is to chlorite and calcite rather than biotite, possibly by reactions such as:

Hornblende → chlorite + tremolite/actinolite + epidote + quartz (5.5)

and Actinolite + epidote + H_2O + CO_2 → chlorite + calcite + quartz (5.6)

(Winkler, 1967)

These reactions involve the introduction of volatiles, and could thus account for the presence of clinozoisite as a common intergranular phase in the calc-silicates of the area.

Again whole rock chemistry determines the point of reaction, and critical CaO/Al_2O_3 ratios may be deduced from a consideration of whether amphibole is breaking down or a second phase of amphibole growth has started.

By the eastern end of Loch Eilt, the critical ratio would appear to be about 0.4, those calc-silicates with a lower ratio showing amphibole breaking down, while those above this ratio have amphibole growing over earlier amphibole/pyroxene. However, on the southern slopes of Glas-charn, 1km north and some 500m higher in altitude, the critical ratio is about 0.5, indicating that at the higher altitude a lower metamorphic grade was achieved in the second metamorphic episode. The breakdown of amphibole by Loch Eilt at about 0.4 might be regarded as an indication that that region was held at about kyanite grade

during the second metamorphic event, if the breakdown to chlorite rather than biotite can be attributed simply to the availability of CO_2 and H_2O. In this respect it is interesting to note that the western margin of a region of large transgressive pegmatites has been mapped by the Geological Survey as lying just to the east of the area (Fig. 5.4) and may indicate the availability of volatiles.

Moving westwards to Arieniskill, amphibole break down to biotite or chlorite and calcite occurs only in those calc-silicates with a CaO/Al_2O_3 ratio less than 0.5, and by Lochailort amphibole breakdown is rare, the main signs of retrogression being in the feldspars.

In most of the calc-silicates east of Lochailort feldspar has suffered breakdown, usually to fine flakes of muscovite aligned with the remnant albite twinning but also in some cases to clinozoisite. Feldspar zoning is common both in the calc-silicates and the adjoining pelites, the outer zones invariably being less calcic than the centre.

Conclusions

The pattern of metamorphism deduced by Kennedy (1949) for this area would appear to be essentially correct when considered in terms of the general pattern of metamorphism. This work confirms the general rise in metamorphic grade eastwards, from upper greenschist facies on the west coast to sillimanite grade (upper almandine-amphibolite facies) by the eastern end of Loch Eilt. However, examination of the calc-silicates also produces evidence of a later stage of metamorphism, which has resulted in a zone of marked retrogression within the area of highest metamorphic grade.

Kennedy's lowest two zones, the biotite-calcite-zoisite zone and the zoisite zone, could not be confirmed because of the limited range

of CaO/Al_2O_3 ratios found in the calc-silicate specimens analysed. In fact, biotite occurs with zoisite throughout the zoisite zone, so that the zone would appear to be of little value or validity.

The western margin of the Lochailort Pelitic Group approximately coincides with the isograd marking the lower boundary of a narrow zone of kyanite grade metamorphism, although kyanite is very rarely developed in the pelites. Further sampling to the north and south would be very useful in helping to clarify the relationship between the boundary of the pelitic unit and the isograd.

Eastwards from this kyanite zone, the area has undergone sillimanite grade metamorphism, indicated both by the calcsilicate mineral assemblages and the rare occurrence of sillimanite and staurolite in the pelitic rocks. It is within this area that the calc-silicates provide evidence for a second metamorphic event, which produced marked retrogression in the area between Lochailort and Ranochan. This seems to indicate either that a lower metamorphic maximum was achieved overall, or that the centre of metamorphism was displaced eastwards, producing metamorphism only to about kyanite grade in the area about Ranochan. Again further sampling would help improve the picture, particularly taking advantage of the 800 metres of vertical relief available to the east on the slopes of Sgurr a Mhuidhe.

Appendix I

Calibration for major element analysis by X-ray fluorescence techniques

Introduction

To calibrate for any single element, drift corrected counts on a number of known standards are regressed against some value representing the proportion of the element (or its oxide) in each of the standards, giving constant terms for the polynomial expression relating the two.

If simple values of element percentage are used, the regression lines are appreciably curved because of mass absorption effects, and can be used only over a very limited range of rock compositions with similar mass absorption characteristics. To analyse a wide variety of rocks, and a larger range of element proportions, a number of such curves for each element will be necessary. Some estimate of composition must be made for any unknown sample which is to be analysed, so that the series of calibrations appropriate to that composition may be selected. Even when mass absorption corrections are to be applied, allowing straight calibration lines (i.e. linear equations) to be used, the initial erection of calibration lines is a problem. Empirically derived straight lines, based on a very limited number of well analysed standards may be used, but errors may be introduced.

In an attempt to eliminate such errors, leaving only random errors of sample preparation, and those inherent in the XRF method, a method of recalculating the composition of rock standards has been derived from a consideration of the mass absorption correction method. This not only reduces error in the initial estimate of composition from the measured characteristic X-ray intensities, but also gives remarkably straight calibration regression lines over a very wide range of element proportions, in a large variety of rock types.

The following sections give the basis of the mass absorption and volatile loss corrections performed in the computer program MUBACK. Some background theory of mass absorption constants and the derivation of mass absorption correction matrices is also given as an introduction to the section on mass absorption corrections.

a) Correction for volatile losses during fusion is essential, since these losses (of CO_2, H_2O, etc.) change the dilution of rock in flux of the finished disc.

Consider first a rock with no volatiles to lose, and SiO_2 content of 50%. The weight before fusion is given by:

0.400g rock powder
2.855g flux
3.255g total weight

Since no volatiles are lost, this is also the weight of the mix after fusion, and the rock forms $(0.4/3.255) \times 100 = 12.289\%$ of the total disc weight, and the SiO_2 in the disc $= \frac{(0.4 \times 0.50)}{3.255} \times 100 = 6.144\%$ of the total.

Now if the rock had contained 50% SiO_2, 25% volatiles and 25% other non-volatiles by weight, then the weight before fusion would be as given above, 3.255g but the weight after fusion would be:

$0.4 \times 0.75 = 0.300$g rock (0.75 is the weight fraction of non-volatiles)
2.855g flux
Total weight 3.155g after fusion

Of this fusion the rock forms $\frac{(0.4 \times 0.75)}{3.155} \times 100 = 9.509\%$ by weight

and the SiO_2 in the disc forms: $\frac{(0.4 \times 0.50)}{3.155} \times 100 = 6.339\%$ by weight.

Since a dilution of 12.289% in a fusion represents 100% of non-volatile components, then a dilution of 9.509% must be equivalent to

$\frac{9.509}{12.289} = 77.378\%$.

This means that a rock with 75% non-volatiles will give an analysis totalling 77.378% (if the only errors are those from fusion losses).

The operation can be reduced to the following general equation:

$$x_2 = \frac{x_1 \times (2.855 + 0.4)}{(2.855 + (0.4T/100))} = \frac{3.255x_1}{(2.855 + (0.004T))} \quad (I.1)$$

where x_1 is the original weight per cent. of an oxide, x_2 is the apparent percentage after volatile losses, and T is the total weight per cent. of non-volatiles in the rock.

If $x_1 = T$, then x_2 is the total expected for the analysis. It can be seen from this that any analysis of a rock containing volatiles will give a higher apparent total of non-volatiles, and a higher value for each of the elements. The size of the effect on totals can be seen in Table I.1.

The error is distributed proportionally among the elements of the total, so that for siliceous rocks most of the error from volatile losses will be apportioned to silica, e.g. rocks with up to 5% volatiles and about 50% SiO_2 will show errors of less than +0.3% in the silica percentage arising purely from this source.

Corrections can be quite easily made, either mathematically, or physically during the preparation of the disc (Padfield & Gray, 1971). From equation I.1 it can be shown that:

$$T_1 = \frac{2.855}{\frac{3.255}{T_2} - 0.004} \quad (I.2)$$

where T_1 is the true total, and T_2 is the total from the analysis. Corrections to individual oxide or element percentages are of the form:

$$x_1 = x_2 \cdot T_1/T_2$$

where x_1 is real and x_2 apparent percentage.

% Volatiles	True Total	Apparent Total
0.5	99.50	99.56
1.0	99.00	99.12
1.5	98.50	98.68
2.0	98.00	98.24
2.5	97.50	97.80
3.0	97.00	97.36
3.5	96.50	96.92
4.0	96.00	96.47
4.5	95.50	96.03
5.0	95.00	95.59
6.0	94.00	94.69
7.0	93.00	93.81
8.0	92.00	92.91
9.0	91.00	92.02
10.0	90.00	91.12
15.0	85.00	86.60
25.0	75.00	77.38
50.0	50.00	53.273

TABLE I.1 Effect on apparent totals of volatile losses during fusion of samples, assuming errors arise from no other source. (For full details see text)

This method makes no allowance for errors in the analysis from any other source, and for more accurate analysis, particularly of high-volatile rocks, corrections can be made to the disc. If the flux-rock mix is weighed in the crucible before and after fusion, then the weight loss can be made up with flux. This brings the dilution of the non-volatile rock components back to its original value (in the ratio 0.4 : 3.255). Analysis of discs prepared in this way should give a true total, and trueelement oxide percentages, any errors arising from other sources (Padfield & Gray, 1971). This has been demonstrated satisfactorily on very volatile-rich rocks, such as the example in Table I.2.

b) Mass absorption Constants

If a beam of monochromatic X-rays passes through a layer of a substance, the intensity of the beam is reduced by absorption. The reduction in intensity is determined by the quantity of matter traversed by the beam, and if the absorber thickness is considered in terms of mass, then the mass absorption coefficient μ (cm^2/g) can be used as a measure of the absorption. μ is strongly dependent on wavelength, but approximately independent of the physical state of the absorber material. Moreover, to a good approximation, μ is additive with respect to the mass absorption coefficients of the elements composing a substance:

$$\mu = \sum_{i=1}^{m} g_i \mu_i \qquad (I.3)$$

where g_i is the mass fraction contributed by the element i, with mass absorption coefficient μ_i, and the summation is over all m constituent elements. This additivity relationship can be interpreted as stating that the total loss of intensity of the beam is the sum of the losses

incurred by its interaction with the individual atoms in its path.

e.g. μ of SiO_2 absorbing Fe Kα radiation:

$$\mu^{Fe}_{Si} = 117 \quad ; \quad \mu^{Fe}_{O} = 22.4$$

Weight fractions in SiO_2 : Si 0.466 ; O_2 0.533

Then $\mu^{Fe}_{SiO_2} = (0.466 \times 117) + (0.533 \times 22.4) = \underline{66.5}$

The matrix used for mass absorption corrections to the XRF data is built up like this, being the values of μ for each of the ten major element oxides (rows) for the characteristic wavelengths for each of the analysed elements (columns). This matrix is laid out in Table I.3.

Using this matrix, the mass absorption coefficients for any whole rock can be found, knowing the weight fractions of the oxides (again using the additive relation) for any wavelength.

e.g. a rock 50% SiO_2, 25% Al_2O_3, 25% Fe_2O_3, μ for Al Kα

Then $\mu^{Al}_{Rock} = (0.50 \times \mu^{Al}_{SiO_2}) + (0.25 \times \mu^{Al}_{Al_2O_3}) + (0.25 \times \mu^{Al}_{Fe_2O_3})$

For a rock with ten analysed oxides, calculation of the mass absorptipn coefficients for the ten characteristic wavelengths can best be shown in matrix algebra form. For simplicity a system of only two components A and B will be considered, but extension into ten or even more components is straightforward.

$$\begin{bmatrix} W_A & W_B \end{bmatrix} \cdot \begin{bmatrix} \mu_{11} & \mu_{12} \\ \mu_{21} & \mu_{22} \end{bmatrix} = \begin{bmatrix} \mu^A_C & \mu^B_C \end{bmatrix} \qquad \text{(I.4)}$$

or: $\underline{W} \cdot \underline{\mu} = \underline{\mu}_C$ (I.4A)

Emitting element	P	Si	Al	Mg	Mn	Fe	Ti	Ca	K	Na
Kα wavelength, Å	6.155	7.126	8.339	9.889	2.103	1.937	2.750	3.360	3.744	11 909
Absorber										
P_2O_5	482	182	1127	1817	94	75	199	347	468	3056
SiO_2	1668	668	1036	1670	84	67	177	310	418	2811
Al_2O_3	1531	2303	912	1471	77	61	162	283	382	2475
MgO	1386	2087	3236	1245	69	55	145	255	345	2095
MnO	1299	1941	2984	4764	69	55	143	247	332	7929
Fe_2O_3	1365	2040	3138	5012	72	57	150	259	349	8346
TiO_2	855	1280	1974	3160	296	236	93	161	217	5277
CaO	703	1052	1620	2593	274	219	571	133	179	4326
K_2O	619	925	1425	2277	278	222	580	1007	158	3794
Na_2O	1234	1858	2880	4641	61	49	130	227	307	1083
Flux	713	1076	1671	2699	35	28	74	130	176	----
Standard Rock	1493	1174	1430	2114	100	79	203	302	376	3308

TABLE I.2 Mass absorption coefficients used in corrections for mass absorption effects in major element analysis by X-ray fluorescence. (For explanation see text)

Where matrix $\underline{W}$ is the vector of weight fractions of elements A and B in the system, $\underline{\mu}$ is the matrix of mass absorption coefficients for elements A and B acting on themselves and on each other (as described above, and Table I.2), and $\underline{\mu_c}$ is the vector of mass absorption coefficients of the substance for the characteristic wavelengths A $K\alpha$ and B $K\alpha$.

c) Mass Absorption Corrections

In the preceding section and those following, secondary absorption only is considered. This is the absorption by the specimen of the characteristic wavelengths emitted within the specimen upon excitation. Primary absorption, i.e. the absorption by the specimen of the exciting primary polychromatic X-ray beam is not dealt with, as polychromatic absorption is a much more complex process to treat adequately, and ignoring its effects does not generate large errors.

Corrections for secondary absorption are made by an iterative process. An initial vector of estimated compositions $\underline{W^1}$ has its vector of mass absorption coefficients $\underline{\mu^1}$ determined. This mass absorption vector is used to improve the estimate of composition $\underline{W^1}$, to gain a better estimate of composition, $\underline{W^2}$. From $\underline{W^2}$ the associated mass absorption coefficients $\underline{\mu^2}$ are found, and these can be used to improve the estimate of composition, again making the correction to the initial vector, $\underline{W^1}$, this time gaining a new vector of composition, $\underline{W^3}$. Again, $\underline{\mu^3}$ associated with $\underline{W^3}$ is found, and used to improve the estimate, $\underline{W^1}$, to the value $\underline{W^4}$. This process is continued until the true composition, $\underline{W^T}$ is reached (or very closely approached). The initial value $\underline{W^1}$ is derived from the calibration lines relating X-ray intensity to element values. The calculation of $\underline{W^1}$ is to be explained later, when the mass absorption correction procedure has been outlined in mathematical terms.

Considering for simplicity a binary system again, the first step is to calculate the vector of mass absorption coefficients for $\underline{W^1}$, using a rearranged form of equations I.4 and I.4A:

$$\begin{bmatrix} \mu_{11} & \mu_{21} \\ \mu_{12} & \mu_{22} \end{bmatrix} \cdot \begin{bmatrix} W_A \\ W_B \end{bmatrix} + \begin{bmatrix} K_A \\ K_B \end{bmatrix} = \begin{bmatrix} \mu_A^1 \\ \mu_B^1 \end{bmatrix} \qquad (I.5)$$

$$\text{or:} \quad \underline{\tilde{\mu}} \cdot \underline{W^1} + \underline{K} = \underline{\mu^1} \qquad (I.5A)$$

where $\underline{\tilde{\mu}}$ is the transpose of matrix $\underline{\mu}$, the set of mass absorption coefficient terms, and $\underline{K}$ is a set of constants to account for the mass absorption of flux or binder in prepared samples, so that $\underline{\mu^1}$ is the set of coefficients for a prepared fusion disc.

The values in $\underline{\mu^1}$ are ratioed to a set of mass absorption coefficients $\underline{a^{st}}$, for a rock of standard composition in a fusion (the composition of the standard rock is arbitrary, but must remain the same in all calculations involved in a particular calibration). The ratios are used to obtain a better estimate of the true composition $\underline{W^T}$ from $\underline{W^1}$:

$$\left.\begin{array}{l} W_A^1 \cdot \mu_A^1 / a_A \\ \\ W_B^1 \cdot \mu_B^1 / a_B \end{array}\right\} \qquad (I.6)$$

This can be expressed in matrix form as follows:

$$\begin{bmatrix} 1/a_A & 0 \\ 0 & 1/a_B \end{bmatrix} \cdot \begin{bmatrix} W_A^1 & 0 \\ 0 & W_B^1 \end{bmatrix} \cdot \begin{bmatrix} \mu_A^1 \\ \mu_B^1 \end{bmatrix} = \begin{bmatrix} W_A^2 \\ W_B^2 \end{bmatrix} \qquad (I.7)$$

$$\text{or} \quad \underline{K} \cdot \underline{W_d^1} \cdot \underline{\mu^1} = \underline{W^2} \qquad (I.7A)$$

where $\underline{W_d^1}$ is the diagonal form of $\underline{W^1}$

The revised value $\underline{W^2}$ has its mass absorption coefficients calculated, using equations I.5 or I.5A

$$\begin{bmatrix} \mu_{11} & \mu_{21} \\ \mu_{12} & \mu_{22} \end{bmatrix} \cdot \begin{bmatrix} W_A^2 \\ W_B^2 \end{bmatrix} + \begin{bmatrix} K_A \\ K_B \end{bmatrix} = \begin{bmatrix} \mu_A^2 \\ \mu_B^2 \end{bmatrix} \qquad (I.8)$$

or $$\underline{\tilde{\mu}} \cdot \underline{W^2} + \underline{K} = \underline{\mu^2} \qquad (I.8A)$$

Equations I.5A and I.8A can be taken together to give the general equation for calculating mass absorption coefficients:

$$\underline{\tilde{\mu}} \cdot \underline{W^n} + \underline{K} = \underline{\mu^n} \qquad (I.9A)$$

Using values $\underline{\mu^2}$ in equation I.7 gives the new estimate of $\underline{W^T}$, $\underline{W^3}$:

$$\begin{bmatrix} 1/\alpha_A & 0 \\ 0 & 1/\alpha_B \end{bmatrix} \cdot \begin{bmatrix} W_A^1 & 0 \\ 0 & W_B^1 \end{bmatrix} \cdot \begin{bmatrix} \mu_A^2 \\ \mu_B^2 \end{bmatrix} = \begin{bmatrix} W_A^3 \\ W_B^3 \end{bmatrix} \qquad (I.10)$$

or

$$\underline{\alpha} \cdot \underline{W_d^1} \cdot \underline{\mu^2} = \underline{W^3} \qquad (I.10A)$$

Equations I.8A and I.10A can also be reduced to a general form:

$$\underline{\alpha} \cdot \underline{W_d^1} \cdot \underline{\mu^n} = \underline{W^{n+1}} \qquad (I.11A)$$

Using equations I.9A and I.11A alternately for values of n=1,2, ..., m, allows correction of $\underline{W^1}$ to $\underline{W^2}$ ..... to $\underline{W^{m+1}}$, $\underline{W^{m+1}}$ approaching W^T. Note that $\underline{W^2}$ to $\underline{W^m}$ are intermediate approximations, it being $\underline{W^1}$ that is corrected in I.11A each time.

The difference between $\underline{W^n}$ and $\underline{W^{n+1}}$ decrease as n increases, approaching zero as $\underline{W^T}$ is reached; the differences are dtermined by the ratio $\underline{\mu^n/\alpha}$, which approach a constant value as n increases.

In practice very few iterations are needed, and $\underline{W^3}$ is a very good approximation to $\underline{W^T}$, certainly to a lower degree of significance than other errors associated with the XRF method.

d) Derivation of analyses for calibration

To gain the first approximate composition $\underline{W^1}$ for an unknown sample, calibration regression lines of characteristic intensity against $\underline{W^1}$ for a series of standard rocks are used. Given the known value $\underline{W^T}$ for a standard rock, $\underline{W^1}$ can be found such that applying mass absorption corrections to $\underline{W^1}$ will give $\underline{W^T}$.

It is important to note that the relationship between $\underline{W^T}$ and $\underline{W^1}$ is unique for any $\underline{W^T}$, so that changing even one element in the vector $\underline{W^T}$ will cause a change in some degree of all the elements in $\underline{W^1}$. $\underline{W^1}$ can be derived empirically, using only one or two standard analyses, but the simplicity of recalculation makes calibration much easier, using a large range of standard compositions, so that any one element can be determined from the same calibration line for a large variety of rock types. The greatest advantage of the method lies in the fact that remarkably straight lines are produced, allowing extrapolation well beyond the calibrated limits of the line with little loss in accuracy. The lines are so straight because the regression is one of intensity (counts/second) against composition as "seen" by the detector. The same proportion of an element in two very different rock types will emit very different amounts of radiation to the detector, because of differing absorption by the different rocks. By eliminating the effect of these absorption differences the "apparent" proportions can be found.

Taking equation I.10A

$$\underline{\alpha} \cdot \underline{W_d^1} \cdot \underline{\mu^2} = \underline{W^3} \qquad \text{(I.10A)}$$

and replacing $\underline{\mu^2}$ by its equivalent from equation 9A (n = 2) gives:

$$\underline{\alpha} \cdot \underline{W_d^1} \cdot (\underline{\tilde{\mu}} \cdot \underline{W^2} + \underline{K}) = \underline{W^3} \qquad \text{(I.12A)}$$

so that

$$\underline{W_d^1} = (\underline{\alpha})^{-1} \cdot \underline{W^3} \cdot (\underline{\mu} \cdot \underline{W^2} + \underline{K})^{-1} \qquad \text{(I.13A)}$$

Now, since $\underline{W^2} = \underline{W^3}$ approximately, and $\underline{W^3} = \underline{W^T}$ to a very good approximation, $\underline{W^2}$ can be replaced by $\underline{W^3}$ in equation I.13A to give an initial estimate of $\underline{W^1_d}$.

Thus:

$$\underline{W^1_d} = (\underline{\alpha})^{-1} \cdot \underline{W^3} \cdot (\underline{\tilde{\mu}} \cdot \underline{W^3} + \underline{K})^{-1} \qquad \text{(I.13B)}$$

This rough approximation to $\underline{W^1_d}$ can be used (as $\underline{W^1}$) first in equation I.5 to find an approximate $\underline{\mu^1}$, then in equation I.7 to find a better value of $\underline{W^2}$.

This procedure can now be repeated; using improved $\underline{W^2}$ in equation I.12A gives a better estimate of $\underline{W^1_d}$ and $\underline{W^1}$. This $\underline{W^1}$ can be used in turn to improve the estimate of $\underline{W^2}$ and so on. After only three or four such iterations, $\underline{W^1}$ and $\underline{W^2}$ converge on their real values, and a check can be made that applying corrections to $\underline{W^1}$ through $\underline{W^2}$ does give $\underline{W^3} = \underline{W^T}$.

The program MUBACK performs this iterative procedure, using an analysis of a rock standard $\underline{W^{T'}}$, correcting for volatile losses to find $\underline{W^T}$, and then generating $\underline{W^1}$ for regression against drift corrected counts for that rock.

e) Results of MUBACK technique

Table I.3 illustrates the changes produced by using this technique to process analyses of standard rocks before using them in calibration regressions. For all elements except MgO there is an improvement in the standard error of regression , the mean residual associated with the regression line and the linear regression coefficient, indicating a more linear correlation between fluorescent yield and element percentage (or apparent percentage).

Variable	Linear Correlation Coefficient		Standard Error of Regression		Mean Residual		Range(%)
	A	B	A	B	A	B	
SiO_2	.99964	.99981	.0035	.0027	.265	.191	35-72
TiO_2	.99900	.99913	.0060	.0042	.055	.046	0-4.5
Al_2O_3	.99924	.99963	.0093	.0065	.251	.182	0-25
ΣFe_2O_3	.99920	.99935	.0040	.0036	.226	.151	0-35
MnO	.99730	.99776	.0030	.0020	.010	.008	0-.6
MgO	.99987	.99972	.0068	.0102	.146	.156	0-45
CaO	.99967	.99980	.0039	.0031	.119	.095	0-15
K_2O	.99942	.99966	.0064	.0048	.069	.057	0-10
P_2O_5	.99267	.99277	.0108	.0107	.140	.044	0-2.5

TABLE I.3 Comparison of parameters for calibration regression lines (counts vs. %)

A) Untransformed data.

B) Data corrected for volatile losses and by MUBACK mass absorption method.

In order to make some assessment of analytical error, 14 samples were analysed by classical wet chemical techniques, and these samples were repeatedly analysed by XRF, at random during the running of the other samples analysed in this study. The results are given in Table I. 5, showing the analyses by wet methods, their equivalents corrected for volatile losses during fusion (which should be the answer obtained by XRF) and the results of the XRF analyses, and table I. 4 gives the relative error associated with each element on the basis of these results. Table I. 4 uses the mean analysis of the samples from the Lochailort and Garnetiferous Pelites to indicate the effect of these errors on a typical analysis.

	Mean Relative Error (%)	Mean Pelite	± Error (%)
SiO_2	.43	60.83	± .26
TiO_2	5.60	.97	.05
Al_2O_3	.85	18.50	.16
Fe_2O_3	3.22	7.81	.25
MnO	5.10	.12	.01
MgO	5.62	2.28	.13
CaO	1.68	2.31	.04
Na_2O	5.17	2.70	.14
K_2O	2.68	3.44	.09
P_2O_5	8.30	.27	.02

TABLE I.4 Relative errors for major element analyses, with typical expected error for mean analysed pelite. Mean pelite analysis is the mean of the 54 analyses in Table III.1. Mean error is derived from analyses in Table I.5, where error is given by: $\frac{(\text{actual\%} - \text{XRF\%})}{\text{actual\%}} \times 100\%$ for each oxide.

TABLE I.5

Tables of major element analyses of rocks analysed by conventional techniques and by the X ray fluorescence method described. The "actual percentages" are derived from the conventional analysis using the program MUBACK, and are the values which an XRF analysis should give if the only errors were those attributable to loss of volatiles during sample preparation.

TABLE I.5.1

	1.	2.	3.	4.	5.	6.	7.
	A304	A304	A304	A304	A304	A3C4	A304
MAJOR ELEMENT ANALYSES							
SiO2	64.56	64.64	64.27	64.77	64.49	64.58	65.27
TiO2	0.85	C.85	0.75	C.80	0.79	0.77	0.79
Al2O3	17.58	17.60	17.73	17.90	17.62	17.70	17.59
Fe2O3	0.66	5.35	5.30	5.36	5.35	5.48	5.60
FeO	4.21	0.00	0.00	0.00	0.00	0.00	0.00
MnO	0.07	0.07	0.C7	0.07	0.07	0.06	0.06
MgO	1.83	1.83	1.78	1.88	1.87	1.64	1.61
CaO	2.27	2.27	2.22	2.23	2.25	2.36	2.29
Na2O	3.27	3.27	3.C2	3.72	3.27	3.05	3.09
K2O	3.08	3.08	3.02	3.01	3.02	3.16	3.25
H2O+	1.59	0.00	0.00	0.00	0.00	0.00	0.00
H2O-	0.03	0.00	0.00	0.00	0.00	0.00	0.00
P2O5	0.14	0.14	0.14	0.14	0.13	0.10	0.10
TOTAL	100.14	99.10	98.30	99.88	98.86	98.90	99.65
CaO/Al2O3	0.129	0.129	0.125	C.125	0.128	0.133	0.130

1. A304 PELITE,UPPER MORAR SCHISTS. WET ANALYSIS.
2. A304 ACTUAL PERCENT
3. A304 XRF ANALYSIS
4. A304 XRF ANALYSIS
5. A304 XRF ANALYSIS
6. A304 XRF ANALYSIS
7. A304 XRF ANALYSIS

	1.	2.	3.	4.	5.	6.	7.
	A305	A305	A305	A305	A305	A305	A305
MAJOR ELEMENT ANALYSES							
SiO2	63.49	63.61	63.50	63.76	63.49	63.83	63.73
TiO2	0.86	0.86	0.84	0.82	0.85	0.85	0.82
Al2O3	18.55	18.59	18.39	19.19	18.50	18.68	18.51
Fe2O3	0.82	5.33	5.35	5.46	5.39	5.34	5.47
FeO	4.05	0.00	0.00	0.00	0.00	0.00	0.00
MnO	0.07	0.07	0.06	0.07	0.06	0.07	0.06
MgO	1.80	1.80	1.79	1.43	1.82	1.82	1.64
CaO	1.67	1.67	1.69	1.62	1.67	1.69	1.73
Na2O	2.53	2.53	2.06	2.10	2.46	2.55	2.68
K2O	4.01	4.02	4.01	4.07	3.97	3.93	4.07
H2O+	1.98	0.00	0.00	0.00	0.00	0.00	0.00
H2O-	0.05	0.00	0.00	0.00	0.00	0.00	0.00
P2O5	0.16	0.16	0.16	0.18	0.16	0.16	0.10
TOTAL	100.04	98.64	97.85	98.70	98.37	98.92	98.81
CaO/Al2O3	0.090	0.090	0.092	0.084	0.090	0.090	0.093

1. A305 PELITE, UPPER MORAR SCHISTS. WET ANALYSIS.
2. A305 ACTUAL PERCENT
3. A305 XRF ANALYSIS
4. A305 XRF ANALYSIS
5. A305 XRF ANALYSIS
6. A305 XRF ANALYSIS
7. A305 XRF ANALYSIS

TABLE I.5.2

	1.	2.	3.	4.	5.	6.	7.	8.	9.	10.
	121K	121K	121K	121K	121K	211K	211K	211K	211K	211K
MAJOR ELEMENT ANALYSES										
SiO2	62.20	62.25	62.12	62.25	62.39	56.19	56.35	56.26	56.11	56.27
TiO2	0.96	0.96	0.95	0.97	0.97	1.16	1.16	1.18	1.16	1.16
Al2O3	17.61	17.62	17.64	17.48	17.69	20.01	20.07	20.02	19.96	19.92
Fe2O3	0.69	7.25	7.14	7.22	7.31	1.44	10.20	9.66	10.21	10.10
FeO	5.90	0.00	0.00	0.00	0.00	7.86	0.00	0.00	0.00	0.00
MnO	0.11	0.11	0.11	0.12	0.12	0.15	0.15	0.14	0.14	0.14
MgO	2.07	2.07	2.02	1.99	2.02	2.42	2.43	2.39	2.42	2.41
CaO	2.78	2.78	2.77	2.85	2.79	1.64	1.64	1.63	1.69	1.70
Na2O	3.45	3.45	3.28	3.35	3.32	1.99	2.00	1.83	2.07	2.10
K2O	2.75	2.75	2.74	2.75	2.70	3.64	3.65	3.63	3.68	3.72
P2O5	0.22	0.22	0.22	0.22	0.22	0.28	0.28	0.29	0.30	0.30
TOTAL	98.74	99.46	98.99	99.20	99.53	96.78	97.93	97.03	97.74	97.82
CaO/Al2O3	0.158	0.158	0.157	0.163	0.158	0.082	0.082	0.081	0.085	0.085

TABLE I.5.3

1. 121K PELITE, LOCHAILORT PELITIC GROUP. WET MAJORS
2. 121K ACTUAL PERCENT
3. 121K XRF ANALYSIS
4. 121K XRF ANALYSIS
5. 121K XRF ANALYSIS
6. 211K PELITE, LOCHAILORT PELITIC GROUP. WET MAJORS
7. 211K ACTUAL PERCENT
8. 211K XRF ANALYSIS
9. 211K XRF ANALYSIS
10. 211K XRF ANALYSIS

	1.	2.	3.	4.	5.	6.	7.	8.	9.	10.
	231K	231K	231K	231K	231K	412K	412K	412K	412K	412K
MAJOR ELEMENT ANALYSES										
SiO2	71.62	71.61	71.73	70.95	71.13	62.24	62.34	61.64	62.13	62.51
TiO2	0.52	0.52	0.53	0.56	0.58	0.89	0.89	0.87	0.92	0.93
Al2O3	14.73	14.73	14.75	14.44	14.34	17.81	17.84	17.82	17.72	17.72
Fe2O3	0.47	3.96	3.83	3.88	3.87	1.11	6.83	6.80	6.86	6.79
FeO	3.14	0.00	0.00	0.00	0.00	5.14	0.00	0.00	0.00	0.00
MnO	0.10	0.10	0.10	0.10	0.10	0.09	0.09	0.08	0.09	0.10
MgO	1.10	1.10	1.18	1.11	1.08	2.19	2.19	2.33	2.17	2.19
CaO	2.58	2.58	2.56	2.56	2.57	2.25	2.25	2.22	2.24	2.22
Na2O	3.67	3.67	3.57	3.63	3.62	2.31	2.31	2.00	2.04	2.02
K2O	1.80	1.80	1.72	1.83	1.84	3.82	3.83	3.81	3.85	3.82
P2O5	0.09	0.09	0.10	0.09	0.10	0.29	0.29	0.28	0.29	0.28
TOTAL	99.82	100.16	100.07	99.15	99.23	98.14	98.86	97.85	98.31	98.58
CaO/Al2O3	0.175	0.175	0.174	0.177	0.179	0.126	0.126	0.125	0.126	0.125

1. 231K SEMIPELITE, LOCHAILORT PELITIC GROUP. WET ANALYSIS.
2. 231K ACTUAL PERCENT
3. 231K XRF ANALYSIS
4. 231K XRF ANALYSIS
5. 231K XRF ANALYSIS
6. 412K PELITE, GARNETIFEROUS PELITE. WET MAJORS
7. 412K ACTUAL PERCENT
8. 412K XRF ANALYSIS
9. 412K XRF ANALYSIS
10. 412K XRF ANALYSIS

TABLE I.5.4

	1.	2.	3.	4.	5.	6.	7.	8.	9.	10.
	622K	622K	622K	622K	622K	631K	631K	631K	631K	631K
MAJOR ELEMENT ANALYSES										
SiO2	59.55	59.64	60.23	59.92	59.89	60.53	60.64	60.66	60.93	60.22
TiO2	0.97	0.97	0.95	0.97	0.98	0.97	0.97	0.94	0.96	0.96
Al2O3	18.50	18.53	18.53	18.57	18.48	18.01	18.04	18.03	18.16	18.13
Fe2O3	1.62	8.28	8.32	8.29	8.50	1.55	7.81	8.03	7.88	7.84
FeO	5.98	0.00	0.00	0.00	0.00	5.62	0.00	0.00	0.00	0.00
MnO	0.14	0.14	0.13	0.14	0.14	0.12	0.12	0.12	0.12	0.12
MgO	2.47	2.47	2.39	2.49	2.50	2.35	2.35	2.28	2.38	2.35
CaO	2.50	2.50	2.57	2.49	2.54	2.49	2.49	2.63	2.49	2.45
Na2O	2.63	2.63	2.82	2.73	2.75	2.54	2.54	2.77	2.78	2.73
K2O	3.41	3.42	3.48	3.39	3.42	3.44	3.45	3.66	3.52	3.54
P2O5	0.34	0.34	0.31	0.34	0.34	0.33	0.33	0.31	0.32	0.32
TOTAL	98.11	98.92	99.73	99.33	99.54	97.95	98.74	99.43	99.54	98.66
CaO/Al2O3	0.135	0.135	0.139	0.134	0.137	0.138	0.138	0.146	0.137	0.135

TABLE I.5.5

1.	622K	PELITE, GARNETIFEROUS PELITE.	WET MAJORS
2.	622K	ACTUAL PERCENT	
3.	622K	XRF ANALYSIS	
4.	622K	XRF ANALYSIS	
5.	622K	XRF ANALYSIS	
6.	631K	PELITE, GARNETIFEROUS PELITE.	WET MAJORS
7.	631K	ACTUAL PERCENT	
8.	631K	XRF ANALYSIS	
9.	631K	XRF ANALYSIS	
10.	631K	XRF ANALYSIS	

	1.	2.	3.	4.	5.	6.	7.	8.	9.	10.
	B341	B341	B341	B341	B341	498	498	498	498	498
MAJOR ELEMENT ANALYSES										
SiO2	70.92	70.96	71.06	71.29	71.00	87.08	87.14	85.33	87.12	87.14
TiO2	0.49	0.49	0.48	0.46	0.44	0.23	0.23	0.22	0.22	0.23
Al2O3	15.14	15.15	15.38	15.58	15.65	7.38	7.38	7.38	7.40	7.43
Fe2O3	0.16	2.85	2.87	2.80	2.91	0.16	1.18	1.13	1.20	1.26
FeO	2.42	0.00	0.00	0.00	0.00	0.92	0.00	0.00	0.00	0.00
MnO	0.07	0.07	0.07	0.05	0.07	0.02	0.02	0.02	0.02	0.03
MgO	0.80	0.80	0.80	0.82	0.97	0.33	0.33	0.17	0.33	0.33
CaO	3.44	3.44	3.43	3.46	3.46	0.72	0.72	0.68	0.71	0.71
Na2O	4.35	4.35	4.37	4.39	4.10	1.21	1.21	1.13	1.27	1.25
K2O	1.27	1.27	1.22	1.22	1.21	1.29	1.29	1.28	1.34	1.33
H2O+	0.52	0.00	0.00	0.00	0.00	0.00	0.00	0.00	0.00	0.00
H2O-	0.02	0.00	0.00	0.00	0.00	0.00	0.00	0.00	0.00	0.00
P2O5	0.23	0.23	0.22	0.22	0.26	0.03	0.03	0.03	0.03	0.03
TOTAL	99.83	99.61	99.90	100.29	100.07	99.37	99.53	97.37	99.64	99.74
CaO/Al2O3	0.227	0.227	0.223	0.222	0.221	0.098	0.098	0.092	0.096	0.096

1. B341 SEMIPELITE E.RANOCHAN PELITE. WET MAJORS
2. B341 ACTUAL PERCENT
3. B341 XRF ANALYSIS
4. B341 XRF ANALYSIS
5. B341 XRF ANALYSIS
6. 498 PSAMMITE, LOCHAILORT PELITIC GROUP. WET MAJORS
7. 498 ACTUAL PERCENT
8. 498 XRF ANALYSIS
9. 498 XRF ANALYSIS
10. 498 XRF ANALYSIS

	1.	2.	3.	4.	5.	6.	7.	8.
	A331	A331	A331	A331	A332	A332	A332	A332
MAJOR ELEMENT ANALYSES								
SiO2	78.47	78.53	77.81	78.52	84.88	84.91	85.27	84.99
TiO2	0.16	0.16	0.13	0.12	0.10	0.10	0.09	0.07
Al2O3	11.65	11.66	11.84	11.90	8.74	8.74	8.83	8.73
Fe2O3	0.42	1.21	1.22	1.10	0.01	0.67	0.84	0.67
FeO	0.71	0.00	0.00	0.00	0.59	0.00	0.00	0.00
MnO	0.13	0.13	0.13	0.12	0.06	0.06	0.06	0.05
MgO	0.21	0.21	0.23	0.18	0.23	0.23	0.23	0.20
CaO	4.47	4.47	4.39	4.57	2.63	2.63	2.65	2.75
Na2O	2.32	2.32	2.45	2.47	1.79	1.79	1.67	1.67
K2O	0.63	0.63	0.60	0.58	0.62	0.62	0.65	0.61
H2O+	0.72	0.00	0.00	0.00	0.34	0.00	0.00	0.00
H2O-	0.04	0.00	0.00	0.00	0.01	0.00	0.00	0.00
P2O5	0.10	0.10	0.11	0.08	0.02	0.02	0.00	0.00
TOTAL	100.03	99.42	98.91	99.64	100.02	99.77	100.29	99.74
CaO/Al2O3	0.384	0.383	0.371	0.384	0.301	0.301	0.300	0.315

1. A331 CALCSILICATE, UPPER PSAMMITIC GROUP. WET ANALYSIS
2. A331 ACTUAL PERCENT
3. A331 XRF ANALYSIS
4. A331 XRF ANALYSIS
5. A332 CALCSILICATE, UPPER PSAMMITIC GROUP. WET ANALYSIS
6. A332 ACTUAL PERCENT
7. A332 XRF ANALYSIS
8. A332 XRF ANALYSIS

TABLE I.5.7

	1.	2.	3.	4.	5.	6.	7.	8.
	A334	A334	A334	A334	A344	A344	A344	A344
MAJOR ELEMENT ANALYSES								
SiO2	69.73	69.67	70.46	69.42	73.87	74.07	73.64	73.44
TiO2	0.24	0.24	0.26	0.21	0.48	0.48	0.49	0.47
Al2O3	17.11	17.10	17.29	17.21	12.60	12.63	12.63	12.51
Fe2O3	0.38	1.67	1.42	1.34	0.46	2.85	2.68	2.87
FeO	1.16	0.00	0.00	0.00	2.14	0.00	0.00	0.00
MnO	0.16	0.16	0.15	0.15	0.20	0.20	0.20	0.19
MgO	0.38	0.38	0.38	0.26	0.87	0.87	0.85	0.87
CaO	5.56	5.56	5.56	5.61	3.86	3.87	3.79	3.96
Na2O	4.00	4.00	3.86	3.97	0.47	0.47	0.50	0.51
K2O	0.60	0.60	0.56	0.53	2.52	2.53	2.54	2.67
H2O+	0.56	0.00	0.00	0.00	0.00	0.00	0.00	0.00
H2O-	0.03	0.00	0.00	0.00	0.06	0.00	0.00	0.00
P2O5	0.23	0.23	0.22	0.20	0.13	0.13	0.16	0.09
TOTAL	100.14	99.61	100.16	98.90	97.66	98.10	97.48	97.58
CaO/Al2O3	0.325	0.325	0.322	0.326	0.306	0.306	0.300	0.317

1. A334 CALCSILICATE, UPPER PSAMMITIC GROUP. WET ANALYSIS
2. A334 ACTUAL PERCENT
3. A334 XRF ANALYSIS
4. A334 XRF ANALYSIS
5. A344 CALCSILICATE, UPPER MORAR SCHISTS. WET ANALYSIS.
6. A344 ACTUAL PERCENT
7. A344 XRF ANALYSIS
8. A344 XRF ANALYSIS

TABLE I.5.8

TABLE I.6

Listing of program MUBACK

MUBACK is the program written to implement the procedures described in Appendix I for deriving "Apparent" analyses from "True" analyses. The "Apparent" analysis is that which will give the true analysis when mass absorption corrections are applied, and also takes into account errors arising from loss of volatiles during fusion of the rock powder and flux mixture used.

Matrices $\underline{W}^1$, $\underline{W}^2$ and $\underline{W}^3$ are represented by arrays W1, W2 and W3.

$\underline{\mu}$ and $\underline{\tilde{\mu}}$ are the arrays MU and MUTRAN.

$\underline{\alpha}$ is the array STMU

$\underline{K}$ is not specifically represented, but is implicitly involved when deriving mass absorption coefficients for a fused disc in the subroutine MUFORD.

```
      PROGRAM MUBACK

C     MUBACK ACCEPTS STANDARD ANALYSES IN BEDFORD COLLEGE DATA FORMAT
C     I.E.  1 - TITLE CARD, 2 - MAJOR ELEMENTS, 3+4 - TRACE ELEMENTS
C     THESE ARE PROCESSED FOR USE IN XRF CALIBRATIONS, MAKING CORRECTIONS
C     FOR VOLATILE LOSS DURING FUSION, AND THEN PERFORMING MASS ABSORPTION
C     CORRECTION 'IN REVERSE' TO OBTAIN VALUES WHICH ARE RELATED TO A
C     COMMON MASS ABSORPTION VALUE, AND SHOULD THUS  GIVE A LINEAR
C     RELATIONSHIP BETWEEN X RAY YIELD AND APPARENT ELEMENT VALUE (W1).

      COMMON MU(10,10),MUTRAN(10,10),W1(10),W2(10),W3(10),STMU(10),
     1 FLUXMA(10),C(10),D(10),E(10),EL(14,9),SORB(13,10),DISCWT,FLUXWT,RKWT
      COMMON/A/ STMUI(10,10)
      REAL MU(10,10),MUTRAN(10,10),ELNAME(14),RKNAME(10)
      DATA STMUI/100*0.0/

C     DISCWT IS WEIGHT OF DISC BEFORE FUSION = 3.255 GRAMS
      DISCWT=3.255

C     FLUXWT IS WEIGHT OF FLUX IN DISC BEFORE FUSION = 2.855 GM
      FLUXWT=2.855

C     RKWT IS WEIGHT OF ROCK IN DISC BEFORE FUSION = 0.400 GRAMS
      RKWT=0.400


C     READ ELEMENT NAMES FOR TITLES
      READ 500,(ELNAME(J),J=1,14)

C     READ IN ARRAY OF MASS ABSORPTION COEFFICIENTS, SORB
      READ 501,((SORB(K,J),J=1,10),K=1,12)
      DO 200 J=1,10

C     FLUXMA IS VECTOR OF M.A. COEFFS. OF FUSION FLUX IN DISC
      FLUXMA(J)=SORB(11,J)*FLUXWT

C     STMU IS VECTOR OF M.A.COEFFS. OF A DISC OF THE STANDARD ROCK
      STMU(J)=(SORB(12,J)*RKWT+FLUXMA(J))/DISCWT

C     STMUI IS DIAGONAL FORM OF ARRAY STMU
      STMUI(J,J)=STMU(J)

C     FORM ARRAY MU, AND ITS TRANSPOSE MUTRAN
      DO 200 I=1,10
      MU(I,J)=SORB(I,J)
      MUTRAN(J,I)=SORB(I,J)
200   CONTINUE

C     READ IN DATA IN STANDARD FORMAT
100   READ 502,(RKNAME(J),J=1,10)
C     CHECK FOR END OF INPUT ( 'FINISH' CARD)
      IF(RKNAME(1).EQ.8HFINISH    )STOP
      READ 503,EL(2,1),EL(7,1),EL(3,1),EL(6,1),EL(11,1),EL(5,1),EL(4,1),
     1EL(8,1),EL(10,1),EL(9,1),EL(12,1),EL(13,1),EL(1,1),EL(14,1)

C     PRINT OUT ORIGINAL INPUT DATA
      PRINT 600,RKNAME,ELNAME
      TOTAL1=TOTAL2=TOTAL3=TOTAL4=0.0
```

```
C   CALCULATE TOTAL FE2O3
      EL(6,1)=EL(6,1)+(EL(11,1)*1.1113)
      DO 201 K=1,14

C   FIND TOTAL OF ANALYSIS(TOTAL1) + TOTAL VOLATILES(TOTAL2)
201   TOTAL1=TOTAL1+EL(K,1)
      TOTAL2=EL(12,1)+EL(14,1)


C   FEO TAKEN FROM TOTAL1,SINCE TOTAL FE2O3 CONSIDERED
      TOTAL1=TOTAL1-EL(11,1)

C   PRINT ORIGINAL DATA
      PRINT 601,(EL(K,1),K=1,14),TOTAL1

C   ROCKS DRIED AT 105 C SO H2O- ALSO TAKEN FROM TOTAL1
      TOTAL1=TOTAL1-EL(13,1)

C   REMOVE VOLATILES FROM TOTAL1
      TOTAL1=TOTAL1-TOTAL2

C   CONVERT PERCENTS OF OXIDES TO ACTUAL PERCENTS IN DISC
      DO 203 K=1,10
203   EL(K,1)=EL(K,1)*DISCWT/(FLUXWT+(RKWT*TOTAL1/100.))

C   PRINT ACTUAL PERCENTS
      PRINT 602,(EL(K,1),K=1,10)
C
C   NEXT MAKE CORRECTIONS TO ACTUAL PERCENTS TO GIVE
C   COMPOSITIONS WHICH WILL RETURN TO 'ACTUAL' ANALYSIS WHEN MASS
C   ABSORPTION CORRECTION IS APPLIED
C
C   FOR FIRST ITERATION MAKE APPROXIMATION THAT W2=W3=ACTUAL %
      DO 204 J=1,10
      W2(J)=EL(J,1)
204   W3(J)=EL(J,1)

C   GMPRD IS A LIBRARY ROUTINE FOR GENERAL MATRIX PRODUCTS
      CALL GMPRD(STMUI,W3,B,10,10,1)

C   THIS LOOP MAKES TEN ITERATIONS TO FIND W1
      DO 207 KOUNT=1,10
      CALL GMPRD(MUTRAN,W2,C,10,10,1)

C   MAKE AN ESTIMATE OF W1, USING W2(APPROXIMATE) AND W3(KNOWN)
      DO 205 J=1,10
      D(J)=(C(J)*RKWT/100.+FLUXMA(J))/DISCWT
      W1(J)=B(J)/D(J)
205   EL(J,3)=W1(J)

C   USE ESTIMATED W1 TO RE-APPROXIMATE W2
      CALL MUFORD(3)
      DO 206 I=1,10
206    W2(I)=EL(I,4)

C  USE W2 TO FIND "W3" FOR CHECKING ACCURACY LATER
C   THEN REITERATE, TO USE W2 IN FINDING NEW ESTIMATE OF W1
      CALL MUFORD(4)
207    CONTINUE
```

```
C
C   PRINT W1, THE ANALYSIS TO BE USED FOR CALIBRATION
      PRINT 603,(W1(I),I=1,10)


C   CHECK THAT %DIFFERENCE BETWEEN ORIGINAL AND DERIVED DATA IS <0.0001
      ISKIP=0
      DO 208 J=1,10
      EL(J,6)=EL(J,1)-EL(J,5)
      EL(J,7)=100.0*EL(J,6)/EL(J,1)
      IF(ABS(EL(J,6)).GT.0.0001 ) ISKIP=ISKIP+1
208   CONTINUE

C   IF ACCURACY OK, GO FOR MORE DATA, OTHERWISE PRINT OUT DIAGNOSTICS
      IF(ISKIP.EQ.0) GO TO 100
      PRINT 604
      PRINT 605,(EL(K,4),K=1,10)
      PRINT 606,(EL(K,5),K=1,10)
      PRINT 607,(EL(K,6),K=1,10)
      PRINT 608,(EL(K,7),K=1,10)
      GO TO 100

C    INPUT FORMATS
500   FORMAT(14A5)
501   FORMAT(10F8.0)
502   FORMAT(10A8)
503   FORMAT(14F4.2,//)

C    OUTPUT FORMATS
600   FORMAT(//10X,10A8/17X,14A7/)
601   FORMAT(15H ORIGINAL DATA   ,14F7.2,' TOTAL ',F7.2)
602   FORMAT(18H ACTUAL PERCENT    ,F4.2,9F7.2)
603   FORMAT(/15H      W1=          10F7.3/)
604   FORMAT(/45H *** CLOSURE INCOMPLETE - CHECK DATA FOLLOWS: /)
605   FORMAT(15H      W2=               10F7.3)
606   FORMAT( 15H   CHECK W3           10F7.3)
607   FORMAT( 15H W3-NEW W3          10F7.4)
608   FORMAT( 15H  > DIFFERENCE      10F7.4//)

      END
```

```
      SUBROUTINE MUFORD(JR)

C     MUFORD RUNS THE MASS ABSORPTION CORRECTION AS USED IN THE MAIN
C     XRF PROGRAM, BOTH FOR REFINING W2 BY ITERATION FROM W1, AND FOR
C     CHECKING FINAL W1 WILL RESULT IN ORIGINAL DATA W3

      COMMON MU(10,10),MUTRAN(10,10),W1(10),W2(10),W3(10),STMU(10),
     1 FLUXMA(10),C(10),D(10),E(10),EL(14,9),SORB(13,10),DISCWT,FLUXWT,RKWT
      REAL MU(10,10),MUTRAN(10,10)

C   JD COUNTS ABSORBER OXIDES 1 - 10
      DO 201 JD=1,10
      RKMA=DISCMA=0.0

C   JQ COUNTS EMITTER ELEMENTS 1 - 10
      DO 200 JQ=1,10
C   RKMA IS THE MASS ABSORPTION FOR THE ROCK ACTING ON ELEMENT JQ
      RKMA=RKMA+MC*SORB(JQ,JD)
200   CONTINUE
C   DISCMA IS THE MASS ABSORPTION FOR THE FUSION DISC ON JQ
      DISCMA=((RKMA*RKWT/100.)+FLUXMA(JD))/DISCWT
      EL(JD,JR+1)=EL(JD,3)*DISCMA/STMU(JD)
201   CONTINUE
      RETURN
      END
```

P2O5	SIO2	AL2O3	MGO	MNO	FE2O3	TIO2	CAO	K2O	NA2O	FEO	H2O+	H2O-	CO2	
	482	182	1127		1817		94	75		199	347	468		3056.0
	1668	668	1036		1670		84	67		177	310	418		2811.0
	1531	2303	912		1471		77	61		162	283	382		2475.0
	1386	2087	3236		1245		69	55		145	255	345		2095.0
	1299	1941	2984		4764		69	55		143	247	332		7928.9
	1365	2040	3138		5012		72	57		150	259	349		8345.9
	355	1280	1974		3160		296	236		93	161	217		5277.0
	703	1052	1620		2593		274	219		571	133	179		4326.0
	619	925	1425		2277		278	222		580	1007	158		3794.0
	1234	1858	2880		4641		61	49		130	227	307		1083.0
	713	1076	1671		2699		34.9	27.8		74.2	130	176		
	1493	1174	1430		2114		100	79		203	302	376		3307.9

Appendix II

Linear Discriminant Function Method

R.A. Fisher (1936) first formulated the theory of the linear discriminant function, and applications to geological problems with simple accounts of the theory may be found in Davis (1973), Krumbein and Graybill (1965) and Miller and Kahn (1962).

The problem essentially consists of: two populations, known to be different on a priori grounds, are sampled. For the samples from population A a number of characters on each of the n_a individuals is measured, and the same characters are measured on each of the n_b individuals of population B. The linear discriminant function provides an "index" which allows any new specimen to be assigned to either population A or B.

Consider a situation where only two characters, x and y, are measured for samples A and B, and plotted on a scattergram, showing a certain amount of overlap (Figure II.1). This overlap may be considered in terms of the degree of separation between the two clusters, and the spread within them. If the scattergram is considered as a plane (2 dimensions) and a third dimension Z is introduced (Figure II.2), then projecting the points from the x,y plane onto Z may achieve a better separation of the two clusters. Optimum separation is achieved by that plane which maximises separation between clusters, and minimises spread within clusters.

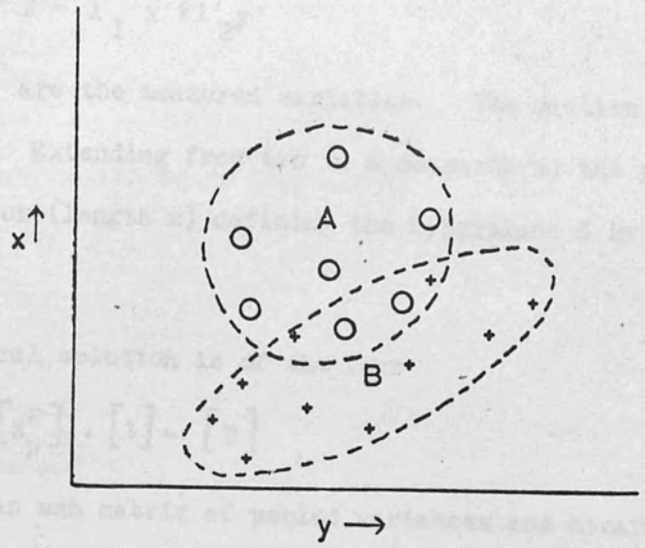

Figure II.1 Scattergram with two groups (A and B) showing overlap.

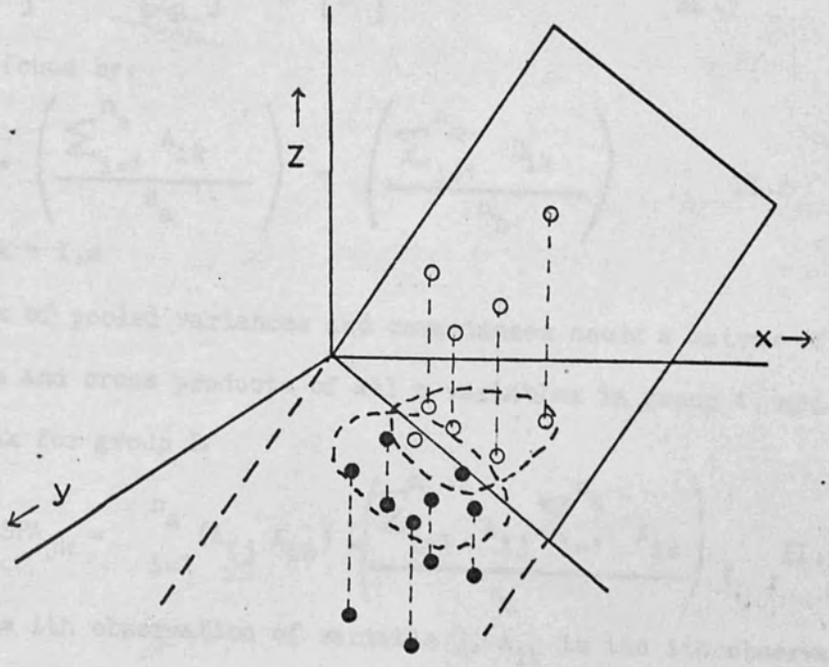

Figure II.2 Projection of points from scattergram onto plane

Let the plane be represented by:

$$Z = \lambda_1 x + \lambda_2 y \qquad \text{II.1}$$

where x and y are the measured variables. The problem is then to find λ_1 and λ_2. Extending from two to m characters, the problem is to find the vector (length m) defining the hyperplane Z in m-dimensional space.

The general solution is of the form

$$\left[S_p^2\right] \cdot \left[\lambda\right] = \left[D\right] \qquad \text{II.2}$$

Where $\left[S_p^2\right]$ is an mxm matrix of pooled variances and covariances of the m variables, the column vector $\left[\lambda\right]$ holds the coefficients of the discriminant equation as defined above, and $\left[D\right]$ is the column vector of the differences between the means of the two groups.

The equation is solved for $\left[\lambda\right]$ simply by inversion and multiplication:

$$\left[\lambda\right] = \left[S_p^2\right]^{-1} \cdot \left[D\right] \qquad \text{II.3}$$

The means are found by:

$$D_k = \bar{A}_k - \bar{B}_k = \left(\frac{\sum_{i=1}^{n_a} A_{ik}}{n_a}\right) - \left(\frac{\sum_{i=1}^{n_b} B_{ik}}{n_b}\right) \qquad \text{II.4}$$

For values of k = 1,m

The matrix of pooled variances and covariances needs a matrix of sums of squares and cross products of all m variables in group A, and a similar matrix for group B.

For A,

$$SPA_{jk} = \sum_{i=1}^{n_a} (A_{ij} A_{ik}) - \left(\frac{\sum_{i=1}^{n_a} A_{ij} \sum_{i=1}^{n_a} A_{ik}}{n_a}\right) \qquad \text{II.5}$$

where A_{ij} is the ith observation of variable j, A_{ik} is the ith observation of variable k. The matrix for B is similarly derived.

If SP_a is the corrected sum of products matrix for A, and SP_B that for B, then the matrix of pooled variances is:

$$\left[s_p^2\right] = \left(\left[SPA\right] + \left[SPB\right] \right) / \left(n_a + n_b - 2 \right) \qquad \text{II.6}$$

The set of coefficients $[\lambda]$ are entries in the discriminant function equation of the form:

$$Z = \lambda_1 x_1 + \lambda_2 x_2 + \ldots \lambda_m x_m \qquad \text{II.7}$$

This is a linear function, i.e. all the terms are summed to yield the single discriminant score, Z.

The discriminant index Z_o is the point along the discriminant function line midway between the centre of group A and the centre of group B. For each value of x_j in II.7 we substitute

$$x_j = \frac{\bar{A}_j + \bar{B}_j}{2} \qquad \text{II.8}$$

to find Z_o, and for the mean scores of A and B we substitute, for Z_a, $x_j = \bar{A}_j$ and for Z_B, $x_j = \bar{B}_j$.

The discriminant index $Z_o = \left(Z_A + Z_B \right)/2$ unless the variances of Z_A and Z_B are different. If so, a weighted estimate of Z_A can be found:

$$Z_o = \left(s_B Z_A + s_A Z_B\right) / \left(s_A + s_B \right) \qquad \text{II.9}$$

where s_A and s_B are the variances of Z_A and Z_B.

A discriminant score can then be found for any individual observation, and its position along the discriminant function line located. It is classified as from population A if the individual score Z_k is closer to Z_A than to Z_B (or on the Z_A side of Z_o), and from population B if the reverse is true.

A "distance" measure can be calculated between the two multivariate means simply by subtracting Z_A from Z_B, i.e. substituting the vector of differences between the group means in the discriminant equation or setting the values of $x_j = D_j$.

$$D^2 = \lambda_1 D_1 + \lambda_2 D_2 + \ldots \lambda_m D_m \qquad \text{II.10}$$

This is Mahalanobis' distance, or the generalised distance D^2, and is a measure of the separation between the two multivariate means expressed in units of the pooled variance.

The F test of this distance takes the form:

$$F = \left(\frac{n_a + n_b - m - 1}{(n_a n + n_b)\, m} \right) \left(\frac{n_a n_b}{n_a + n_b} \right) D^2 \qquad \text{II.11}$$

with m and $(n + n - m - 1)$ degrees of freedom.

The null hypothesis is:

$$H_o : D_j = 0$$

i.e. that the multivariate means are equal or that the distance between them is zero.

The probability of misclassifying a sample known to belong to one of the two groups can be estimated from the probability of a standardised normal curve with a deviation from the mean of $\frac{1}{2}D$ (i.e. $\sqrt{D^2/2}$)

Rao (1952) gives a test of whether a loss in discrimination results from eliminating some of the variables, and using a discriminant function based on the remainder. The test statistic is:

$$\frac{n_a + n_b - p - q - 1}{q} \cdot U_{p,q} \qquad \text{II.12}$$

where p is the number of variables retained, and q is the number of variables eliminated, and

$$U_{p,q} = \left(\frac{1 + \frac{n_a n_b}{(n_a + n_b)(n_a + n_b - 2)} D^2_{p+q}}{1 + \frac{n_a n_b}{(n_a + n_b)(n_a + n_b - 2)} D^2_p} \right) \qquad \text{II.13}$$

Under the null hypothesis that D^2_p discriminates just as well as D^2_{p+q}, this test statistic has an F distribution with A and $(n_a + n_b - p - q - 1)$ degrees of freedom. If the test is significant, a loss of discrimination would result from eliminating the q variables, so that all $(p+q)$ should be used. If non-significant, the q variables can be dropped without any loss of discrimination.

Five basic assumptions are made in tests of significance:

1) Observations in each group are randomly chosen.
2) None of the observations used for classification are misclassified.
3) Probability of an unknown belonging to either group is equal.
4) Variables are normally distributed in each group.
5) Variance -covariance matrices of the groups are equal in size.

It is most difficult to justify 3-5. However, limited deviations from normality or limited inequality of variances do not have serious effects.

APPENDIX III

TABLES OF ANALYSES

Table III.1 Random samples from the Lochailort Pelitic Group and Garnetiferous Pelite, used as basic data for the analysis of variance and discriminant function studies. See Chapter 3, page 27 for sampling design, and Figure 3.1 for sampling distribution.

Table III.2 Random samples from pelitic units of the Morar area used as "unknowns" with which to test effectiveness of linear discriminant functions. See Chapter 4, Figure 4.1 for sampling distribution.

Table III.3 Calc silicate rock analyses. An indication has been given of the presence of significant index minerals. Quartz, garnet and plagioclase feldspar are always present, unless otherwise indicated. Plagioclase compositions (by Michel-Levy method) are given where possible, ALT. indicating alteration. Mineral abbreviations are:-

AM - amphibole	PX - pyroxene
BT - biotite	CC - calcite
MUS - muscovite	CHL - chlorite
ZS - zoisite	CZS - clinozoisite
EP - epidote	

Where a replacement relationship has been established, the mineral being replaced is given in brackets(), with / before the replacing mineral. e.g. (AM)/BT indicates biotite replacing amphibole. AM/BT indicates that amphibole is unstable, biotite is stable. AM-BT would indicate coexistence of biotite and amphibole.

TABLE III.1.1

	1. NC111K	2. NC112K	3. NC113K	4. NC121K	5. NC122K	6. NC123K	7. NC131K	8. NC132K	9. NC133K
MAJOR ELEMENT ANALYSES									
SiO2	59.33	60.88	60.73	62.12	60.78	61.19	59.68	60.45	60.67
TiO2	1.03	0.95	0.87	0.95	1.06	1.11	0.98	1.06	1.01
Al2O3	19.81	19.18	18.72	17.64	17.85	17.82	17.97	19.51	18.76
Fe2O3	8.08	7.56	6.92	7.14	8.88	8.41	7.48	7.94	8.24
MnO	0.13	0.11	0.12	0.11	0.13	0.13	0.10	0.12	0.12
MgO	2.34	2.19	2.23	2.02	2.24	2.23	2.54	1.98	2.31
CaO	1.40	1.30	1.91	2.77	2.62	2.35	3.04	1.79	2.20
Na2O	1.98	2.00	2.44	3.28	2.62	2.80	3.70	2.24	2.34
K2O	4.10	4.67	3.90	2.74	2.88	2.83	2.18	3.41	2.99
P2O5	0.25	0.16	0.24	0.22	0.22	0.24	0.29	0.21	0.24
TOTAL	98.45	99.00	98.08	98.99	99.28	99.11	97.96	98.71	98.88
TRACE ELEMENT ANALYSES PPM									
Zr	172	198	174	290	280	303	211	231	230
Y	48	44	49	55	65	64	55	61	62
Rb	173	179	168	118	132	129	136	135	137
Nb	20	22	20	18	18	18	14	22	21
Sr	204	200	261	281	280	269	328	220	270
Zn	145	117	125	103	130	127	152	131	144
Nd	36	50	64	51	56	59	54	56	52
Ce	113	142	153	182	150	138	116	127	124
Ba	880	982	762	596	595	611	366	705	603
La	48	62	71	55	65	64	54	56	52

TABLE III.1.2

	1. NC211K	2. NC212K	3. NC213K	4. NC221K	5. NC222K	6. NC223K	7. NC231K	8. NC232K	9. NC233K
MAJOR ELEMENT ANALYSES									
SiO2	56.26	62.11	62.29	61.75	60.54	58.01	71.73	70.75	60.90
TiO2	1.18	0.88	0.82	1.06	1.07	1.14	0.53	0.65	1.05
Al2O3	20.02	18.80	18.40	18.83	19.88	19.37	14.75	14.65	18.45
Fe2O3	9.66	6.78	6.75	8.40	7.35	9.69	3.83	3.66	7.19
MnO	0.14	0.14	0.12	0.12	0.12	0.15	0.10	0.04	0.10
MgO	2.39	2.38	2.28	2.12	1.78	2.37	1.18	1.46	2.15
CaO	1.63	2.39	1.48	2.00	2.36	1.97	2.56	0.69	1.90
Na2O	1.83	3.05	2.14	2.86	3.28	2.40	3.57	1.53	2.18
K2O	3.63	3.13	4.31	2.90	2.64	3.14	1.72	5.67	4.34
P2O5	0.29	0.26	0.23	0.24	0.19	0.27	0.10	0.11	0.18
TOTAL	97.03	99.92	98.82	100.28	99.21	98.51	100.07	99.21	98.44
TRACE ELEMENT ANALYSES PPM									
Zr	224	184	171	227	229	209	218	398	311
Y	73	46	32	64	60	67	33	32	43
Rb	165	143	164	132	121	154	83	155	159
Nb	24	19	18	20	22	23	11	14	20
Sr	195	296	219	264	337	242	294	215	244
Zn	155	106	100	134	96	137	57	58	103
Nd	46	56	34	35	42	45	48	21	18
Ce	132	125	124	95	92	120	88	85	47
Ba	795	781	1067	608	668	639	472	1311	1135
La	58	61	44	41	37	49	39	29	21

TABLE III.1.3

	1. NC311K	2. NC312K	3. NC313K	4. NC321K	5. NC322K	6. NC323K	7. NC331K	8. NC332K	9. NC333K
MAJOR ELEMENT ANALYSES									
SiO2	58.15	58.00	61.00	65.06	61.25	59.30	59.83	59.20	58.74
TiO2	0.94	0.96	1.00	0.88	1.02	1.16	0.98	1.10	1.10
Al2O3	20.22	20.08	18.44	16.54	18.58	18.47	19.44	19.52	19.55
Fe2O3	7.78	7.96	7.92	6.40	8.14	9.04	7.94	8.86	8.64
MnO	0.12	0.17	0.11	0.10	0.12	0.13	0.11	0.13	0.13
MgO	2.52	2.51	2.36	1.93	2.14	2.48	2.18	2.49	2.38
CaO	1.63	2.53	2.59	2.73	2.65	2.01	1.94	1.93	1.78
Na2O	2.00	3.48	2.33	3.40	3.31	2.19	2.52	2.32	2.45
K2O	4.46	3.31	2.76	1.88	2.76	3.60	3.32	3.78	3.60
P2O5	0.27	0.28	0.26	0.20	0.24	0.26	0.21	0.26	0.24
TOTAL	98.09	99.28	98.77	99.12	100.21	98.64	98.47	99.59	98.61
TRACE ELEMENT ANALYSES PPM									
Zr	150	150	152	296	237	285	191	225	206
Y	49	46	51	48	59	72	60	59	57
Rb	170	144	168	101	128	156	135	151	155
Nb	19	17	18	15	20	22	16	22	21
Sr	224	301	273	322	302	228	233	227	205
Zn	117	123	115	109	130	141	112	137	122
Nd	53	30	49	31	40	57	24	48	38
Ce	147	103	153	67	103	149	70	126	104
Ba	953	788	929	358	590	806	796	751	646
La	64	36	61	28	39	64	25	53	38

TABLE III.1.4

	1. NC411K	2. NC412K	3. NC413K	4. NC421K	5. NC422K	6. NC423K	7. NC431K	8. NC432K	9. NC433K
MAJOR ELEMENT ANALYSES									
SiO2	59.18	61.64	61.50	65.95	58.02	66.98	60.39	59.13	58.05
TiO2	0.91	0.87	0.94	0.82	1.00	0.92	1.04	1.00	0.99
Al2O3	18.76	17.82	18.13	16.89	18.85	15.67	18.23	19.56	20.59
Fe2O3	7.86	6.80	7.28	6.16	8.95	5.88	7.55	8.26	8.95
MnO	0.12	0.08	0.14	0.11	0.13	0.13	0.11	0.14	0.11
MgO	2.50	2.33	2.63	2.22	2.79	2.06	2.73	2.59	2.49
CaO	2.43	2.22	2.20	2.13	2.44	3.70	2.66	2.65	1.92
Na2O	2.54	2.00	2.68	2.61	2.87	3.12	2.78	3.68	2.61
K2O	3.97	3.81	4.01	3.08	3.87	1.92	3.38	2.77	3.73
P2O5	0.27	0.28	0.36	0.23	0.32	0.22	0.37	0.33	0.32
TOTAL	98.54	97.85	99.87	100.20	99.24	100.60	99.24	100.11	99.76
TRACE ELEMENT ANALYSES PPM									
Zr	164	217	206	198	173	381	228	185	163
Y	27	34	37	30	26	53	41	38	41
Rb	130	114	128	112	134	83	132	119	132
Nb	18	15	15	29	16	19	14	14	18
Sr	323	277	363	260	306	372	319	363	291
Zn	107	92	112	111	127	89	116	124	114
Nd	26	29	45	28	21	55	55	32	1
Ce	86	95	123	80	66	117	136	86	38
Ba	1066	1166	1163	908	980	507	1082	673	892
La	32	38	49	27	24	50	66	33	8

TABLE III.1.5

	1. NC511K	2. NC512K	3. NC513K	4. NC521K	5. NC522K	6. NC523K	7. NC531K	8. NC532K	9. NC533K
MAJOR ELEMENT ANALYSES									
SiO2	61.02	58.59	58.79	59.34	59.94	62.83	57.03	61.08	61.72
TiO2	0.97	1.01	1.00	0.96	0.94	0.93	1.03	0.94	0.94
Al2O3	17.78	18.80	18.82	20.12	19.61	18.00	19.05	17.81	18.09
Fe2O3	7.47	8.91	9.01	7.82	7.81	6.29	9.64	7.67	8.06
MnO	0.12	0.14	0.13	0.11	0.11	0.11	0.15	0.12	0.13
MgO	2.41	2.44	2.58	2.14	2.04	1.77	2.55	2.47	2.33
CaO	2.71	2.61	2.70	2.05	2.20	3.07	2.75	2.62	2.70
Na2O	2.91	2.88	3.19	2.87	2.72	4.06	3.04	3.03	3.06
K2O	3.24	3.71	3.52	3.79	4.10	2.50	3.63	3.24	3.22
P2O5	0.35	0.34	0.35	0.31	0.28	0.23	0.38	0.34	0.32
TOTAL	98.98	99.43	100.09	99.51	99.75	99.79	99.25	99.32	100.57
TRACE ELEMENT ANALYSES PPM									
Zr	189	173	173	166	172	250	173	203	181
Y	43	57	35	48	31	28	25	40	35
Rb	126	125	123	128	134	104	128	121	113
Nb	15	16	16	18	18	17	15	14	16
Sr	321	293	309	280	290	416	314	326	324
Zn	111	124	128	120	124	88	127	119	121
Nd	48	64	24	55	11	35	3	34	50
Ce	116	144	86	131	58	82	47	106	106
Ba	893	974	921	864	1024	809	991	855	839
La	47	74	28	49	16	35	11	43	48

	1.	2.	3.	4.	5.	6.	7.	8.	9.
	NC611K	NC612K	NC613K	NC621K	NC622K	NC623K	NC631K	NC632K	NC633K
MAJOR ELEMENT ANALYSES									
SiO2	61.66	59.72	66.03	59.41	60.23	58.92	60.66	58.52	57.38
TiO2	0.96	1.02	0.81	0.97	0.95	1.01	0.94	0.97	0.97
Al2O3	17.51	18.48	16.48	18.88	18.53	18.55	18.03	19.02	19.65
Fe2O3	7.51	8.93	6.55	8.54	8.32	8.58	8.03	9.15	9.16
MnO	0.10	0.14	0.10	0.14	0.13	0.13	0.12	0.15	0.15
MgO	2.29	2.52	1.91	2.38	2.39	2.34	2.28	2.43	2.43
CaO	2.36	2.83	2.18	2.55	2.57	2.73	2.63	2.55	2.07
Na2O	1.25	3.19	2.27	2.74	2.82	2.98	2.77	2.94	2.10
K2O	4.40	3.35	3.17	3.62	3.48	3.47	3.66	3.82	4.39
P2O5	0.32	0.34	0.23	0.32	0.31	0.31	0.31	0.33	0.32
TOTAL	98.36	100.52	99.73	99.55	99.73	99.02	99.43	99.88	98.62
TRACE ELEMENT ANALYSES PPM									
Zr	209	171	204	163	176	188	188	146	130
Y	47	32	52	30	29	33	39	34	29
Rb	133	116	98	125	127	125	124	132	137
Nb	17	17	16	16	17	16	17	17	16
Sr	251	331	271	295	302	314	311	315	239
Zn	115	117	89	133	123	125	106	117	117
Nd	54	35	46	5	9	23	37	24	9
Ce	123	95	124	42	49	91	105	88	54
Ba	903	608	909	949	917	905	886	927	1170
La	61	41	55	9	15	26	36	31	15

TABLE III.1.6

	1.	2.	3.	4.	5.	6.	7.	8.	9.	10.
	NC533	NC534	NC535	NC536	NC360	NC362	NC363	NC364	NC365	NC366
MAJOR ELEMENT ANALYSES										
SiO2	61.71	58.05	62.37	60.62	56.85	60.32	57.15	58.39	63.48	60.30
TiO2	0.95	1.08	1.01	0.93	0.94	0.94	0.92	0.95	0.87	0.97
Al2O3	18.05	19.08	17.17	17.85	19.52	17.74	19.83	18.69	17.71	18.24
Fe2O3	6.25	7.92	6.64	6.95	8.41	6.56	9.07	7.75	5.40	6.22
MnO	0.11	0.10	0.10	0.10	0.10	0.10	0.12	0.13	0.10	0.09
MgO	2.00	2.58	2.08	2.23	2.28	2.11	2.16	2.27	1.66	1.93
CaO	2.25	1.95	2.21	2.42	2.27	2.69	1.90	2.84	2.55	2.28
Na2O	3.11	2.35	2.60	2.37	2.28	2.59	2.16	2.69	2.54	1.90
K2O	3.67	4.85	3.77	4.08	3.42	3.06	3.34	3.13	3.16	4.15
P2O5	0.23	0.29	0.23	0.41	0.48	0.25	0.33	0.36	0.27	0.28
TOTAL	98.33	98.25	98.18	97.96	96.55	96.36	96.98	97.20	97.74	96.36
TRACE ELEMENT ANALYSES PPM										
Zr	259	246	312	201	179	248	147	242	318	258
Y	25	30	33	40	53	30	53	39	19	25
Rb	129	159	122	128	113	114	121	139	98	120
Nb	17	16	16	15	20	16	17	17	14	17
Sr	419	309	322	347	294	399	276	390	377	296
Zn	88	108	95	107	113	89	112	118	71	99
Nd	0	0	0	0	7	23	11	26	4	16
Ce	0	0	0	0	70	122	62	132	70	98
Ba	0	0	0	0	997	932	852	868	1244	1126
La	0	0	0	0	10	30	16	20	7	20

1. NC533 GARNETIFEROUS PELITE, MORAR BAY. XRF ANALYSIS.
2. NC534 GARNETIFEROUS PELITE, MORAR BAY. XRF ANALYSIS.
3. NC535 GARNETIFEROUS PELITE, MORAR BAY. XRF ANALYSIS.
4. NC536 GARNETIFEROUS PELITE, MORAR BAY. XRF ANALYSIS.
5. NC360 LOCH MAMA PELITE. XRF ANALYSIS.
6. NC362 LOCH MAMA PELITE. XRF ANALYSIS.
7. NC363 LOCH MAMA PELITE. XRF ANALYSIS.
8. NC364 LOCH MAMA PELITE. XRF ANALYSIS.
9. NC365 LOCH MAMA PELITE. XRF ANALYSIS.
10. NC366 LOCH MAMA PELITE. XRF ANALYSIS.

TABLE III.2.1

TABLE III.2.2

	1. NC352	2. NC353	3. NC354	4. NC355	5. NC356	6. NC357	7. NC358	8. NC359
MAJOR ELEMENT ANALYSES								
SiO2	79.40	59.42	57.16	56.40	57.93	55.12	58.83	55.57
TiO2	0.36	1.01	1.01	0.93	1.01	1.04	1.04	0.97
Al2O3	11.48	19.31	20.65	21.07	19.41	21.53	19.50	20.91
Fe2O3	2.03	7.72	9.59	9.35	9.37	10.29	7.58	9.08
MnO	0.03	0.09	0.14	0.15	0.16	0.16	0.07	0.12
MgO	0.73	2.58	2.55	2.44	2.67	2.72	2.45	2.80
CaO	0.72	1.81	1.89	1.90	2.50	2.12	3.06	2.23
Na2O	1.46	2.21	1.99	2.52	2.58	2.13	3.29	2.08
K2O	2.59	3.93	3.87	3.58	3.42	3.59	3.03	4.26
P2O5	0.10	0.26	0.31	0.32	0.32	0.36	0.30	0.29
TOTAL	98.90	98.34	99.16	98.66	99.37	99.06	99.15	98.31
TRACE ELEMENT ANALYSES PPM								
Zr	197	200	150	152	152	174	197	143
Y	14	49	53	52	45	63	41	41
Rb	58	136	139	137	120	145	110	141
Nb	3	16	19	20	15	19	15	17
Sr	171	275	245	283	327	278	392	313
Zn	0	121	108	119	120	112	119	130
Nd	25	33	37	39	32	39	40	29
Ce	59	104	120	114	109	120	108	96
Ba	615	1007	1050	953	902	965	803	1048
La	16	42	49	49	42	48	43	33

1. NC352 ARIENISKILL PELITIC GROUP. XRF ANALYSIS
2. NC353 ARIENISKILL PELITIC GROUP. XRF ANALYSIS
3. NC354 ARIENISKILL PELITIC GROUP. XRF ANALYSIS
4. NC355 ARIENISKILL PELITIC GROUP. XRF ANALYSIS
5. NC356 ARIENISKILL PELITIC GROUP. XRF ANALYSIS
6. NC357 ARIENISKILL PELITIC GROUP. XRF ANALYSIS
7. NC358 ARIENISKILL PELITIC GROUP. XRF ANALYSIS
8. NC359 ARIENISKILL PELITIC GROUP. XRF ANALYSIS

TABLE III.2.3

	1.	2.	3.	4.	5.	6.	7.
	NC320	NC327	DP589	DP631	DP633	DP634	DP694
MAJOR ELEMENT ANALYSES							
SiO2	58.96	59.14	55.95	52.46	59.04	60.16	58.09
TiO2	0.99	0.95	0.87	1.13	0.98	0.86	0.92
Al2O3	17.33	17.61	19.60	20.16	17.78	17.57	19.82
Fe2O3	7.45	7.99	8.35	9.84	7.48	7.67	8.70
MnO	0.14	0.16	0.13	0.14	0.12	0.14	0.14
MgO	2.45	2.21	1.87	3.02	2.39	2.24	2.11
CaO	3.43	3.41	2.35	2.72	3.35	2.53	2.31
Na2O	1.39	3.31	2.29	2.85	3.17	2.26	2.35
K2O	3.71	2.51	4.03	4.05	2.53	3.37	3.62
P2O5	0.27	0.32	0.27	0.39	0.35	0.37	0.37
TOTAL	96.12	97.61	95.71	96.76	97.19	97.17	98.43
TRACE ELEMENT ANALYSES PPM							
Zr	270	191	166	200	231	158	154
Y	47	49	47	37	43	45	38
Rb	118	103	134	133	97	122	126
Nb	17	16	18	17	14	14	18
Sr	307	408	340	401	426	282	329
Zn	107	107	102	122	118	102	107
Nd	51	62	43	36	47	45	0
Ce	123	125	131	129	110	119	0
Ba	687	538	914	1187	682	865	0
La	53	56	53	50	47	51	0

1. NC320 GARNETIFEROUS PELITE, GLENUIG. XRF ANALYSIS
2. NC327 GARNETIFEROUS PELITE, SMEARISARY. XRF ANALYSIS
3. DP589 GARNETIFEROUS PELITE, GLENUIG. XRF ANALYSIS.
4. DP631 GARNETIFEROUS PELITE, GLENUIG. XRF ANALYSIS.
5. DP633 GARNETIFEROUS PELITE, GLENUIG. XRF ANALYSIS.
6. DP634 GARNETIFEROUS PELITE, SOUTH MOIDART. XRF ANALYSIS.
7. DP694 GARNETIFEROUS PELITE, SOUTH MOIDART. XRF ANALYSIS.

TABLE III.2.4

	1.	2.	3.	4.	5.	6.	7.	8.
	NC369	NC478	NC498	NC500	NC563	NC564	NC565	NC566
MAJOR ELEMENT ANALYSES								
SiO2	60.52	65.62	87.08	79.21	49.84	57.21	64.01	58.02
TiO2	0.81	0.71	0.23	0.33	1.57	0.95	0.57	0.99
Al2O3	17.19	15.97	7.38	9.27	21.22	19.63	18.11	19.51
Fe2O3	6.94	4.90	0.16	2.25	8.02	8.01	4.67	6.65
FeO	0.00	0.00	0.92	0.00	0.00	0.00	0.00	0.00
MnO	0.16	0.09	0.02	0.04	0.18	0.10	0.08	0.13
MgO	2.12	1.47	0.33	0.37	2.49	2.42	1.62	2.02
CaO	2.52	3.26	0.72	0.86	5.83	2.43	2.79	3.49
Na2O	2.73	3.18	1.21	1.71	4.53	2.87	3.59	3.65
K2O	2.97	2.18	1.29	2.41	3.02	4.25	3.40	3.83
P2O5	0.21	0.12	0.03	0.07	0.41	0.25	0.17	0.26
TOTAL	96.17	97.50	99.37	96.52	97.11	98.12	99.01	98.55
TRACE ELEMENT ANALYSES PPM								
Zr	178	218	255	350	1173	172	129	266
Y	44	35	10	17	52	37	20	33
Rb	142	105	43	83	111	129	85	102
Nb	19	14	5	7	36	15	8	15
Sr	312	256	133	179	842	374	564	604
Zn	109	70	8	33	103	132	62	86
Nd	47	50	26	32	0	0	0	0
Ce	118	113	33	60	0	0	0	0
Ba	634	670	462	681	0	0	0	0
La	49	49	16	28	0	0	0	0

1. NC369 LOCHAILORT PELITIC GROUP. XRF ANALYSIS.
2. NC478 LOCHAILORT PELITIC GROUP. XRF ANALYSIS.
3. NC498 LOCHAILORT PELITIC GROUP. WET ANALYSIS.
4. NC500 LOCHAILORT PELITIC GROUP. XRF ANALYSIS.
5. NC563 BASAL PELITIC GROUP. XRF ANALYSIS
6. NC564 BASAL PELITIC GROUP. XRF ANALYSIS
7. NC565 BASAL PELITIC GROUP. XRF ANALYSIS
8. NC566 BASAL PELITIC GROUP. XRF ANALYSIS

	1.	2.	3.	4.	5.	6.	7.
	NC545	NC546	NC547	NC548	NC550	NC558	NC559
MAJOR ELEMENT ANALYSES							
SiO2	53.87	58.05	56.68	68.20	59.43	58.63	57.81
TiO2	1.13	1.01	1.12	0.58	0.94	1.06	1.04
Al2O3	21.92	20.59	20.41	17.27	19.06	19.22	19.62
Fe2O3	9.73	8.56	9.10	3.84	7.39	6.74	8.35
MnO	0.20	0.14	0.13	0.04	0.11	0.18	0.12
MgO	2.56	2.34	2.42	1.02	2.19	1.99	2.47
CaO	1.36	1.96	1.94	2.21	2.43	4.92	2.66
Na2O	1.31	2.94	2.92	4.16	3.71	3.92	3.31
K2O	5.21	3.55	3.66	3.02	3.28	2.27	3.57
P2O5	0.28	0.26	0.30	0.04	0.30	0.49	0.33
TOTAL	97.57	99.40	98.68	100.38	98.84	99.42	99.28
TRACE ELEMENT ANALYSES PPM							
Zr	193	180	172	89	193	209	203
Y	67	61	63	12	51	55	59
Pb	197	148	164	97	129	102	160
Nb	26	22	20	11	18	19	21
Sr	161	270	233	451	299	339	322
Zn	137	119	131	64	108	93	132

1. NC545 WEST RANOCHAN PELITE. XRF ANALYSIS.
2. NC546 WEST RANOCHAN PELITE. XRF ANALYSIS.
3. NC547 WEST RANOCHAN PELITE. XRF ANALYSIS.
4. NC548 WEST RANOCHAN PELITE. XRF ANALYSIS.
5. NC550 WEST RANOCHAN PELITE. XRF ANALYSIS.
6. NC558 WEST RANOCHAN PELITE. XRF ANALYSIS.
7. NC559 WEST RANOCHAN PELITE. XRF ANALYSIS.

TABLE III.2.6

	1.	2.	3.	4.	5.	6.	7.	8.	9.
	NC538	NC539	NC540	NC541	NC542	NC543	NC544	NC556	NC557
MAJOR ELEMENT ANALYSES									
SiO2	59.38	54.72	58.31	73.61	66.45	62.28	59.10	60.00	59.75
TiO2	0.90	1.04	1.04	0.63	0.81	0.89	0.95	0.93	0.94
Al2O3	19.41	21.28	19.33	13.40	16.36	18.14	19.07	18.60	18.25
Fe2O3	7.13	8.32	9.05	3.81	5.55	6.96	7.41	6.94	6.99
MnO	0.10	0.13	0.16	0.04	0.09	0.13	0.18	0.20	0.15
MgO	2.28	2.84	3.00	1.13	1.82	2.38	2.40	2.19	2.13
CaO	2.17	1.82	0.76	2.07	2.55	2.07	2.26	2.96	1.78
Na2O	2.68	2.38	0.58	3.71	3.73	3.50	3.37	4.48	4.55
K2O	3.96	4.54	5.22	1.66	2.74	3.43	3.80	2.57	4.09
P2O5	0.28	0.12	0.21	0.16	0.23	0.24	0.28	0.35	0.19
TOTAL	98.29	97.19	97.66	100.22	100.33	100.02	98.82	99.22	98.82
TRACE ELEMENT ANALYSES PPM									
Zr	172	167	178	325	268	170	202	166	187
Y	52	51	52	30	34	42	43	52	48
Rb	153	185	208	85	116	171	163	126	171
Nb	18	20	22	13	17	19	18	19	22
Sr	315	313	103	313	408	305	481	514	436
Zn	114	142	145	80	92	114	120	121	106

1. NC538 EAST RANOCHAN PELITE. XRF ANALYSIS.
2. NC539 EAST RANOCHAN PELITE. XRF ANALYSIS.
3. NC540 EAST RANOCHAN PELITE. XRF ANALYSIS.
4. NC541 EAST RANOCHAN PELITE. XRF ANALYSIS.
5. NC542 EAST RANOCHAN PELITE. XRF ANALYSIS.
6. NC543 EAST RANOCHAN PELITE. XRF ANALYSIS.
7. NC544 EAST RANOCHAN PELITE. XRF ANALYSIS.
8. NC556 EAST RANOCHAN PELITE. XRF ANALYSIS.
9. NC557 EAST RANOCHAN PELITE. XRF ANALYSIS.

TABLE III.2.7

	1.	2.	3.	4.	5.	6.	7.	8.
MAJOR ELEMENT ANALYSES								
SiO2	48.52	58.97	57.73	59.36	57.97	58.20	58.97	55.04
TiO2	1.42	1.06	1.06	0.92	1.03	1.04	0.88	1.00
Al2O3	20.16	17.55	18.87	18.34	18.23	17.95	18.36	21.37
Fe2O3	9.99	7.67	8.23	7.14	8.62	8.26	6.68	8.07
MnO	0.09	0.09	0.12	0.06	0.15	0.13	0.08	0.20
MgO	3.00	2.28	2.36	1.66	2.45	2.29	1.91	2.22
CaO	3.31	2.48	2.53	1.26	2.65	2.68	2.37	1.05
Na2O	4.71	3.07	2.47	1.80	2.78	3.55	4.07	1.35
K2O	3.85	3.25	3.12	4.12	3.14	2.88	2.90	5.23
P2O5	0.56	0.24	0.29	0.29	0.28	0.30	0.29	0.29
TOTAL	95.61	96.66	96.78	94.95	97.30	97.28	96.51	95.82
TRACE ELEMENT ANALYSES PPM								
Zr	417	241	229	211	241	234	199	161
Y	70	38	59	55	59	59	52	51
Rb	151	144	126	153	140	121	130	181
Nb	22	21	21	21	23	23	20	23
Sr	1494	477	334	236	288	541	479	210
Zn	114	107	114	102	130	120	110	119
Nd	76	45	57	64	50	57	62	59
Ce	167	95	141	136	119	127	130	130
Ba	1619	880	888	791	870	845	654	1272
La	69	45	53	59	40	55	60	53

1. RA 022/ES/121 MHUIDHE PELITE. XRF ANALYSIS.
2. RA 022/ES/174 MHUIDHE PELITE. XRF ANALYSIS.
3. RA 022/ES/175 MHUIDHE PELITE. XRF ANALYSIS.
4. RA 020/WS/1 MHUIDHE PELITE. XRF ANALYSIS.
5. RA 020/WS/5 MHUIDHE PELITE. XRF ANALYSIS.
6. RA 020/WS/6 MHUIDHE PELITE. XRF ANALYSIS.
7. RA 020/WS/9 MHUIDHE PELITE. XRF ANALYSIS.
8. RA 020/WS/12 MHUIDHE PELITE. XRF ANALYSIS.

	1.	2.	3.	4.	5.	6.	7.	8.	9.	10.
	NCA300	NCA301	NCA302	NCA306	NCA308	NCA309	NC529	NC530	NC531	NC532
MAJOR ELEMENT ANALYSES										
SiO2	70.86	59.37	64.69	65.30	60.16	62.64	61.56	54.45	59.75	54.98
TiO2	0.13	0.81	0.72	0.84	0.60	0.59	0.78	0.61	0.65	0.44
Al2O3	11.15	16.86	16.14	15.59	15.04	15.05	17.79	14.85	19.26	17.80
Fe2O3	1.69	5.34	4.58	3.38	4.88	4.87	3.44	3.14	3.74	3.71
MnO	0.20	0.26	0.29	0.23	0.29	0.33	0.29	0.39	0.27	0.37
MgO	0.64	1.34	0.89	0.52	1.47	1.28	0.85	0.69	1.00	0.97
CaO	7.69	9.19	7.79	6.55	9.78	9.53	8.80	14.89	9.54	13.19
Na2O	2.50	2.47	2.67	3.00	2.07	2.00	3.37	2.28	3.01	2.65
K2O	0.49	1.20	0.89	0.85	1.75	0.69	0.81	0.53	0.85	0.69
P2O5	0.24	0.19	0.25	0.14	0.17	0.19	0.25	0.21	0.32	0.27
TOTAL	95.59	97.03	98.91	96.80	96.21	97.17	97.94	92.04	98.39	95.07
CaO/Al2O3	0.690	0.545	0.483	0.446	0.650	0.633	0.495	1.003	0.495	0.741
TRACE ELEMENT ANALYSES PPM										
Zr	67	182	425	388	170	179	268	206	186	78
Y	15	43	50	43	47	32	43	31	43	33
Rb	18	35	33	33	62	23	33	22	34	29
Nb	9	18	11	14	16	15	17	14	21	14
Sr	335	365	367	373	409	314	388	340	380	393
Zn	13	56	40	30	45	40	24	9	32	19
Ce	40	83	109	90	82	0	0	0	0	0
Ba	185	197	257	302	329	0	0	0	0	0

1.	NCA300	ET-ZS-CC. AN15	NM677968
2.	NCA301	ET-ZS-CC. AN15	NM677968
3.	NCA302	ET-ZS-CC. AN15	NM677968
4.	NCA306	ET-ZS-CC. AN15	NM677968
5.	NCA308	ET-ZS-CC. AN15	NM673946
6.	NCA309	AM-ET-ZS-CC.	NM673945
7.	NC529	ET-ZS-CC. AN20	NM675945
8.	NC530	ET-ZS-CC.	NM675945
9.	NC531	ET-ZS-CC.	NM675945
10.	NC532	ET-ZS-CC.	NM675945

TABLE III.3.1

TABLE III.3.2

	1. NCA312	2. NCA312	3. NCA313	4. NCA314	5. NCA315	6. NCA318
MAJOR ELEMENT ANALYSES						
SiO2	67.78	56.58	65.93	65.85	59.86	64.32
TiO2	0.90	0.77	0.49	0.54	0.53	0.42
Al2O3	14.56	17.21	15.85	15.34	18.43	13.55
Fe2O3	3.01	6.27	3.44	4.60	3.52	0.47
FeO	0.00	0.00	0.00	0.00	0.00	1.79
MnO	0.22	0.31	0.24	0.24	0.24	0.28
MgO	0.44	1.78	0.36	0.95	0.58	0.79
CaO	5.61	7.83	4.82	6.87	9.74	11.27
Na2O	3.51	4.15	6.34	2.71	3.33	1.68
K2O	0.84	1.28	0.72	0.94	0.71	0.72
H2O+	0.00	0.00	0.00	0.00	0.00	0.95
H2O-	0.00	0.00	0.00	0.00	0.00	0.04
P2O5	0.07	0.36	0.27	0.41	0.31	0.10
CO2	0.00	0.00	0.00	0.00	0.00	3.71
TOTAL	96.94	96.50	98.46	98.45	97.25	100.09
CaO/Al2O3	0.385	0.455	0.304	0.448	0.528	0.832
TRACE ELEMENT ANALYSES PPM						
Zr	523	189	0	303	160	204
Y	39	43	0	48	38	26
Rb	35	56	0	45	26	24
Nb	22	12	0	11	12	16
Sr	432	397	0	335	475	264
Zn	29	70	0	38	27	17
Ce	73	78	0	66	62	57
Ba	296	335	0	371	364	99

1.	NCA312	BT-ZS-CC.	AN20	NM677919
2.	NCA312B	BT-ZS-CC.	AN20	NM677919
3.	NCA313A	BT-ZS-CC.		NM677919
4.	NCA314	BT-ZS-CC.	AN<20	NM677919
5.	NCA315	BT-ZS-CC.	AN<20	NM677920
6.	NCA318A	(WET MAJORS)	BT-ZS-CC. AN20	NM651779

TABLE III.3.3

	1.	2.	3.	4.	5.	6.	7.	8.	9.	10.
	NC516	NC517	NC518	NC520	NC522	NC511	NC512	NC513	NC514	NC515
MAJOR ELEMENT ANALYSES										
SiO2	72.75	70.12	73.98	68.20	65.50	74.38	74.93	70.12	82.44	71.67
TiO2	0.35	0.32	0.31	0.32	0.79	0.57	0.42	0.45	0.23	0.46
Al2O3	14.77	15.26	12.67	13.08	16.72	13.49	12.76	13.76	8.90	13.25
Fe2O3	1.89	1.43	1.93	1.97	3.80	2.31	1.88	3.69	1.38	2.72
MnO	0.21	0.32	0.24	0.33	0.31	0.11	0.22	0.37	0.10	0.34
MgO	0.40	0.30	0.53	0.49	1.10	0.55	0.35	0.62	0.26	0.56
CaO	4.89	5.78	5.44	9.00	6.77	6.00	5.17	5.83	2.68	5.77
Na2O	4.16	4.79	3.34	2.65	3.53	1.97	3.57	2.56	2.81	2.35
K2O	0.47	0.43	0.69	0.59	1.11	0.82	0.44	1.53	0.65	1.18
P2O5	0.27	0.34	0.25	0.20	0.33	0.21	0.14	0.43	0.15	0.42
TOTAL	100.16	99.09	99.38	96.83	99.96	100.41	99.88	99.36	99.60	98.72
CaO/Al2O3	0.331	0.379	0.429	0.688	0.405	0.445	0.405	0.424	0.301	0.435
TRACE ELEMENT ANALYSES PPM										
Zr	157	115	114	96	368	219	236	147	136	176
Y	24	29	31	32	59	29	35	47	26	53
Rb	15	13	26	23	50	33	16	81	23	60
Nb	8	12	9	11	22	12	17	20	8	21
Sr	318	304	288	337	417	308	330	438	201	393
Zn	5	4	9	4	31	7	2	13	0	14

1.	NC516	BT-ZS ?AN15-20	NM671837
2.	NC517	BT-ZS-CC. ?AN15-20	NM671837
3.	NC519	BT-ZS-CC. ?AN15-20	NM671837
4.	NC520	BT-ZS-CC. ?AN15-20	NM671837
5.	NC522	BT-ZS-CC. ?AN15-20	NM671837
6.	NC511	BT-ZS. ALT.	NM743836
7.	NC512	BT-ZS. AN36	NM744833
8.	NC513	BT-ZS-CC. ALT.	NM744833
9.	NC514	BT-CZS/ZS. ALT(?20+)	NM744833
10.	NC515	BT-ZS-CC. ALT.	NM744833

	1.	2.	3.	4.	5.	6.	7.	8.	9.
	NCA320	NCA326	NCA325	NCA323	NCA322	DP653	DP676	DP683	DP686
MAJOR ELEMENT ANALYSES									
SiO2	63.54	67.73	77.88	64.28	56.52	67.88	75.12	73.08	75.28
TiO2	0.80	0.51	0.24	0.35	0.57	0.38	0.11	0.37	0.13
Al2O3	15.75	14.59	11.33	17.93	21.29	17.42	13.47	14.39	13.55
Fe2O3	4.27	1.88	1.37	2.54	2.13	1.85	1.19	2.10	1.30
MnO	0.21	0.25	0.13	0.21	0.21	0.28	0.17	0.06	0.19
MgO	0.94	0.27	0.09	0.76	0.61	0.49	0.36	0.39	0.38
CaO	8.79	6.47	4.28	7.81	7.27	8.29	6.21	5.28	6.00
Na2O	1.31	4.29	2.89	2.70	4.06	2.99	2.26	3.68	2.31
K2O	1.00	0.74	0.52	1.24	3.09	0.47	0.41	0.88	0.40
P2O5	0.22	0.21	0.00	0.19	0.20	0.33	0.20	0.11	0.20
TOTAL	96.83	96.94	98.73	98.01	95.95	100.38	99.50	100.34	99.74
CaO/Al2O3	0.558	0.443	0.378	0.436	0.341	0.476	0.461	0.367	0.443
TRACE ELEMENT ANALYSES PPM									
Zr	294	303	100	119	134	94	50	105	57
Y	44	27	14	14	16	9	7	7	9
Rb	37	27	20	39	103	7	12	17	9
Nb	28	19	8	14	13	9	1	4	4
Sr	323	358	304	422	935	372	201	514	205
Zn	37	12	11	23	14	3	0	6	4
Ce	99	45	51	48	35	0	0	0	0
Ba	224	186	277	300	612	0	0	0	0

1.	NCA320	BT-ZS-CC-MUS. AN20	NM6527EC
2.	NCA326	BT-CC-ZS. AN30	NM676779
3.	NCA325A	BT-ZS-CC. AN30	NM
4.	NCA323	BT-ZS-CC. AN40	NM695783
5.	NCA322	BT-ZS/CZS. ALT.	NM697783
6.	DP653	ZS-CC. ALT.	NM688733
7.	DP676	ZS-BT-CC. AN42	NM679735
8.	DP683	BP-PLAG-Q-BT. NO GT. -ARNIECI TYPE	NM676736
9.	DP686	BT-ZS-CC. AN38	NM676736

TABLE III.3.4

TABLE III.3.5

	1. NCA329	2. NCA330	3. NCA331	4. NCA332	5. NCA333	6. NCA334
MAJOR ELEMENT ANALYSES						
SiO2	62.35	77.79	78.47	84.88	70.71	69.73
TiO2	1.74	0.36	0.16	0.10	0.47	0.24
Al2O3	17.23	11.47	11.65	8.74	15.29	17.11
Fe2O3	4.60	1.66	0.42	0.01	2.31	0.38
FeO	0.00	0.00	0.71	0.59	0.00	1.16
MnO	0.45	0.16	0.13	0.06	0.22	0.16
MgO	0.77	0.03	0.21	0.23	0.45	0.38
CaO	7.17	4.02	4.47	2.63	6.63	5.56
Na2O	2.79	2.78	2.32	1.79	2.47	4.00
K2O	1.16	0.38	0.63	0.62	0.65	0.60
H2O+	0.00	0.00	0.72	0.34	0.00	0.56
H2O-	0.00	0.00	0.04	0.01	0.00	0.03
P2O5	0.26	0.01	0.10	0.02	0.12	0.23
TOTAL	98.52	98.66	100.03	100.02	99.32	100.14
CaO/Al2O3	0.416	0.350	0.384	0.301	0.434	0.325
TRACE ELEMENT ANALYSES PPM						
Zr	807	283	36	46	159	67
Y	46	36	9	8	19	14
Rb	52	23	39	17	27	14
Nb	41	14	5	2	10	5
Sr	325	243	266	205	362	559
Zn	25	8	5	8	10	11
Ce	101	70	27	27	62	39
Ba	273	117	68	474	217	203

1.	NCA329A	BT AN49		NM763823
2.	NCA330	BT-CZS. ALT.,ZONED		NM763823
3.	NCA331	(WET MAJORS) BT.		NM764822
4.	NCA332	(WET MAJORS) BT.	AN50(CENTRE) - AN40(EDGE)	NM766823
5.	NCA333	BT+CHL-CZS. AN58		NM766833
6.	NCA334	(WET MAJORS) BT.		NM766833

TABLE III.3.6

	1.	2.	3.	4.	5.	6.
	NC501	NC502	NC503	NC504	NC505	NC506
MAJOR ELEMENT ANALYSES						
SiO2	76.30	72.43	71.08	70.35	60.16	65.36
TiO2	0.44	0.87	0.66	0.38	0.90	0.35
Al2O3	11.84	14.18	15.36	16.19	17.25	18.29
Fe2O3	2.48	2.13	1.84	1.57	5.41	2.69
MnO	0.08	0.10	0.11	0.16	0.23	0.22
MgO	0.72	0.54	0.44	0.35	1.68	0.68
CaO	2.99	3.86	4.59	3.73	8.80	6.04
Na2O	3.08	4.44	3.58	4.38	2.60	3.20
K2O	1.20	0.89	1.09	1.49	1.06	1.44
P2O5	0.02	0.53	0.19	0.29	0.39	0.23
TOTAL	99.15	99.97	98.94	98.89	98.48	98.50
CaO/Al2O3	0.253	0.272	0.299	0.230	0.510	0.330
TRACE ELEMENT ANALYSES PPM						
Zr	128	207	217	122	283	106
Y	17	19	39	20	43	17
Rb	24	26	35	56	26	52
Nb	7	11	27	6	16	7
Sr	259	328	236	442	428	577
Zn	15	9	7	4	49	14

1.	NC501	(AM)/BT-C2S. AN34	NM772828
2.	NC502	(AM)-BT. ALT.	NM772828
3.	NC503	BT. ALT.	NM772828
4.	NC504	BT. ALT.	NM772828
5.	NC505	AM-C2S. AN42	NM767823
6.	NC506	BT. AN44	NM767822

TABLE III.3.7

	1.	2.	3.	4.	5.	6.	7.
	NC484	NC485	NC487	NC491	NC476	NC480	NC481
MAJOR ELEMENT ANALYSES							
SiO2	73.71	73.11	67.46	66.42	78.64	74.73	81.15
TiO2	0.36	0.35	0.70	0.50	0.37	0.33	0.14
Al2O3	13.48	12.89	15.37	17.24	9.77	13.79	10.68
Fe2O3	2.60	2.61	3.74	2.86	2.31	1.90	1.14
MnO	0.21	0.19	0.11	0.13	0.26	0.33	0.11
MgO	0.63	0.67	0.97	0.91	0.55	0.65	0.43
CaO	6.76	8.69	6.78	5.90	5.89	6.31	4.46
Na2O	2.12	0.90	2.81	3.75	0.85	1.47	1.13
K2O	0.44	0.24	1.23	1.11	0.51	0.40	0.43
P2O5	0.16	0.16	0.23	0.29	0.22	0.12	0.08
TOTAL	100.47	99.81	99.40	99.11	99.37	100.03	99.75
CaO/Al2O3	0.501	0.674	0.441	0.342	0.603	0.458	0.418
TRACE ELEMENT ANALYSES PPM							
Zr	261	256	253	152	201	331	103
Y	17	13	22	15	11	29	16
Rb	16	7	24	23	16	7	21
Nb	8	9	11	6	7	10	3
Sr	315	337	440	577	324	209	194
Zn	15	2	25	20	6	7	1

1.	NC484	AM-CZS. ALT.	NM777843
2.	NC485	AM-ZS-CZS. ALT.	NM777843
3.	NC487	BT-CZS. AN42(CENTRE) - AN32(EDGE)	NM773844
4.	NC491	BT-CHL. AN45	NM767822
5.	NC476	AM-BT-CZS. AN56	NM765843
6.	NC480	AM-CZS. AN64	NM784843
7.	NC481	AM. ALT.	NM784843

TABLE III.3.8

	1.	2.	3.	4.	5.	6.	7.	8.	9.
	NC436	NC442	NC443	NC449	NC450	NC450	NC451	NC453	NC455
MAJOR ELEMENT ANALYSES									
SiO2	66.13	66.69	73.30	76.74	81.97	82.16	77.85	69.04	69.39
TiO2	0.62	0.50	0.54	0.40	0.29	0.29	0.33	0.29	0.69
Al2O3	17.25	17.75	13.31	11.79	9.53	9.62	12.91	17.79	14.22
Fe2O3	3.99	2.48	2.49	2.09	1.23	1.25	1.32	2.29	3.84
MnO	0.34	0.30	0.19	0.34	0.14	0.14	0.07	0.21	0.26
MgO	0.99	0.56	0.65	0.51	0.23	0.23	0.31	0.56	1.16
CaO	6.96	9.33	4.16	5.66	2.89	2.94	3.48	6.75	5.18
Na2O	0.85	0.74	2.81	0.80	1.88	1.89	3.14	1.21	0.37
K2O	1.31	0.94	1.08	0.46	0.65	0.64	0.62	1.43	2.50
P2O5	0.31	0.23	0.41	0.31	0.03	0.03	0.17	0.35	0.18
TOTAL	98.75	99.52	98.94	99.10	98.84	99.19	100.20	99.92	97.79
CaO/Al2O3	0.403	0.526	0.313	0.480	0.303	0.306	0.270	0.379	0.364
TRACE ELEMENT ANALYSES PPM									
Zr	168	113	169	181	196	196	221	61	239
Y	42	20	50	40	28	28	33	21	45
Rb	82	49	44	25	29	29	24	76	136
Nb	15	13	12	13	8	8	4	12	16
Sr	251	183	281	89	181	181	266	201	242
Zn	25	3	5	5	1	1	8	5	31

1.	NC436	BT-CHL-MUS. AN71	NM793848
2.	NC442	(AM)-ZS-CZS-SPH. AN75	NM793848
3.	NC443	(AM)/BT-MUS. ALT.(48+?)	NM793848
4.	NC449	(AM)/CHL.	NM799844
5.	NC450	BT. AN56CENTRE(>EDGE)	NM799844
6.	NC450	BT. AN56CENTRE(>EDGE)	NM799844
7.	NC451	(BT)/CHL. AN58	NM79984
8.	NC453	(BT)/CHL-MUS. ALT.	NM801837
9.	NC455	(AM)-(BT)-CHL-MUS. ALT.	NM796832

TABLE III.3.9

	1.	2.	3.	4.	5.	6.
	NCA343	NCB343	NCA344	NCA345	NCA346	NCA348
MAJOR ELEMENT ANALYSES						
SiO2	68.93	66.82	73.87	68.46	65.20	81.02
TiO2	0.59	0.63	0.48	0.51	0.49	0.19
Al2O3	14.10	15.30	12.60	13.40	17.69	10.14
Fe2O3	3.84	3.95	0.46	3.24	3.21	1.04
FeO	0.00	0.00	2.14	0.00	0.00	0.00
MnO	0.38	0.41	0.20	0.25	0.28	0.09
MgO	0.87	0.88	0.87	0.97	0.99	0.30
CaO	5.42	6.13	3.86	5.61	6.86	3.12
Na2O	1.14	1.00	0.47	0.36	1.94	2.48
K2O	2.00	2.10	2.52	5.14	1.25	0.35
P2O5	0.19	0.18	0.13	0.09	0.26	0.02
TOTAL	97.46	97.40	97.60	98.03	98.17	98.75
CaO/Al2O3	0.384	0.401	0.306	0.419	0.388	0.308
TRACE ELEMENT ANALYSES PPM						
Zr	314	283	588	532	339	135
Y	70	71	100	94	107	28
Pb	110	114	350	535	153	13
Nb	17	17	24	37	38	6
Sr	150	166	434	777	752	158
Zn	25	23	47	56	54	7
Ce	87	91	73	70	76	46
Ba	239	262	317	773	275	112

1.	NCA343A BT/CHL. ALT.	NM794829
2.	NCB343B BT/CHL. ALT.	NM794829
3.	NCA344 (WET MAJORS) BT-CHL-MUSC. ALT.	NM794829
4.	NCA345 (AM)/BT/CHL. ALT.	NM794829
5.	NCA346 CHL. ALT.	NM799828
6.	NCA348 BT-ZS-CC-CRS. AN>30	NM815826

TABLE III.3.10

	1.	2.	3.	4.	5.	6.
	NC456	NC458	NC460	NC461	NC463	NC465
MAJOR ELEMENT ANALYSES						
SiO2	63.50	70.06	60.46	76.09	66.80	69.74
TiO2	0.60	0.44	0.36	0.43	0.53	0.67
Al2O3	19.38	16.22	20.20	12.79	16.94	14.13
Fe2O3	3.49	2.08	2.42	1.80	2.75	4.06
MnO	0.34	0.27	0.25	0.14	0.17	0.26
MgO	0.80	0.47	0.61	0.42	0.71	1.34
CaO	9.37	6.16	7.95	4.21	6.24	4.98
Na2O	1.06	2.26	1.87	2.55	2.20	0.31
K2O	0.83	0.85	2.68	0.65	1.63	2.77
P2O5	0.62	0.41	0.60	0.18	0.40	0.18
TOTAL	99.99	99.22	97.40	99.26	98.37	98.44
CaO/Al2O3	0.483	0.380	0.394	0.329	0.368	0.352
TRACE ELEMENT ANALYSES PPM						
Zr	184	126	144	251	236	246
Y	42	37	42	40	43	47
Rb	34	39	135	27	68	146
Nb	31	12	6	8	11	16
Sr	255	217	412	245	312	212
Zn	15	8	13	11	22	36

1.	NC456	BT/CHL. AN>62	NM799827
2.	NC458	BT/CHL. AN68	NM799827
3.	NC460	BT. ALT.	NM799827
4.	NC461		NM
5.	NC463	BT/CHL-MUSC. ALT.	NM797829
6.	NC465	BT/CHL-MUSC. AN43(CENTRE) - AN36(EDGE)	NM797829

TABLE III.3.11

	1.	2.	3.	4.	5.	6.	7.	8.	9.
	NC423	NC424	NC430	NC433	NC435	NC553	NC554	NC560	NC561
MAJOR ELEMENT ANALYSES									
SiO2	65.30	71.16	77.01	72.08	76.57	70.55	72.36	65.36	84.41
TiO2	0.44	0.60	0.36	0.38	0.33	0.61	0.60	0.57	0.26
Al2O3	13.21	12.17	10.25	11.84	12.69	14.34	13.80	17.85	7.92
Fe2O3	4.95	3.86	1.95	3.70	1.90	3.10	2.86	3.23	1.43
MnO	0.32	0.17	0.33	0.57	0.44	0.41	0.52	0.29	0.12
MgO	1.17	1.24	0.48	0.89	0.42	0.88	0.65	0.72	0.21
CaO	10.26	8.06	7.23	8.67	5.13	6.41	7.19	4.16	1.77
Na2O	0.83	0.49	0.77	0.76	1.26	0.84	0.67	4.80	0.49
K2O	0.38	0.16	0.30	0.21	0.72	0.97	0.53	1.13	2.19
P2O5	0.26	0.18	0.28	0.29	0.12	0.15	0.11	0.45	0.03
TOTAL	97.12	98.09	98.96	99.39	99.58	98.26	99.29	98.56	98.83
CaO/Al2O3	0.777	0.662	0.705	0.732	0.404	0.447	0.521	0.233	0.223
TRACE ELEMENT ANALYSES PPM									
Zr	202	351	284	267	169	344	349	265	215
Y	42	34	32	56	40	52	51	49	15
Rb	23	3	14	17	39	48	40	54	25
Nb	12	17	12	20	10	14	13	20	6
Sr	203	173	221	171	173	255	177	519	295
Zn	40	28	9	15	7	24	25	19	1

1.	NC423	(PX)/AMPH-CZS. AN61	NM833826
2.	NC424	AM. AN70	NM833826
3.	NC430	(PX)/AM-CZS. AN88	NM832827
4.	NC433	(PX)/AM-CZS. AN74	NM833827
5.	NC435	AM-CZS. AN?>60	NM829824
6.	NC553	AM/CHL. AN80	NM837832
7.	NC554	AM-CZS. AN80	NM838832
8.	NC560		NM
9.	NC561		NM

	1.	2.	3.	4.	5.	6.	7.	8.	9.	10.
	NCA336	NCA337	NCA339	NCA340	NCA341	NC400	NC401	NC403	NC421	
MAJOR ELEMENT ANALYSES										
SiO2	71.39	78.98	78.82	75.49	67.34	71.97	77.28	63.37	62.01	83.60
TiO2	0.40	0.39	0.48	0.48	0.53	0.52	0.36	0.56	0.60	0.26
Al2O3	13.17	9.94	10.18	12.55	17.30	14.99	10.34	16.79	13.52	8.26
Fe2O3	3.15	2.23	2.67	2.53	3.49	2.52	2.26	3.40	4.90	1.63
MnO	0.38	0.13	0.20	0.23	0.27	0.48	0.46	0.50	0.26	0.20
MgO	0.65	0.38	0.33	0.38	0.73	0.60	0.36	0.92	1.24	0.48
CaO	5.85	3.19	4.36	3.81	6.39	7.03	7.38	11.94	10.85	4.35
Na2O	0.55	2.43	1.49	2.67	2.36	1.16	0.39	0.32	0.51	0.46
K2O	2.83	0.74	0.43	0.68	1.30	0.45	0.18	0.11	0.61	0.24
P2O5	0.12	0.23	0.02	0.08	0.38	0.16	0.11	0.27	0.37	0.06
TOTAL	98.49	98.64	98.38	98.90	100.09	99.88	99.12	98.18	94.87	99.54
CaO/Al2O3	0.444	0.321	0.428	0.304	0.369	0.469	0.714	0.711	0.803	0.527
TRACE ELEMENT ANALYSES PPM										
Zr	179	227	549	394	206	350	284	168	283	252
Y	33	41	26	38	41	52	39	39	52	25
Rb	171	43	23	37	88	25	5	1	36	14
Nb	14	11	11	9	20	19	13	24	23	8
Sr	560	281	216	295	301	165	117	185	264	169
Zn	15	29	13	17	31	8	6	25	66	11
Ce	53	76	71	71	79	0	0	0	0	0
Ba	289	170	190	357	273	0	0	0	0	0

1.	NCA336 (PX)/AM. AIT.	NM833820
2.	NCA337B BT/CHL. ALT.	NM883819
3.	NCA339 (AM)/BT/CHL-ZS. AN55	NM835819
4.	NCA340A BT/CHL. AN49(CENTRE) - AN43(EDGE)	NM794829
5.	NCA341 CHL. ALT.	NM838818
6.	NC400 AM. AN86	NM838818
7.	NC401 (PX)/AM-CZS. AN75	NM838818
8.	NC403 (PX)/AM. AN72	NM838818
9.	NC421 PX/AM-ZS-CZS. NO PLAG.	NM838826
10.	RA 022/ES/28 (PX)/AM. AN80	NM858815

TABLE III.3.12

	1.	2.	3.	4.	5.	6.	7.	8.	9.
	NC414	NC415	NC416	NC417	NC418	NC419	NC404	NC408	NC409
MAJOR ELEMENT ANALYSES									
SiO2	67.94	72.28	72.21	66.53	75.35	72.14	64.14	78.02	86.57
TiO2	0.42	0.43	0.55	0.55	0.43	0.46	0.41	0.28	0.19
Al2O3	13.59	13.05	14.49	15.57	12.04	14.27	16.79	9.51	6.40
Fe2O3	3.77	2.38	2.35	3.65	2.45	2.50	5.03	2.79	0.70
MnO	0.40	0.26	0.26	0.35	0.58	0.50	0.46	0.39	0.02
MgO	0.38	0.51	0.52	0.94	0.45	0.47	0.56	0.46	0.20
CaO	9.75	8.35	7.02	10.17	6.45	8.54	9.99	4.68	3.80
Na2O	0.84	0.91	0.82	0.42	0.65	0.55	0.70	1.09	0.46
K2O	0.41	0.77	1.10	0.12	0.31	0.10	0.25	0.46	0.12
P2O5	0.19	0.13	0.42	0.26	0.14	0.16	0.18	0.33	0.06
TOTAL	98.19	99.07	99.74	98.56	98.85	99.69	98.51	98.01	98.52
CaO/Al2O3	0.717	0.640	0.484	0.653	0.536	0.598	0.595	0.492	0.594
TRACE ELEMENT ANALYSES PPM									
Zr	207	274	334	202	334	257	152	209	185
Y	34	36	38	36	46	36	30	36	16
Rb	20	44	66	1	21	2	11	26	1
Nb	12	12	29	15	17	19	14	7	8
Sr	158	259	228	177	121	177	293	123	126
Zn	54	14	11	24	6	5	11	15	0

1.	NC414	*PX-AM-ZS. AN78	NM840822
2.	NC415	(PX)/AM-CZS. ALT	NM841827
3.	NC416	(AM)/CT+ZS-MUSC. ALT(?65)	NM841827
4.	NC417	AM. AN68	NM841827
5.	NC418	AM. AN70	NM841827
6.	NC419	AM. AN72	NM841827
7.	NC404	AM. AN74	NM855816
8.	NC408	(AM)/(PX)/CHL. AN60	NM864815
9.	NC409	PX-ZS-GT-Q ROCK. NC PLAG.	NM864815

TABLE III.3.13

TABLE III.3.14

	1.	2.	3.	4.	5.	6.
	DP52	DP14A	DP121	DP157	DP127	DP8E
MAJOR ELEMENT ANALYSES						
SiO2	72.81	78.40	55.73	71.82	56.56	64.72
TiO2	0.65	0.45	0.70	1.00	0.69	0.49
Al2O3	12.61	10.37	22.72	13.40	19.91	18.61
Fe2O3	3.82	2.72	3.50	3.56	6.25	3.98
MnO	0.29	0.16	0.23	0.25	0.27	0.20
MgO	1.99	1.31	2.43	1.51	1.87	2.17
CaO	6.07	4.45	10.26	4.68	12.14	6.46
Na2O	0.23	0.12	3.47	0.30	1.23	1.93
K2O	0.67	1.53	0.64	2.37	0.93	0.80
H2O-	0.00	0.09	0.00	0.00	0.00	0.00
P2O5	0.11	0.05	0.10	0.54	0.39	0.09
CO2	0.05	0.00	0.12	0.28	0.07	0.09
TOTAL	99.20	99.65	99.90	99.71	99.81	99.53
CaO/Al2O3	0.481	0.429	0.452	0.349	0.642	0.347

1.	DP52	AM-CZS.	NM7984
2.	DP14A	AM-CZS. AN63	NM8082
3.	DP121	AM-ET-CZS. AN43	NM7682
4.	DP157	AM-CZS.	NM7982
5.	DP127	AM-ET-ZS-CZS. ALT.	NM7585
6.	DP8E	AM-ET-CZS. AN62	NM8377

REFERENCES

Anderson, R.L. & Bancroft, T.A. (1952) Statistical theory in research, McGraw-Hill, New York.

Atherton, M.P. (1965) The chemical significance of isograds, In: Controls of metamorphism (Pitcher, W.S. & Flinn, G.W.) (eds.) Oliver & Boyd (London).

Bailey, E.B. (1955) Moine tectonics and metamorphism in Skye, Trans. Geol. Soc. Edin., 16, 93-166.

Brown, R.L., Dalziel, I.W.S. & Johnson, M.R.W. (1970) A review of the structure and stratigraphy of the Moinian of Ardgour, Moidart and Sunart, Scott. Journ. Geol., 6, 309-335.

Butler, B.C.M. (1965) A chemical study of some rocks of the Moine series of Scotland, Q. Jl. geol. Soc. Lond., 121, 163-209.

Dalziel, I.W.S. (1966) A structural study of the granitic gneiss of western Ardgour, Argyll and Inverness-shire, Scot. J. Geol., 2, 125-152.

Davis, J.C. (1973) Statistics and data analysis in geology, John Wiley, New York.

Deer, W.A., Howie, R.A. & Zussman, J. (1963) Rock forming minerals (5 vols.), Longmans, London.

Emery, J.R. & Griffiths, J.C. (1954) Differentiation of oil-bearing from barren sediments by quantitative petrographic analysis, Producers Monthly, 19, 33-37.

Fisher, R.A. (1936) The use of multiple measurements in taxonomic problems, Annals of Eugenics, 7, 179-188.

Flett, J.S. (1923) The geology of lower Findhorn and lower Strathnairn, Mem. Geol. Survey.

Giletti, B.J., Moorbath, S. & Lambert, R.St.J. (1961) A geochronological study of the metamorphic complexes of the Scottish Highlands, Quart. J. Geol. Soc. Lond., 117, 233-272.

Griffiths, J.C. (1957) Petrographical investigations of Salt Wash sediments, U.S. At. Energy Comm. RME3151, 37 pp.

Harvey, P.K., Taylor, D.M., Bancroft, R.D. & Bancroft, F. (1973) An accurate fusion method for the analysis of rocks and chemically related materials by XRF, X-Ray Spectrometry, 2, 33-44.

Huitson, A. (1966) The analysis of variance, Charles Griffin & Co., London.

Johnstone, G.S. (1975) The Moine Succession. In: A correlation of Precambrian rocks in the British Isles, Geol. Soc. Lond., Spec. Publ. 6.

Johnstone, G.S., Smith, D.I. & Harris, A.L. (1969) Moinian assemblage of Scotland, Mem. Am. Ass. Petrol. Geol., 12, 159-180.

Kennedy, W.Q. (1949) Zones of progressive regional metamorphism in the Moine schists of the Western Highlands of Scotland, Geol. Mag., 86, 43-56.

Kennedy, W.Q. (1951) Sedimentary differentiation as a factor in the Moine-Torridonian correlation, Geol. Mag., 88, 257-266.

Krumbein, W.C. & Graybill, F.A. (1965) An introduction to statistical models in geology, McGraw-Hill, New York.

Lambert, R.St.J. (1969) Isotopic studies relation to the Precambrian history of the Moinian of Scotland, Proc. Geol. Soc. Lond., 1652, 243-5.

Long, L.E. & Lambert, R.St.J. (1936) Rb-Sr isotopic ages from the Moine Series. In: The British Caledonides, Johnson, M.R.W. & Stewart, R.H. (eds.), Oliver & Boyd, Edinburgh.

Middleton, G.V. (1962) A multivariate statistical technique applied to the study of sandstone composition, Trans. Roy. Soc. Can., 56, 119-126.

Miller, R.L. & Kahn, J.S. (1962) Statistical analysis in the geological sciences, John Wiley, New York.

Myer, G. H. (1966) New data on zoisite and epidote, Amer. Journ. Sci., 264, 364-385.

Padfield, T. & Gray, A. (1971) Major element and rock analysis by XRF - a simple method, Phillips analytical equipment Bulletin.

Potter, P.E., Shimp, N.F. & Witters, J. (1963) Trace elements in marine and fresh water argillaceous sediments, geochim. et. Cosmochim. Acta, 27, 669-694.

Powell, D. (1964) The stratigraphical succession of the Moine schists around Lochailort, and its regional significance, Proc. Geol. Ass., 75, 223-250.

Powell, D. (1974) Stratigraphy and structure of the western Moine and the problem of Moine orogenesis, Jl. geol. soc. Lond., 130, 575-593.

Ramsay, J. & Spring, J. (1962) Moine stratigraphy in the western Highlands of Scotland, Proc. Geol. Ass., 73, 295-326.

Rao, C.R. (1962) Advanced statistical methods in biometric research, John Wiley, New York.

Read, H. H. (1934) Age problems of the Moine Series of Scotland, Geol. Mag., 71, 302-317.

Richey, J.E. & Kennedy, W.Q. (1939) Moine and sub-Moine series of Morar, Bull. Geol. Surv. Gt.Br., 2, 26-45.

Shaw, D.M. (1954) Trace elements in pelitic rocks, Part I & II, Geol. Soc. Am. Bull., 65, 1151-1182.

Shaw, D.M. (1956) Geochemistry of pelitic rocks, Part III: Major elements and general geochemistry, Geol. Soc. Am. Bull., 67, 919-934.

Steveson, B.G. (1971) Chemical variability in some Moine rocks of Lochailort, Scott. Journ. Geol., 7, 51-60.

Sutton, J. & Watson, J.V. (1964) Some aspects of Torridonian stratigraphy on Skye, Proc. Geol. Ass., 75, 251-289.

Tanner, P.W.G. (1970) The Sgurr Beag Slide, a major tectonic break within the Moinian of the western Highlands of Scotland, Q. Jl. geol. Soc. Lond., 126, 435-463.

Tanner, P.W.G., Johnstone, G.S., Smith, D.I. & Harris, A.L. (1970) Moinian stratigraphy and the problem of the Central Ross-shire inliers, Bull. Geol. Soc. Am., 81, 299-305.

Tillman, R.W. (1973) Multiple group discriminant analysis of Gulf of Mexico river, beach and coastal aeolian sands, Geol. Soc. Amer. Abs. with Programs, (Ann.Mtg.), 5, 842.

van Breemen, O., Pidgeon, R.T. & Johnson, M.R.W. (1974) Precambrian and Palaeozoic pegmatites in the Moines of Northern Scotland, Jl. Geol. Soc. Lond., 130, 493-507.

Winchester, J.A. (1970) The geology of Fannich Forest, D.Phil. thesis, University of Oxford (unpublished).

Winchester, J.A. (1972) Moinian calc-silicate gneisses from Fannich Forest, and their significance as indicators of metamorphic grade, J. Pet., 13, 405-424.

Winchester, J.A. (1973) Pattern of regional metamorphism suggests sinistral displacement of 160km along Great Glen Fault, Nature (Phys. Sci.), 246, 81-84.

Winchester, J.A. (1974a) The zonal pattern of regional metamorphism in the Scottish Caledonides, Jl. geol. Soc. Lond., 130, 509-524.

Winchester, J.A. (1974b) The control of the whole rock content of CaO and Al_2O_3 on the occurrence of the Al_2SiO_5 polymorphs in amphibolite facies pelites, Geol. Mag., 111, 205-211.

Winkler, H.G.F. (1967) Petrogenesis of Metamorphic Rocks, Springer-Verlag, New York.

Wood, C.V. (1961) Discriminating between refractory and non-refractory quartzite by quantitative petrography, Journ. Sed. Petr., 31, 530-533.